The grass subfamily Pooideae: Cretaceous-Paleocene origin and climate-driven Cenozoic diversification

Running title: Climate-driven evolution of Pooideae

Abstract

- **Aim:** Frost is among the most dramatic stresses a plant can experience and complex physiological adaptations are needed to endure long periods of sub-zero temperatures. Due to the need to evolve these complex adaptations, transitioning from tropical to temperate climates is regarded difficult. Here, we study the transition from tropical to temperate climates in the grass subfamily Pooideae, which dominates cool temperate, continental and Arctic regions. We produce a dated phylogeny and investigate the role of climate cooling in diversification.
- **Location** Global, temperate regions
- **Time period** Cretaceous-Cenozoic
- **Major taxa** Pooideae
- **Methods** Using newly available fossils and methods we dated a comprehensive Pooideae phylogeny and tested for the impact of paleoclimates on diversification rates. Using ancestral state reconstruction, we investigated if Pooideae ancestors experienced frost and winter. To locate the ancestral distribution area of Pooideae we performed biogeographical analyses.
- **Results** We estimated a late Cretaceous/early Paleocene origin of the Pooideae (61–77 million years ago (Ma)), with all major clades already diversified at the Eocene-Oligocene climate cooling (34 Ma). Climate cooling was a probable driving force of Pooideae diversification. Pooideae likely evolved in a temperate niche experiencing frost, but not long winters.
- **Main conclusion** Pooideae likely originated in a temperate niche and experienced cold temperatures and frost long before expansion of temperate biomes after the Eocene-Oligocene transition. This suggests that the Pooideae ancestor had adaptations to temperate climate and that certain responses to low temperature stress are shared in extant Pooideae grasses. Throughout the Cenozoic falling temperatures and expansion of temperate biomes were associated with increase in diversification. However, complex mechanisms for enduring strongly seasonal climate with long, cold winters most likely evolved independently in daughter lineages. Our findings provide insight

into how adaptations to historic changes in chill and frost exposure influence distribution of plant diversity today.

Keywords: Diversification, evolution, grasses, niche transition, paleoclimate, phylogeny, Poaceae, Pooideae, temperate adaptations

Introduction

Temperate climates occupy major parts of the global landmass, but the temperate biomes as we know them today originated and expanded relatively recently in Earth's history when the global climate cooling intensified in the late Eocene (Eldrett, Greenwood, Harding, & Huber, 2009; Fine & Ree, 2006; Morley, 2000; Strömberg, 2011; Zachos, Pagani, Sloan, Thomas, & Billups, 2001). Many temperate–adapted lineages evolved around and after the Eocene-Oligocene (E-O) transition, ca 34 Ma, along with the expansion of cold temperate biomes, especially in the Northern Hemisphere (Favre et al., 2016; Kerkhoff, Moriarty, & Weiser, 2014; Marcussen, Heier, Brysting, Oxelman, & Jakobsen, 2015; Meseguer et al., 2018; Meseguer, Lobo, Ree, Beerling, & Sanmartín, 2015; Near et al., 2012). The concurrence of E-O transition and diversification into temperate climates suggests that global cooling around 34 Ma sparked the evolution of adaptations to cold seasonal climates. However, whereas approximately 80% of all seed plant families (The Angiosperm Phylogeny Group, 2016) are represented in tropical climates, only approximately 40% of plant families have members in cold temperate, continental and arctic climates with high seasonality and prolonged periods of sub-zero conditions (Stevens, 2017). This pattern has led to the assumption that transitioning from tropical to highly seasonal, cold climates requires the evolution of complex physiological adjustments not so readily accomplished (see e.g. Donoghue, 2008). Although, (historic) climate cooling likely impacted the evolution of angiosperm lineages, it is still unknown how it influenced today's distribution of species diversity.

An example of a highly successful temperate lineage is the grass subfamily Pooideae. It is the largest subfamily of Poaceae and comprises almost 4000 species distributed worldwide (Soreng et al., 2017). Its remarkable ability to endure in the coldest environments is reflected by its distribution and dominance in cold temperate, continental and Arctic grass floras (Hartley, 1973; Visser, Clayton, Simpson, Freckleton, & Osborne, 2014). Pooideae have the ability to make physiological adjustments to tackle physical damages from cold temperatures as well as mechanisms for timing of life history events to a highly seasonal climate, such as flowering, seasonal growth cessation and cold acclimation (Fjellheim, Boden, & Trevaskis, 2014; Preston & Sandve, 2013). These adaptations make them particularly well adapted to tolerate the extreme environments in cold temperate, contintental and Arctic areas. These capacities are well described in the model grass *Brachypodium distachyon* (tribe Brachypodieae) and in its species-rich sister clade, the "core" Pooideae (Soreng & Davis, 1998). The core Pooideae comprise 3232 species (Soreng et al., 2017), and include all

commercially important Pooideae crops, like bread wheat (*Triticum aestivum*) and barley (*Hordeum vulgare*) and forage grasses such as fescues (*Festuca* spp.) and ryegrass (*Lolium perenne*). The Pooideae share a common ancestor with the mainly tropical and subtropical subfamilies Oryzoideae (previously Ehrhartoideae) and Bambusoideae, and together they form the BOP clade (Soreng et al., 2017). A shift in climatic preferences from warm, tropical to colder, more temperate climates has been inferred in the stem-lineage of the Pooideae (Edwards & Smith, 2010).

The age of Pooideae has been difficult to establish, but ages ranging from 45 to 64 Ma have been suggested (Bouchenak-Khelladi, Verboom, Savolainen, & Hodkinson, 2010; Burke, Lin, Wysocki, Clark, & Duvall, 2016; Christin et al., 2014; Prasad et al., 2011; The International Brachypodium Initiative, 2010; Vanneste, Maere, & Van de Peer, 2014; Wang et al., 2015). During the time range of suggested origin for Pooideae the global climate was warm with little differences in temperatures at high and low latitudes, (Mudelsee, Bickert, Lear, & Lohmann, 2014; Zachos et al., 2001), there were few or no incidents of frost and seasonality in temperature was relatively low (Archibald, Bossert, Greenwood, & Farrell, 2010). In the late Eocene gradual climate cooling lead to an expansion of temperate climates (Liu et al., 2009; Potts & Behrensmeyer, 1992; Zachos et al., 2001). A drop in global temperature around the E-O transition 34 Ma (Pound & Salzmann, 2017), concomitant with increased seasonality (Eldrett et al., 2009; Zachos et al., 2001) intensified the expansion of the temperate niche. However, disentangling how falling temperatures throughout the Cenozoic have impacted the evolutionary history of Pooideae is hampered by the lack of a properly dated, comprehensive Pooideae phylogeny.

The difficulties establishing an age for Pooideae appears to reflect the overall poor macrofossil record of Poaceae (Strömberg, 2011) as well as grasses having lower nucleotide substitution rates than other angiosperms (Gaut, Muse, Clark & Clegg, 1992; Christin et al., 2014). The earliest firm records of grass pollen are 55-60 Ma, with older pollen fossils of grasses or grass relatives known from 70 Ma, and it was long assumed that the family was not much older than this (Kellogg, 2001). However, recent findings of around 100 Ma old fossils assignable to Poaceae contradict a Paleogene origin of grasses. The first fossil, a grass spikelet infected by a *Claviceps*-like fungus trapped in Burmese amber, suggests a stem node age of Poaceae of at least 98 Ma (Poinar Jr., Alderman, & Wunderlich, 2015; Shi et al., 2012) and the second set of fossils, silicised epidermal fragments with preserved cell patterning and phytoliths, have synapomorphies that suggest a crown node age of Poaceae of at least 101 Ma

(Wu, You, & Li, 2018). Furthermore, 66 Ma old epidermal fragments containing phytoliths (Prasad, Strömberg, Alimohammadian, & Sahni, 2005) show diagnostic features of subfamily Oryzoideae (Prasad et al., 2011). When used as age constraints in dating analyses, these fossils indicate older ages for all major clades of Poaceae, Pooideae included (Christin et al., 2014; Marcussen et al., 2014; Prasad et al., 2011). Age estimates for Pooideae are however largely based on external calibrations and the known Pooideae fossil record has so far not been fully explored in dating analyses (but see Marcussen et al., 2014).

In this study we aim to reconstruct the paleoclimatic impact on phylogenetic and diversification history of the grass subfamily Pooideae. Firstly, we provide a comprehensive, fossil-dated chloroplast phylogeny of Pooideae. Preservation rates of macrofossils are low in Poaceae and therefore ages are likely to be underestimated using classical node dating where the oldest available fossil is applied as a minimum age constraint. We circumvent this problem by employing a new method (PyRate; Silvestro, Schnitzler, Liow, Antonelli, & Salamin, 2014) that estimates the speciation time probability distribution based on the entire fossil record for each clade, thereby also eliminating the subjective choice of a maximum age constraint. Secondly, we estimate diversification rates and test for an impact of paleoclimates on diversification trajectories, using recently-developed paleoenvironmental birth-death models (Condamine, Rolland, & Morlon, 2013). Thirdly, we reconstruct the temperature niche of Pooideae to establish if the ancestor experienced frost or longer periods of cold temperatures. Lastly, we reconstruct the biogeographical history of Pooideae under the dispersal–extinction–cladogenesis (DEC) model.

Materials and Methods

Materials and sampling

A data matrix containing three chloroplast (cp) DNA regions (*matK*, *ndhF*, *rbcL*) for 421 species, including 30 Poaceae outgroups from all 11 subfamilies and 3 far outgroups from the closest sister families (*Ecdeicolea monostachya*, *Joinvillea plicata*, *Flagellaria indica*), was assembled from GenBank and from own accessions (see Table S1.1 in Appendix 1). Pooideae sampling was aimed at being exhaustive at the genus level. We followed the most recent taxonomies for each lineage on a case-to-case basis. For lineages resistant to taxonomic change (e.g. *Festuca*/*Lolium*) we aimed at sampling deep lineages exhaustively. Sequences for some taxa were obtained *de novo* by PCR and Sanger sequencing using custom Pooideae-specific primers (Table S1.2). Clustal alignments were generated and manually adjusted in BioEdit (Hall, 1999). The final alignments for *matK*, *ndhF* and *rbcL* were 1629,

907 and 720 nucleotides long, respectively (sum: 3256), and had 2% (8), 14% (54) and 34% (135) of missing ingroup sequences, respectively.

Sampling of fossils and estimation of fossil origination times

We performed a dating analysis with a total of 11 fossil calibration points (Table 1); for a justification for the use of fossils and priors see Appendix 2. Based on the Pooideae fossil record (Iles, Smith, Gandolfo, & Graham, 2015; Strömberg, 2011; Thomasson, 1988) we identified six fossil calibration points and estimated for five of them the probability density of origination time for the respective clade (Table 1) using PyRate (Silvestro et al., 2014). A fossil matrix (see Appendix 2) containing associated lineage minimum and maximum age bounds was entered in PyRate and an MCMC chain was run for 1 million generations. Ages were sampled randomly from within the age bounds under a uniform probability distribution. The analysis was replicated 20 times. For each lineage, the posterior distribution of speciation times was summarised over all replicates in Tracer v1.6.0 (Rambaut, Suchard, & Drummond, 2013). For each posterior distribution we used mean, variance, 0.025 quantile and 0.975 quantile (Table 1) to translate it into a log-normal distribution with three parameters (mean, standard deviation (stdev), offset) using ParameterSolver v3.0 (Cook, Wathen, & Nguyen, 2013), which was then used as a calibration prior in a conventional BEAST dating analysis.

We used regular node dating for the remaining fossil calibrations (Table 1), with fossils applied as minimum age constraints for their respective clades (Table 1), an exponential prior distribution with an arbitrary mean of in most cases 10 Ma, i.e. a 95% highest probability density (HPD) of 30 Ma. The uninformative exponential distribution was chosen over the uniform one to avoid convergence problems. A larger mean (50 Ma) was applied to the *Lygeum* stem node (*Lygeum* fossils) and to the Stipeae stem node (fossil *Stipa florissantii*) because ages inferred from explorative analyses (not shown) suggest that these fossils are stem lineage fossils on a long branch. Finally, we constrained the root node with an exponential prior having a 95% HPD between 101 and 144 Ma and a hard maximum bound at 144 Ma, corresponding to the Angiosperm crown node age previously obtained by PyRate analysis of the entire Angiosperm fossil record (Silvestro, Cascales-Miñana, Bacon, & Antonelli, 2015). To our knowledge, this is the most informed estimate for this node published to date. The calibration of Poaceae crown to ≥101 Ma is used for the first time here; it is based on newly described silicised leaf epithel fragments with convincing diagnostic cell pattern and phytoliths (Wu, You & Li, 2018) extracted from the teeth structure

of a basal hadrosauroid dinosaur (*Equijubus normani*) recovered in the late Early Cretaceous (Albian, 113–101 Ma) Zhonggou Formation of Gongpoquan Basin, Mazongshan area, Gansu Province in northwestern China. These grass fossils display dimorphic epidermal patterning of long and short cells, which is a unique feature shared by Poaceae and Joinvilleaceae (Rudall, Prychid & Gregory, 2014; Kellogg, 2000), and further short-cell pairs which first appear in Poaceae:Anomochlooideae and are considered a synapomorphy of crown-node grasses (Rudall et al. 2014), which node it hence calibrates. We note that including or excluding the calibration of Oryzeae ≥66 Ma based on fossil epithel containing phytoliths (Prasad et al., 2005), although having been considered controversial (Prasad et al., 2011; Christin et al., 2014; Spriggs, Christin, & Edwards, 2014), did not alter the inferred ages significantly in our exploratory dating analyses (not shown), except for the nodes surrounding the calibration.

Dating Pooideae

The dating analysis was set up in BEAUti v1.7.4 and performed in BEAST v1.8 (Drummond & Rambaut, 2007; Drummond, Suchard, Xie, & Rambaut, 2012). The three cpDNA partitions were analysed using unlinked site models, linked clocks, and linked partition trees. Nucleotide substitution model priors were set to GTR + G (four gamma categories) for all partitions, as suggested by JModelTest v.2.1.10 (Darriba, Taboada, Doallo, & Posada, 2012). To account for rate heterogeneity among lineages the tree was given an uncorrelated lognormal relaxed molecular clock prior assuming a Yule speciation process (birth-only); initial analyses applying a parameter richer birth-death model did not alter the outcome. The clock rate was given an uninformative uniform prior between 0 and 10^{100}. For three basal nodes the topology was constrained by enforcing monophyly for Pooideae, Pooideae + Bambusoideae, and the BOP clade. Constraints for fossils and secondary calibrations are shown in Table 1. Two MCMC chains were run for 200 million generations while parameters were logged every 20,000 generations. After confirming proper chain mixing, convergence (i.e. ESS >200) and burn-in removal (20 million generations) the two chains were merged in LogCombiner v1.7.4 (part of BEAST package). We used TreeAnnotator v1.7.4 (part of BEAST package) to summarise the data in a maximum clade credibility (MCC) tree with mean node heights. This tree was used for further downstream analyses.

Diversification analyses

We investigated modes of species diversification in Pooideae. Using two complementary approaches (TreePar and RPANDA), we estimated whether a clades' diversification deviates

from a constant birth-death model or if shifts in speciation and extinction rates occurred. We further tested the impact of past environmental changes on the diversification using RPANDA. To this end, we took into account incomplete taxon sampling and age uncertainties (100 randomly selected trees from the posterior distribution of trees; stdevs are reported in Tables S1.3, S1.4). For TreePar 2.1 (Stadler, 2011), potential rate shift times were evaluated in a grid of 1 Ma time intervals. The sampling fraction for the first time interval (present) was set to 0.1 according to the taxon sampling in the present, while the probability of survival per lineage was alternatively set to 1 (no extinction, i.e. the sampling of deep branches is complete) or 0.1 (10% of lineages survive to the next period). The likelihood ratio test and AIC was used to compare nested models of increasing complexity, from 1 to 2 additional rate shifts.

In the paleoenvironmental birth-death models (Condamine et al., 2013) implemented in RPANDA (Morlon et al., 2016), speciation (λ) and extinction rates (μ) can change according to an environmental variable, which itself varies through time. We compared the fit of a set of models where diversification rates vary continuously as a function of an environmental variable (here the temperature) against a constant-rate birth–death model and a set of models in which speciation and/or extinction vary continuously according to time alone (Table S1.4). When rates varied with temperature or time, we assumed exponential variation. For the temperature and time models, the parameters α and β control the variation of λ and μ, respectively, and measure the sign and strength of the temperature/time dependence. For example, in temperature models, a positive α (β) indicates that speciation (extinction) rates decrease exponentially from the past to the present in association with decreasing global temperatures, so rates are higher under warm climatic periods. Conversely, a negative α (β) indicates that these rates are higher under cold periods, so speciation (extinction) increases in association with decreasing global temperatures. Similarly, for the time models, a positive α (β) indicates that speciation (extinction) rates decrease from the past to the present in association with decreasing time. Global paleotemperature data were retrieved from Condamine et al. (2013) and based on the global Cenozoic deep-sea oxygen isotope record as a proxy for global temperatures (Veizer & Prokoph, 2015~~Zachos, Dickens, & Zeebe, 2008~~). We assessed the strength of support for constant, time-dependent, and temperature-dependent diversification by computing the corrected Akaike criteria and selecting the best model among these four categories.

Geo-referenced records and climatic data

Geo-referenced records for Pooideae and outgroup taxa were downloaded from the Global Biodiversity Information Facility (GBIF.org 2016, 2019~~; www.gbif.org~~) using the rgbif package in R (Chamberlain, 2017). To exclude unreliable records we discarded coordinates with less than three decimals and employed additional filtering implemented in the SpeciesGeoCoder package (Töpel et al., 2016) in R. In short we discarded records where coordinates a) were not valid (not part of the coordinate system, or marine coordinates), b) were exactly or close to zero (threshold 0.5), c) were the same for latitude and longitude, d) had the same values as the country's capital, e) lay outside the country's polygon, or f) had the same value as the GBIF institutions. Taxa with synonymous names were merged using taxonomic information from GBIF. For each of the filtered geo-referenced records, 19 Bioclim variables were downloaded from the WorldClim database (http://www.worldclim.org/) in a 2.5 arc-minutes resolution using the 'raster' package in R. After excluding the lower and upper 5% of each Bioclim variable and taxon we calculated mean and standard deviation, which were used in downstream phylogenetic analyses.

ASR of climatic space

To assess the phylogenetic information contained in each Bioclim variable we determined the phylogenetic signal of the grand total means represented by Pagel's lambda (λ) (Pagel, 1999) using phylosig function of the R package phytools (Revell, 2012). For the Bioclim variable with the strongest phylo~~l~~genetic signal (BIO3, isothermality) we reconstructed ancestral states as a continuous trait evolving under an Ornstein-Uhlenbeck model (AIC_C=2880.39 compared to AIC_C=2911.59 under Brownian motion) using the R packages Rphylopars (Goolsby, Bruggeman, & Ané, 2017). To investigate the Pooideae most recent common ancestor's (MRCA) exposure to frost and prolonged cold, we scored BIO6 (minimum temperature of the coldest month) and BIO11 (mean temperature of the coldest quarter) as binary traits. In case of BIO6, we scored a single binary trait, measuring exposure to frost as either "yes" (BIO6 <0) or "no" (BIO6 ≥0). To measure exposure to winter severity, we explored which winter temperatures comprised the strongest phylogenetic signal. We found that the amount of months below a monthly mean temperature of 2°C and 3°C exhibited the two strongest phylogenetic signals (data not shown). Based on these findings we scored BIO11 as three binary traits, whether BIO11 (i.e. the mean temperature of the coldest quarter) was below ("yes"), or not below ("no") 2°C, 3°C and 4°C, respectively. To test if the binary traits were distributed non-randomly along the phylogeny we estimated Fritz & Purvis'

(2010) *D* using the phylo.d function in the R package caper (Orme, 2013; Table S1.5). The binary ASRs were performed with BEAST using a separate data partition on the previously obtained timetree. The state of the root was not constraint and we assumed an asymmetrical evolution model, due to a better fit for the binarized BIO11 below 2°C (Table S1.6). We supplied the MCC timetree as starting tree and turned off all tree operators. Remaining settings and priors were left unchanged.

Historical biogeography

To investigate the ancestral distribution of the Pooideae we reconstructed the biogeographic history using the maximum likelihood model DEC implemented in Lagrange (Ree, Moore, Webb, & Donoghue, 2005; Ree & Smith, 2008). Taxa distributions were defined by six broadly defined biogeographic regions, i.e. Africa, North America, South America, Arctic, Australasia and Eurasia, based on GBIF distribution data. This analysis was run on the MCC tree, excluding outgroup taxa. We considered that all ranges comprised of three areas could be an ancestral state (maxareas =3). We coded the two North American Brachyelytreae species as distributed in Eurasia + North America. This was done to correct for the absence from our analysis of Asian species of this lineage (i.e. *Brachyelytrum japonicum*).

Results

Dating analysis

The obtained chloroplast phylogeny for 421 species and 11 calibrations is shown in Fig. 1a, and the ages of key nodes are given in Table 2. The crown node of Pooideae (stem node of Brachyelytreae) was inferred to a 95% credibility interval (CI) of 61–77 Ma (mean 69 Ma), at the Cretaceous-Paleocene boundary (Fig. 1, Table 2). Reconstructed ages for the stem nodes of the main subclades of Pooideae showed a rapid succession of speciation events between 58–74 Ma (mean 66 Ma; Lygeeae+Nardeae stem) and 47–61 Ma (mean 54 Ma; Diarrheneae stem). The stem node of Brachypodieae, i.e. the split between *Brachypodium* and core Pooideae, was reconstructed to 45–59 Ma (mean 52 Ma). The 95% CI of the crown node ages for the largest subclades, i.e. Stipeae, Meliceae (minus *Brylkinia*) and the three core Pooideae lineages, all overlapped with the E-O transition boundary 34 Ma (means 36–39 Ma, 95% CI 31–47 Ma) (Fig. 1; Table 2). The crown node of Poaceae was inferred at 101–112 Ma (mean 105 Ma) and the split between the two major clades of subfamilies BOP and PACMAD at 73–88 Ma (mean 74 Ma).

Diversification analyses

We estimated episodic changes in diversification rates in TreePar evaluating two extreme survival probability models (Table S1.3). For the no extinction scenario (100% of the lineages survive to the next period), the best model was the one with a single rate shift and diversification increasing through time (AICw = 0.41; Table S1.3), although this model was not significantly better than a constant rate model based on delta AIC values (ΔAIC =0.77; AICw = 0.28; Table S1.3). For the high extinction model (10% survival), the hypothesis of constant diversification could not be rejected (AICw = 0.89; Table S1.3).

Among the continuous models in RPANDA, we ccould not exclude that diversification was constant (AICw = 0.35; Table S1.4). Nonetheless, the constant birth-death model was not significantly better than a temperature-dependent model where speciation remains constant and extinction decreases with decreasing temperatures (i.e. diversification increases; $\beta>0$; ΔAIC =0.66; AICw = 0.25).

Phylogenetic signal and ASR of climate niche

All investigated Bioclim variables expressed a statistically significant phylogenetic signal, i.e. Pagel's λ significantly different from zero (p <0.001, Table S1.7). Bioclim variables for isothermality (BIO3), temperature seasonality (BIO4) and variables linked to winter season temperatures (BIO6 and BIO11) contained the strongest phylogenetic signals (Pagel's λ >0.86). For the remaining Bioclim variables, Pagel's λ ranged between 0.34 and 0.85, with variables linked to precipitation containing the weakest phylogenetic signal.

Isothermality (BIO3) was the Bioclim variable with the strongest and most significant phylogenetic signal (Table S1.7). The reconstruction of isothermality as a continuous trait (Fig. 2, 3b–d) produced ancestral estimates for the Pooideae ancestor and the Pooideae backbone nodes that were comparable with values of present warm temperate and subtropical climates (Fig. 3a). Isothermality estimates associated with cold temperate and frigid climates were reconstructed late in the phylogeny and only in a few lineages (Fig. 2, 3b–d).

The analysis of the binarized BIO6 variable indicated that the ancestor of the Pooideae, as well as the ancestor of each major lineage, might have experienced frost (Fig. 2). Our analyses for ancestral winter severity (binarized BIO11 variable, Fig. 3b–d) indicated that ancestors of all major lineages might have experienced winters with mean temperatures below 3°C (Fig. 3c). However, a mean winter temperature of 2°C seems to be the lower limit

for most extant and ancestral lineages (Fig. 3b). Tolerance to such cold winters was reconstructed later in independent Pooideae lineages.

Reconstruction of historical biogeography

The DEC analyses (Fig. S3.1 in Appendix 3) reconstructed Eurasia as most likely area for ancestral Pooideae lineages (relative probabilities in Appendix 4). We identified numerous dispersals from Eurasia to different continents occurring after the divergence of all tribes. Most notably are the early independent dispersals of Stipeae (in agreement with the fossil record) and Meliceae lineages to the Americas in the late Eocene. Most other dispersals occurred later, starting in the Miocene around 20 Ma.

Discussion

The age of Poaceae and Pooideae

Compared to many earlier estimates, our age estimates (Fig. 1a, Table 2) indicate a relatively older age of the Pooideae and Poaceae, with crown node ages at 61–77 Ma and 101–112 Ma, respectively. Our findings are however in line with recent analyses that have taken into account updated information from the fossil record (Bouchenak-Khelladi et al., 2009; Prasad et al., 2011; Christin et al., 2014; Marcussen et al., 2014; Burke et al., 2016; Vanneste et al., 2014; Wang et al., 2015). Studies that found considerably younger ages (i.e. 59–70 Ma for Poaceae) typically did not include these fossils (Kellogg, 2001; Vicentini, Barber, Aliscioni, Giussani, & Kellogg, 2008; Bouchenak-Khelladi, Muasya, & Linder, 2014; Christin et al., 2014; Marcussen et al., 2014) or inferred ages by molecular substitution rates rather than fossil calibration (Goff et al., 2002; Paterson, Bowers, & Chapman, 2004; Schlueter et al., 2011; Wang et al., 2005; The International Brachypodium Initiative, 2010). Importantly, also angiosperm-wide dating projects, which necessarily include few grass samples and fossils, have similarly inferred young ages for Poaceae (Bell, Soltis, & Soltis, 2010; Hertweck et al., 2015; Magallón, 2010; Magallón, Gómez-Acevedo, Sánchez-Reyes, & Hernández-Hernández, 2015; Magallón, Hilu, & Quandt, 2013; Vanneste et al., 2014). Apart from a limiting fossil record, difficulties dating the grasses have also been attributed to a slowdown in substitution rates, especially in chloroplast markers, in grasses compared to other angiosperms (Christin et al., 2014).

In recent years a series of newly discovered fossils point to Poaceae being an older lineage than previously estimated. Phytoliths and fossilized epidermal fragments from *Changii indicum*, that were found in Indian dinosaur coprolites, possess synapomorphies with

Oryzoideae (Prasad et al., 2005, 2011). These coprolites were dated to 66 Ma (cf. Iles et al., 2015). They have been considered controversial, mainly because they implied a higher age for this lineage than previously believed (Christin et al., 2014; Kellogg, 2015; Prasad et al., 2011; Spriggs et al., 2014). Subsequently the discovery of a fossil grass spikelet infected with a *Claviceps*-like fungus (Poinar Jr. et al., 2015), alongside other spikelet-like structures (Poinar Jr., 2004), from Burmese amber deposits, has pushed the age of the grasses back to at least 98–99 Ma (Shi et al., 2012). However, the fossil of the infected spikelet (Poinar Jr. et al., 2015) only calibrates the stem node of Poaceae and is no longer the oldest fossil available. Most recently, 101–113 Ma old epidermis fragments from the Zhonggou Formation of northwestern China have been convincingly assigned to crown node grasses (Wu et al., 2018) based on the existence of long-short epidermal cell patterning which is a synapomorphy of Poaceae and Joinvilleaceae (Rudall et al., 2014; Kellogg, 2000), short-cell pairs which is a synapomorphy of crown-group Poaceae (Rudall et al. 2014), and equidimensional-unlobed phytoliths which are considered ancestral in the family (Rudall et al. 2014). The age of the Zhonggou Formation is Albian, perhaps early Albian (Zheng et al., 2015). Together these newly discovered grass fossils (Poinar Jr. et al., 2015; Prasad et al., 2005, 2011; Wu et al., 2018), two of which are included in our analyses, all point to Poaceae being far older than previously assumed. A Poaceae crown node age of more than 100 Ma becomes now difficult to reject.

Did cooling climate and expansion of temperate biomes throughout the Cenozoic drive diversification in Pooideae?

We found evidence indicating that diversification rates have changed through time in Pooideae, increasing since the origin of the group until present, and possibly as a function of the temperature decrease during the Cenozoic (Fig. 1b; Tables S1.3, S1.4). The positive correlation (β>0) found between global temperature and extinction indicates that these groups diversified more during periods of global cooling compared to warmer periods. The peak in diversification rates toward the present is concurrent with the intensified global cooling trend that culminated with the Pleistocene glaciations. Pooideae might not be unique in this regard. Several radiations following the appearance of temperate biomes have been identified in other plant groups (Favre et al., 2016; Meseguer et al., 2018). The temperature dependent model was not significantly better than a constant birth-death diversification model based on the analysis of the posterior sample of trees. However, it seems unlikely that a group of almost 4000 species diversifies at a constant rate during more than 60 million years of profound environmental changes. The reduced power to select among models and to detect

diversification rate changes in our study (i.e. we obtained rather low AIC weights for the most supported models) might be associated with our relatively low sampling of taxa for this extremely species-rich group: our sampling was designed to be exhaustive at the genus level, which implies that all basal and median nodes and lineages in the tree have been sampled while the tips are under-sampled. In any case, our temperature-dependent RPANDA results are congruent with the increase in diversification rates detected by TreePar in the recent past (Table S1.3). Nonetheless, future studies with increased taxon sampling will probably help to shed light on this issue.

A likely driver of the association between cold and diversification is the availability of new niches as the temperate climates greatly expanded across the Holarctic during the mid-late Cenozoic (Eldrett et al., 2009; Liu et al., 2009; Potts & Behrensmeyer, 1992; Pound & Salzmann, 2017; Zachos et al., 2001). In addition, frost might have eliminated most of the boreotropical woody elements thus creating habitats for frost-hardy grasses and reducing competition. Particularly important would have been the reduced fitness of frost sensitive grass lineages that otherwise would have been direct competitors of Pooideae. Preadaptations to endure cold may explain the expansion of Pooideae into temperate climates and increased diversification rates as this lineage successively exploited cooler niches associated with the overall colder climates. Furthermore, higher diversification rates have been found across Poales lineages inhabiting “open” and “dry” habitats compared to lineages inhabiting “shade” and “wet” habitats (Bouchenak-Khelladi et al., 2014). For Pooideae, ancestral habitat reconstruction indicates that transitions from “closed” to “open” habitats occurred after the major tribes had diverged (Bouchenak-Khelladi et al., 2010). Thus, the potentially increased diversification rates (Fig. 1b) not only coincide with climate cooling, but also with transitions to more open habitats.

Frost tolerance and ancestral niche

We calculated the time of Pooideae origin to be 61–77 Ma, at a time when global temperatures were relatively warm and boreotropical forest elements were abundant in the Northern Hemisphere (Greenwood, Basinger, & Smith, 2010; Pross et al., 2012; Tiffney, 1985; Wolfe, 1975). Nevertheless, our reconstruction of ancestral niches (based on bioclimatic variables) indicates that ancestors of all major Pooideae lineages experienced and could withstand frosts and mild winters in a seasonal climate (Fig. 2, Figs. 3b–d). Thus, we hypothesize that Pooideae were adapted to temperate-like climates long before the expansion of temperate biomes, contrary to many other temperate plant lineages (Favre et al., 2016;

Kerkhoff et al., 2014; Meseguer et al., 2018, 2015). This hypothesis is supported by two recent studies. In a study of three Pooideae species, Zhong, Robbett, Poire, & Preston (2017) identified several gene clusters exhibiting conserved cold response, many of which had previously been characterized as ancient stress response genes. Another study found sixteen cold responsive genes that exhibited conserved expression in five distantly related Pooideae species (Schubert et al., 2019). Interestingly, most of these genes were induced in response to short-term cold, and are known to be stress-responsive in other angiosperms. Taken together, these results point to a common response to short-term cold stress among Pooideae lineages, but also to a lack of common adaptation to prolonged periods of cold.

It is however, intrinsically difficult to precisely estimate a species fundamental niche (Soberon & Arroyo-Peña, 2017). Hence, absence of a species from environments experiencing frost does not necessarily imply sensitivity to frost. Although climate is commonly considered the major determinant of species distribution, it may well be that other biotic and abiotic factors confound the link between a specific climate parameter and the fundamental niche (Soberon & Arroyo-Peña, 2017). A study of the realized niche of cold tolerance in the southern temperate grass subfamily Danthonioideae indeed underestimated the fundamental niche (Humphreys & Linder 2013). However, Humphreys & Linder (2013) also showed that species experiencing cold temperatures in their native range showed a higher survival rate in a growth experiment of overwintering capacity, indicating a close correlation between realized niche and physical tolerance to frost. In the grass family, much focus has been put on characterizing frost tolerance of the Pooideae and Danthonioideae (see eg. Sandve et al., 2011; Humphreys & Linder 2013), but less so on tropical grasses not exposed to frost in their native range. However, Ludlow (1980) shows that the resistance to frost in tropical grasses is low compared to temperate grasses and that subtropical or high elevation tropical grasses have better frost resistance than more broadly adapted tropical grasses, indicating that species in frost-free environments indeed are more sensitive to frost. Furthermore, an underestimation of the number of frost-sensitive species will not contradict our conclusion that the ancestor of Pooideae experienced frost.

Our reconstruction of ancestral (temperature) niches is based on contemporary bioclimatic data and thus corresponds to the geographic locations the taxa have been collected from (GBIF records). As noted by Grandcolas, Nattier, Legendre & Pellens (2011), such extrinsic traits can contain non-heritable components, which violate the assumptions underlying ASR. The bioclimatic variables used here are proxies for the cold stress experienced in a taxa's

realized temperature niche, which exerts strong selection pressure on plants. Cold tolerance in itself is a highly complex trait, but its constituents are heritable. Nonetheless, our ASRs of these (extrinsic) traits are not able to distinguish convergent and parallel evolution which increases the uncertainty of inferred states on ancestral nodes. The abundance of frost-experiencing taxa in all tribes suggests however, that their ancestors possessed features that allowed them to evolve cold adaptation, which is supported by the sixteen cold responsive genes shared by five distantly related Pooideae species identified by Schubert et al. (2019).

Did the Pooideae ancestor live in cold microhabitats?

Under the DEC model the Pooideae ancestor and all tribes are reconstructed with a clear ancestral Eurasian distribution (Figs. S3.1). This is in line with previous analyses of Pooideae based on a more restricted set of Pooideae lineages (Bouchenak-Khelladi et al., 2010). The early dispersals of Meliceae and Stipeae lineage into North and South America in the late Eocene and early Oligocene appear as distinct events, since almost all other dispersals took place after the early Miocene. In agreement with this result, the fossil *Stipa florissantii* documents the presence of Stipeae in North America at 34 Ma. The paradoxical early evolution of cold adaptations in a globally warm climate (Fig. 2, Figs. 3b–d) might be explained by cold microhabitats existing in the early Paleocene. One possible area for the existence of early Pooideae is high elevation habitats in mountains of the nascent Alpine orogeny in Eurasia. These mountain chains resulted from the collision of the African and Arabian plates with the European (Eurasian) plate from Late Cretaceous onwards, with major phases of mountain building from the Paleocene (Gee & Stephenson, 2006; Moores & Fairbridge, 1997; Sharkov et al., 2015). In cold microhabitats of such nascent Eurasian mountains, the early Pooideae may have evolved some crucial stress responses to cold that may have given them sufficient fitness advantage to enable diversification into the temperate niche as temperate biomes expanded throughout the Oligocene. However, this hypothesis needs to be tested in a further study. The delay of some 20 Ma from the origin of Pooideae to the intensification of its diversification at the Eocene (after 50 Ma; Fig. 1) might reflect long ecological and geographic confinement, e.g. to high-elevation sky islands. Similar delays in diversification following evolution of pre-adaptive traits have been identified in both animals (Bininda-Edmonds et al., 2007; Nel, Roques, Nel, Prokop, & Steyer, 2007) and plants (Arakaki et al., 2011; Marazzi & Sanderson, 2010), and include diversification following evolution of C_4 photosynthesis in grasses (Bouchenak-Khelladi et al., 2009; Spriggs et al., 2014).

Lineage-specific adaptations to long winters

Despite the evidence for a temperate ancestral niche (Fig. 2, Figs. 3b–d) our analyses also indicate that tolerance of more extreme temperate conditions, i.e. colder and longer winters, is not shared among the major Pooideae lineages. Coinciding with the intensification of the global cooling trend and the increased seasonality, particularly during and after the E-O transition (Eldrett et al., 2009), we observe emergence of niches with stronger seasonality (low isothermality) and more severe winters (mean temperature of the coldest quarter below 2°C, Fig. 3b) in separate lineages. A similar evolutionary history has been reconstructed for Danthonioideae, where the coldest habitats are occupied by distantly related clades (Humphreys & Linder, 2013). We suggest that complex adaptive pathways for tolerating long, severe winters, (e.g. cold acclimation and adaptations to short growing seasons) evolved independently in Pooideae lineages. Our findings corroborate recent studies of molecular evolution of cold adaptation. Although all species from distantly-related Pooideae lineages are able to cold acclimate, most of the cold responsive genes identified by Schubert et al., (2019) were differentially expressed in only one of five investigated species representing different tribes. Finally, flowering in response to vernalization is widespread in the Pooideae (McKeown, Schubert, Marcussen, Fjellheim, & Preston, 2016). In the core Pooideae, vernalization is highly regulated by the *VRN1* and *VRN2* regulon (Fjellheim et al., 2014). Although cold induction of *VRN1* was found to be an ancestral trait in the Pooideae lineage (McKeown et al., 2016), the regulatory role of *VRN2* is not conserved in the subfamily, but has been co-opted into the vernalization pathway in the core Pooideae (Woods, McKeown, Dong, Preston, & Amasino, 2016).

Conclusions

Despite an old age of 61–77 Ma, we inferred an ancestrally temperate niche with episodic frost for Pooideae. An ultimate sieve for persisting in large parts of the temperate regions is the ability to survive winter, but other characters, such as timing of flowering, growth and life history strategies would also have played central roles. Our dated phylogeny provides a rigorous framework for future testing of hypotheses regarding evolution of adaptations to temperate climate from tropical ancestors in light of climate and diversification history of Pooideae. Our study is also the first on grasses to demonstrate the usefulness of employing speciation times, estimated from the entire fossil record of the clade using PyRate, as calibration prior instead of oldest fossil. This method increases objectivity and accuracy in

molecular dating, especially for lineages with a sparse fossil record such as grasses, and should be put to use also for other grass lineages where ages are still controversial.

References

The Angiosperm Phylogeny Group, Chase, M. W., Christenhusz, M. J. M., Fay, M. F., Byng, J. W., Judd, W. S., Soltis, D. E., Mabberley, D. J., Sennikov, A. N., Soltis, P. S., Stevens, P. F. (2016). An update of the Angiosperm Phylogeny Group classification for the orders and families of flowering plants: APG IV. *Botanical Journal of the Linnean Society*, 181(1), 1–20.

Arakaki, M., Christin, P.A., Nyffeler, R., Lendel, A., Eggli, U., Ogburn, R. M., … Edwards, E. J. (2011). Contemporaneous and recent radiations of the world's major succulent plant lineages. *Proceedings of the National Academy of Sciences of the United States of America*, *108*(20), 8379–8384.

Archibald, S. B., Bossert, W. H., Greenwood, D. R., & Farrell, B. D. (2010). Seasonality, the latitudinal gradient of diversity, and Eocene insects. *Paleobiology*, *36*(03), 374–398.

Barba-Montoya, J., dos Reis, M., Schneider, H., Donoghue, P. C. J., & Yang, Z. (2018). Constraining uncertainty in the timescale of angiosperm evolution and the veracity of a Cretaceous Terrestrial Revolution. *New Phytologist*, *218*(2), 819–834.

Bell, C. D., Soltis, D. E., & Soltis, P. S. (2010). The age and diversification of the angiosperms re-revisited. *American Journal of Botany*, *97*(8), 1296–1303.

Bininda-Emonds, O. R. P., Cardillo, M., Jones, K. E., MacPhee, R. D. E., Beck, R. M. D., Grenyer, R., … Purvis, A. (2007). The delayed rise of present-day mammals. *Nature*, *446*(7135), 507–512.

Bouchenak-Khelladi, Y., Muasya, A. M., & Linder, H. P. (2014). A revised evolutionary history of Poales: Origins and diversification. *Botanical Journal of the Linnean Society*, *175*(1), 4–16.

Bouchenak-Khelladi, Y., Verboom, A. G., Savolainen, V., & Hodkinson, T. R. (2010). Biogeography of the grasses (Poaceae): a phylogenetic approach to reveal evolutionary history in geographical space and geological time. *Botanical Journal of the Linnean Society*, *162*(4), 543–557.

Bouchenak-Khelladi, Y., Verboom, G. A., Hodkinson, T. R., Salamin, N., Francois, O., Ni Chonghaile, G., & Savolainen, V. (2009). The origins and diversification of C_4 grasses and savanna-adapted ungulates. *Global Change Biology*, *15*(10), 2397–2417.

Burke, S. V, Lin, C.-S., Wysocki, W. P., Clark, L. G., & Duvall, M. R. (2016). Phylogenomics and plastome evolution of tropical forest grasses (*Leptaspis*, *Streptochaeta*: Poaceae). *Frontiers in Plant Science*, *7*, 1993.

Chamberlain, S. (2017). rgbif: Interface to the Global 'Biodiversity' Information Facility 'API.'

Christin, P.-A., Spriggs, E., Osborne, C. P., Strömberg, C. A. E., Salamin, N., & Edwards, E. J. (2014). Molecular dating, evolutionary rates, and the age of the grasses. *Systematic Biology*, *63*(2), 153–165.

Condamine, F. L., Rolland, J., & Morlon, H. (2013). Macroevolutionary perspectives to environmental change. *Ecology Letters*, *16*, 72–85.

Cook, J., Wathen, K. J., & Nguyen, H. (2013). Parametersolver v3. 0 Available from https://biostatistics. mdanderson. org/SoftwareDownload/SingleSoftware. aspx.

Darriba, D., Taboada, G. L., Doallo, R., & Posada, D. (2012). jModelTest 2: more models, new heuristics and parallel computing. *Nature Methods*, *9*(8), 772.

Donoghue, M. J. (2008). A phylogenetic perspective on the distribution of plant diversity. *Proceedings of the National Academy of Sciences*, *105*(Supplement 1), 11549–11555.

Drummond, A. J., & Rambaut, A. (2007). BEAST: Bayesian evolutionary analysis by sampling trees. *BMC Evolutionary Biology*, *7*(1), 214.

Drummond, A. J., Suchard, M. A., Xie, D., & Rambaut, A. (2012). Bayesian phylogenetics with BEAUti and the BEAST 1.7. *Molecular Biology and Evolution*, *29*(8), 1969–1973.

Edwards, E. J., & Smith, S. A. (2010). Phylogenetic analyses reveal the shady history of C_4 grasses. *Proceedings of the National Academy of Sciences*, *107*(6), 2532–2537.

Eldrett, J. S., Greenwood, D. R., Harding, I. C., & Huber, M. (2009). Increased seasonality through the Eocene to Oligocene transition in northern high latitudes. *Nature*, *459*(7249), 969–973.

Favre, A., Michalak, I., Chen, C. H., Wang, J. C., Pringle, J. S., Matuszak, S., … Muellner-Riehl, A. N. (2016). Out-of-Tibet: the spatio-temporal evolution of *Gentiana* (Gentianaceae). *Journal of Biogeography*, *43*(10), 1967–1978.

Fine, P. V. A., & Ree, R. H. (2006). Evidence for a time-integrated species-area effect on the latitudinal gradient in tree diversity. *The American Naturalist*, *168*(6), 796–804.

Fjellheim, S., Boden, S., & Trevaskis, B. (2014). The role of seasonal flowering responses in adaptation of grasses to temperate climates. *Frontiers in Plant Science*, *5*, 431.

Fritz, S. A., & Purvis, A. (2010). Selectivity in mammalian extinction risk and threat types: A new measure of phylogenetic signal strength in binary traits. *Conservation Biology*, *24*(4), 1042–1051.

Gaut, B.S., Muse, S.V., Clark, W.D., & Clegg M.T. (1992). Relative rates of nucleotide substitution of the *rbcL* locus of monocotyledonous plants. *Journal of Molecular Evolution*, *35(4)*, 292–303.

GBIF.org (19-20'th October 2016) GBIF Occurrence Download http://doi.org/10.15468/dl.obmdq7, http://doi.org/10.15468/dl.zwbz44, http://doi.org/10.15468/dl.kyz82l, http://doi.org/10.15468/dl.h6fdbn

GBIF.org (11'th January 2019) GBIF Occurrence Download https://doi.org/10.15468/dl.vzezkq

Gee, D. G., & Stephenson, R. A. (2006). European lithosphere dynamics. *Geological Society, Memoirs*, *32*(1999), 662.

Goff, S. A., Ricke, D., Lan, T. H., Presting, G., Wang, R., Dunn, M., … Briggs, S. (2002). A draft sequence of the rice genome (*Oryza sativa* L. ssp. japonica). *Science*, *296*(5565), 92–100.

Goolsby, E. W., Bruggeman, J., & Ané, C. (2017). Rphylopars : fast multivariate phylogenetic comparative methods for missing data and within-species variation. *Methods in Ecology and Evolution*, *8*(1), 22–27.

GPWG, Grass Phylogeny Working Group (2001). Phylogeny and subfamilial classification of the grasses (Poaceae). *Annals of the Missouri Botanical Garden*, *88*(3), 373–457.

Grandcolas, P., Nattier, R., Legendre, F., & Pellens, R. (2011). Mapping extrinsic traits such as extinction risks or modelled bioclimatic niches on phylogenies: does it make sense at all? *Cladistics*, *27*(2), 181-185.

Greenwood, D. R., Basinger, J. F., & Smith, R. Y. (2010). How wet was the Arctic Eocene rain forest? Estimates of precipitation from Paleogene Arctic macrofloras. *Geology*, *38*(1), 15–18.

Hartley, W. (1973). Studies on origin, evolution, and distribution of Gramineae. 5. The subfamily Festucoideae. *Australian Journal of Botany*, *21*(2), 201–234.

Hertweck, K. L., Kinney, M. S., Stuart, S. A., Maurin, O., Mathews, S., Chase, M. W., … Pires, J. C. (2015). Phylogenetics, divergence times and diversification from three genomic partitions in monocots. *Botanical Journal of the Linnean Society*, *178*(3), 375–393.

Humphreys, A. M., & Linder, H. P. (2013). Evidence for recent evolution of cold tolerance in grasses suggests current distribution is not limited by (low) temperature. *New Phytologist*, *198*(4), 1261–1273.

Iles, W. J. D., Smith, S. Y., Gandolfo, M. A., & Graham, S. W. (2015). Monocot fossils suitable for molecular dating analyses. *Botanical Journal of the Linnean Society*, *178*(3), 346-374.

Kellogg, E. A. 2000. The grasses: a case study in macroevolution. *Annual Review in Ecology and Systematics*, 31(1), 217–38.

Kellogg, E. A. (2001). Evolutionary History of the Grasses. *Plant Physiology*, *125*(3), 1198–1205.

Kellogg, E. A. (2015). Fossil record and rates of diversification. In *The families and genera of vascular plants, vol 13. flowering plants monocots* (pp. 103–107). Cham: Springer International Publishing.

Kerkhoff, A. J., Moriarty, P. E., & Weiser, M. D. (2014). The latitudinal species richness gradient in New World woody angiosperms is consistent with the tropical conservatism hypothesis. *Proceedings of the National Academy of Sciences*, *111*(22), 8125–8130.

Liu, Z., Pagani, M., Zinniker, D., Deconto, R., Huber, M., Brinkhuis, H., … Pearson, A. (2009). Global cooling during the Eocene-Oligocene climate transition. *Science*, *323*(5918), 1187–1190.

Magallón, S. (2010). Using Fossils to Break Long Branches in Molecular Dating: A Comparison of Relaxed Clocks Applied to the Origin of Angiosperms. *Systematic Biology*, *59*(4), 384–399.

Magallón, S., Gómez-Acevedo, S., Sánchez-Reyes, L. L., & Hernández-Hernández, T. (2015). A metacalibrated time-tree documents the early rise of flowering plant phylogenetic diversity. *New Phytologist*, *207*(2), 437–453.

Magallón, S., Hilu, K. W., & Quandt, D. (2013). Land plant evolutionary timeline: Gene effects are secondary to fossil constraints in relaxed clock estimation of age and substitution rates. *American Journal of Botany*, *100*(3), 556–573.

Marazzi, B., & Sanderson, M. J. (2010). Large-scale patterns of diversification in the widespread legume genus senna and the evolutionary role of extrafloral nectaries. *Evolution*, *64*(12), 3570–3592.

Marcussen, T., Heier, L., Brysting, A. K., Oxelman, B., Jakobsen, K. S. (2015). From gene trees to a dated allopolyploid network: insights from the Angiosperm genus *Viola* (Violaceae). Systematic Biology, 64(1), 84–101.

Marcussen, T., Sandve, S. R., Heier, L., Spannagl, M., Pfeifer, M., Jakobsen, K. S., … Olsen, O.-A. (2014). Ancient hybridizations among the ancestral genomes of bread wheat. *Science*, *345*(6194), 1250092.

McKeown, M., Schubert, M., Marcussen, T., Fjellheim, S., & Preston, J. C. (2016). Evidence for an early origin of vernalization responsiveness in temperate Pooideae grasses. *Plant Physiology*, *172*(1), 416–426.

Meseguer, A. S., Lobo, J. M., Cornuault, J., Beerling, D., Ruhfel, B. R., Davis, C. C., … Sanmartín, I. (2018). Reconstructing deep-time palaeoclimate legacies in the clusioid Malpighiales unveils their role in the evolution and extinction of the boreotropical flora. *Global Ecology and Biogeography*, *27*(5), 616-628.

Meseguer, A. S., Lobo, J. M., Ree, R., Beerling, D. J., & Sanmartín, I. (2015). Integrating fossils, phylogenies, and niche models into biogeography to reveal ancient evolutionary history: The case of *Hypericum* (Hypericaceae). *Systematic Biology*, *64*(2), 215–232.

Moores, E. M., & Fairbridge, R. W. (1997). *Encyclopedia of European and Asian Regional Geology*. London: Chapman & Hall.

Morley, R. J. (2000). *Origin and evolution of tropical rain forests.* Chichester: John Wiley & Sons.

Morlon, H., Lewitus, E., Condamine, F. L., Manceau, M., Clavel, J., & Drury, J. (2016). RPANDA: An R package for macroevolutionary analyses on phylogenetic trees. *Methods in Ecology and Evolution*, *7*(5), 589–597.

Mudelsee, M., Bickert, T., Lear, C. H., & Lohmann, G. (2014). Cenozoic climate changes: A review based on time series analysis of marine benthic δ 18 O records. *Reviews of Geophysics*, *52*(3), 333–374.

Near, T. J., Dornburg, A., Kuhn, K. L., Eastman, J. T., Pennington, J. N., Patarnello, T., … Jones, C. D. (2012). Ancient climate change, antifreeze, and the evolutionary diversification of Antarctic fishes. *Proceedings of the National Academy of Sciences*, *109*(9), 3434–3439.

Nel, A., Roques, P., Nel, P., Prokop, J., & Steyer, J. S. (2007). The earliest holometabolous insect from the Carboniferous: A “crucial” innovation with delayed success (Insecta Protomeropina Protomeropidae). *Annales de La Societe Entomologique de France*, *43*(3), 349–355.

Orme, D. (2013). The caper package : comparative analysis of phylogenetics and evolution in R. *R Package Version 0.5*, *2*, 1–36.

Pagel, M. (1999). Inferring the historical patterns of biological evolution. *Nature*, *401*(6756), 877–884.

Paterson, A. H., Bowers, J. E., & Chapman, B. A. (2004). Ancient polyploidization predating divergence of the cereals, and its consequences for comparative genomics. *Proceedings of the National Academy of Sciences*, *101*(26), 9903–9908.

Poinar Jr., G. O. (2004). *Programinis burmitis* gen. et sp. nov., and *P. laminatus* sp. nov., Early Cretaceous grass-like monocots in Burmese amber. *Australian Systematic Botany*, *17*(5), 497–504.

Poinar Jr., G. O., Alderman, S., & Wunderlich, J. (2015). One hundred million year old ergot : psychotropic compounds in the Cretaceous ? *Paleodiversity*, *8*(December), 13–19.

Potts, R., & Behrensmeyer, A. (1992). Late Cenozoic terrestrial ecosystems. In A. K. Behrensmeyer, J. D. Damuth, W. A. DiMichele, R. Potts, H.-D. Sues, & S. L. Wing (Eds.), *Terrestrial ecosystems through time: evolutionary paleoecology of terrestrial plants and animals* (1st ed., pp. 419–451). Chicago: The University of Chicago Press.

Pound, M. J., & Salzmann, U. (2017). Heterogeneity in global vegetation and terrestrial climate change during the late Eocene to early Oligocene transition. *Scientific Reports*, *7*, 43386.

Prasad, V., Strömberg, C. A. E., Alimohammadian, H., & Sahni, A. (2005). Dinosaur coprolites and the early evolution of grasses and grazers. *Science*, *310*(5751), 1177–1180.

Prasad, V., Strömberg, C. A. E., Leaché, A. D., Samant, B., Patnaik, R., Tang, L., … Sahni, A. (2011). Late Cretaceous origin of the rice tribe provides evidence for early diversification in Poaceae. *Nature Communications*, (2), 480.

Preston, J. C., & Sandve, S. R. (2013). Adaptation to seasonality and the winter freeze. *Frontiers in Plant Science*, *4*, 167.

Pross, J., Contreras, L., Bijl, P. K., Greenwood, D. R., Bohaty, S. M., Schouten, S., … Yamane, M. (2012). Persistent near-tropical warmth on the Antarctic continent during the early Eocene epoch. *Nature*, *488*(7409), 73–77.

Rambaut, A., Suchard, M., & Drummond, A. J. (2013). Tracer v1.6. Available from http://tree.bio.ed.ac.uk/software/tracer/.

Ree, R. H., Moore, B. R., Webb, C. O., & Donoghue, M. J. (2005). A likelihood framework for inferring the evolution of geographic range on phylogenetic trees. *Evolution*. John Wiley & Sons, Ltd (10.1111).

Ree, R. H., & Smith, S. A. (2008). Maximum likelihood inference of geographic range evolution by dispersal, local extinction, and cladogenesis. *Systematic Biology*, *57*(1), 4–14.

Revell, L. J. (2012). phytools: An R package for phylogenetic comparative biology (and other things). *Methods in Ecology and Evolution*, *3*(2), 217–223.

Rudall, P., Prychid, C., & Gregory, T. (2014). Epidermal patterning and silica phytoliths in grasses: an evolutionary history. *Botanical Review*, 80(1), 59–71.

Sandve, S. R., Kosmala, A., Rudi, H., Fjellheim, S., Rapacz, M., Yamada, T., & Rognli, O. A. (2011). Molecular mechanisms underlying frost tolerance in perennial grasses adapted to cold climates. *Plant Science*, *180*(1), 69–77.

Schlueter, J. A., Dixon, P., Granger, C., Grant, D., Clark, L., Doyle, J. J., & Shoemaker, R. C. (2004). Mining EST databases to resolve evolutionary events in major crop species. *Genome*, *47*(5), 868–876.

Schubert, M., Grønvold, L., Sandve, S,. Hvidsten T. R., Fjellheim, S. (2019). Evolution of cold acclimation and its role in niche transition in the temperate grass subfamily Pooideae. *Plant Physiology*, DOI: 10.1104/pp.18.01448

Sharkov, E., Lebedev, V., Chugaev, A., Zabarinskaya, L., Rodnikov, A., Sergeeva, N., & Safonova, I. (2015). The Caucasian-Arabian segment of the Alpine-Himalayan collisional belt: Geology, volcanism and neotectonics. *Geoscience Frontiers*, *6*(4), 513–522.

Shi, G., Grimaldi, D. A., Harlow, G. E., Wang, J. J., Wang, J. J., Yang, M., … Li, X. (2012). Age constraint on Burmese amber based on U-Pb dating of zircons. *Cretaceous Research*, *37*, 155–163.

Soberon, J., & Arroyo-Peña, B. (2017). Are fundamental niches larger than the realized? Testing a 50-year-old prediction by Hutchinson. *PLoS ONE*, *12*(4), e0175138.

Silvestro, D., Cascales-Miñana, B., Bacon, C. D., & Antonelli, A. (2015). Revisiting the origin and diversification of vascular plants through a comprehensive Bayesian analysis of the fossil record. *New Phytologist*, *207*(2), 425–436.

Silvestro, D., Schnitzler, J., Liow, L. H., Antonelli, A., & Salamin, N. (2014). Bayesian estimation of speciation and extinction from incomplete fossil occurrence data. *Systematic Biology*, *63*(3), 349–367.

Soreng, R. J., & Davis, J. I. (1998). Phylogenetics and character evolution in the grass family (Poaceae): Simultaneous analysis of morphological and Chloroplast DNA restriction site character sets. *The Botanical Review*, *64*(1), 1–85.

Soreng, R. J., Peterson, P. M., Romaschenko, K., Davidse, G., Teisher, J. K., Clark, L. G., … Zuloaga, F. O. (2017). A worldwide phylogenetic classification of the Poaceae (Gramineae) II: An update and a comparison of two 2015 classifications. *Journal of Systematics and Evolution, 55(4), 259–290.*

Spriggs, E. L., Christin, P. A., & Edwards, E. J. (2014). C_4 photosynthesis promoted species diversification during the miocene grassland expansion. *PLoS ONE*, *9*(5), e97722.

Stadler, T. (2011). TreePar in R - Estimating diversification rates in phylogenies. Available from http://cran.r-project.org/web/packages/TreePar/index.html.

Stevens, P. F. (2001 onwards). *Angiosperm Phylogeny Website*. Version 14, July 2017

Strömberg, C. A. E. (2005). Decoupled taxonomic radiation and ecological expansion of open-habitat grasses in the Cenozoic of North America. *Proceedings of the National Academy of Sciences*, *102*(34), 11980–11984.

Strömberg, C. A. E. (2011). Evolution of grasses and grassland ecosystems. *Annual Review of Earth and Planetary Sciences*, *39*(1), 517–544.

Strömberg, C. A. E., & McInerney, F. A. (2011). The Neogene transition from C_3 to C_4 grasslands in North America: assemblage analysis of fossil phytoliths. *Paleobiology*, *37*(01), 50–71.

The International Brachypodium Initiative. (2010). Genome sequencing and analysis of the model grass *Brachypodium distachyon*. *Nature*, *463*(7282), 763–768.

Thomasson, J. R. (1988). Fossil grasses: 1820–1986 and beyond. In *International Symposium on Grass Systematics and Evolution, Washington, DC (USA), 27–31 Jul 1986*.

Tiffney, B. H. (1985). The Eocene North Atlantic land bridge : Its importance in Tertiary and modern phytogeography of the northern hemisphere. *Journal of the Arnold Arboretum*, *66*(2), 243–273.

Töpel, M., Zizka, A., Calió, M. F., Scharn, R., Silvestro, D., & Antonelli, A. (2016). SpeciesGeoCoder: Fast categorization of species occurrences for analyses of biodiversity, biogeography, ecology, and evolution. *Systematic Biology*, *66*(2), 145–151.

Vanneste, K., Maere, S., & Van de Peer, Y. (2014). Tangled up in two: a burst of genome duplications at the end of the Cretaceous and the consequences for plant evolution. *Philosophical Transactions of the Royal Society B: Biological Sciences*, *369*(1648), 20130353.

Veizer, J., & Prokoph, A. (2015). Temperatures and oxygen isotopic composition of Phanerozoic oceans. *Earth-Science Reviews*, *146*, 92-104.

Vicentini, A., Barber, J. C., Aliscioni, S. S., Giussani, L. M., & Kellogg, E. A. (2008). The age of the grasses and clusters of origins of C_4 photosynthesis. *Global Change Biology*, *14*(12), 2963–2977.

Visser, V., Clayton, W. D., Simpson, D. A., Freckleton, R. P., & Osborne, C. P. (2014). Mechanisms driving an unusual latitudinal diversity gradient for grasses. *Global Ecology and Biogeography*, *23*(1), 61–75.

Wang, X., Wang, J., Jin, D., Guo, H., Lee, T. H., Liu, T., & Paterson, A. H. (2015). Genome alignment spanning major poaceae lineages reveals heterogeneous evolutionary rates and alters inferred dates for key evolutionary events. *Molecular Plant*, *8*(6), 885–898.

Wolfe, J. A. (1975). Some aspects of plant geography of the Northern Hemisphere during the late Cretaceous and Tertiary. *Annals of the Missouri Botanical Garden*, *62*(2), 264.

Woods, D. P., McKeown, M. A., Dong, Y., Preston, J. C., & Amasino, R. M. (2016). Evolution of *VRN2/Ghd7*-like genes in vernalization-mediated repression of grass flowering. *Plant Physiology*, *170*(4), 2124–2135.

Wu, Y., You, H.-L., & Li, X.-Q. (2018). Dinosaur-associated Poaceae epidermis and phytoliths from the Early Cretaceous of China. *National Science Review*.

Zachos, J. C., Dickens, G. R., & Zeebe, R. E. (2008). An early Cenozoic perspective on greenhouse warming and carbon-cycle dynamics. *Nature*, *451*(January), 279–283.

Zachos, J., Pagani, M., Sloan, L., Thomas, E., & Billups, K. (2001). Trends, rhythms, and aberrations in global climate 65 Ma to present. *Science*, *292*(5517), 686–693.

Zheng, D., Zhang, H., Zhang, Q., Li, Q., Wang, H., Fang, Y., Liu, Q., Jarzembowsky, E. A., Yan, E., & Wang, B. 2015. The discovery of an Early Cretaceous dragonfly *Hemeroscopus baissicus* Pritykina, 1977 (Hemeroscopidae) in Jiuquan, Northwest China, and its stratigraphic implications. *Cretaceous Research*, *52*(B),: 316-322.

Zhong, J., Robbett, M., Poire, A., & Preston, J. C. (2018~~7~~). Successive evolutionary steps drove Pooideae grasses from tropical to temperate regions. *New Phytologist*, *217*(2), 925–938.

Data accessibility All data used in this manuscript are presented in the manuscript and its supplementary material or have been previously published or archived elsewhere.

Tables

Table 1 Calibrations used for the dating analysis of Pooideae including secondary calibrations derived from an initial dating analysis of Poaceae (for justifications see Appendix 2).

		Posterior estimate from PyRate					Calibration priors for Pooideae BEAST analysis			
Node	**Fossil**	**mean**	**variance**	**0.025Q**	**0.975Q**		**type**	**offset**	**mean**	**stdev**
Pooideae: *Hesperostipa* stem	*Berriochloa* spp.	30.746	11.740	26.022	37.377	→	logN	26	1.348	0.648
Pooideae: narrow-leaved Loliineae stem	*Festuca* cf. *capillata*	27.352	96.976	16.252	45.084	→	logN	16	2.149	0.749
Pooideae: *Lygeum* stem	*Lygeum* sp.	19.945	10.441	16.000	26.302		exp	16	50	.
Pooideae: *Nassella* stem	*Nassella* spp.	17.590	67.934	8.020	34.234	→	logN	8	1.984	0.744
Pooideae: *Piptatheropsis* stem	*Paleoeriocoma hitchcockii*	17.166	54.198	8.053	31.864	→	logN	8	1.967	0.706
Pooideae: Stipeae stem	*Stipa florissantii*	.	.	.	.		exp	34	50	.
Bambusoideae: *Chusquea* stem	Bambusoideae cf. *Chusquea*	.	.	.	.		exp	33.9	10	.
Oryzoideae: *Leersia* stem	*Leersia seifhennersdorfensis*	.	.	.	.		exp	30.7	10	.
Oryzoideae crown	*Changii indicum*	.	.	.	.		exp	66	10	.
Pharoideae crown	*Pharus primuncinatus*	.	.	.	.		exp	15	10	.
Poaceae crown	Poaceae sp.	.	.	.	.		exp	101	10	.
root	secondary calibration	.	.	.	.		exp + U(101,144)	101	11	.
Oryzeae stem	*Changii indicum*	.	.	.	.		exp	66	10	.
Chusquea stem	*Bambusoideae cf. Chusquea*	.	.	.	.		exp	33.9	10	.
Leersia stem	*Leersia seifhennersdorfensis*	.	.	.	.		exp	30.7	10	.

→, arrows link posterior estimates in initial analysis with priors in the Pooideae dating analysis; exp, exponential distribution; N, normal distribution; logN, log-normal distribution; U, uniform distribution; offset, youngest possible node age.

Table 2 Estimated node ages for Pooideae (rows 1-10) and other Poaceae clades (rows 11-16) obtained by fossil-calibrated dating analyses.

		Stem node age (Ma)				**Crown node age (Ma)**			
	Taxon/clade	mean	stdev	0.025Q	0.975Q	mean	stdev	0.025Q	0.975Q
1	Aveneae	44.3	3.2	38.1	50.8	35.6	3.3	28.8	41.8
2	Poeae	44.3	3.2	38.1	50.8	38.5	3.1	32.4	44.5
3	Triticeae	49.0	3.5	42.3	55.9	37.0	4.2	29.4	45.9
4	Brachypodieae	51.8	3.5	44.8	58.6	18.9	4.7	10.1	28.5
5	Diarrheneae	53.9	3.6	47.1	61.3	13.5	7.0	2.2	29.8
6	Meliceae	57.9	3.8	50.8	65.6	45.6	5.0	35.8	55.4
7	Stipeae	59.6	3.8	52.1	67.0	38.6	4.3	30.6	47.3
8	Duthieae	60.9	3.9	52.9	68.0	30.1	7.9	16.7	47.8
9	Lygeeae+Nardeae	65.5	4.0	57.8	73.5	32.1	8.0	16.4	47.8
10	Pooideae	73.7	3.9	66.0	81.3	68.7	4.0	60.9	76.7
11	BOP clade	80.2	4.0	72.9	88.4	77.8	3.8	70.3	85.3
12	PACMAD clade	80.2	4.0	72.9	88.4	55.1	6.9	41.6	68.8
13	Puelioideae	84.8	4.1	76.8	93.0	51.6	17.7	16.5	85.7
14	Pharoideae	93.9	4.3	86.0	102.8	25.0*	5.9*	15.0*	38.2*
15	Anomochlooideae**	105.1*	2.9*	101.0*	112.4*	n/a**	n/a**	n/a**	n/a**
16	Poaceae	120.8	6.2	108.9	133.2	105.1*	0.6*	101.0*	112.4*

0.025Q, 0.025 quantile of the highest probability density (HPD) interval; 0.975Q: 0.975 quantile of the HPD interval; stdev: standard deviation; *: fossil-calibrated nodes; **: non-monophyletic for the chloroplast.

Figures

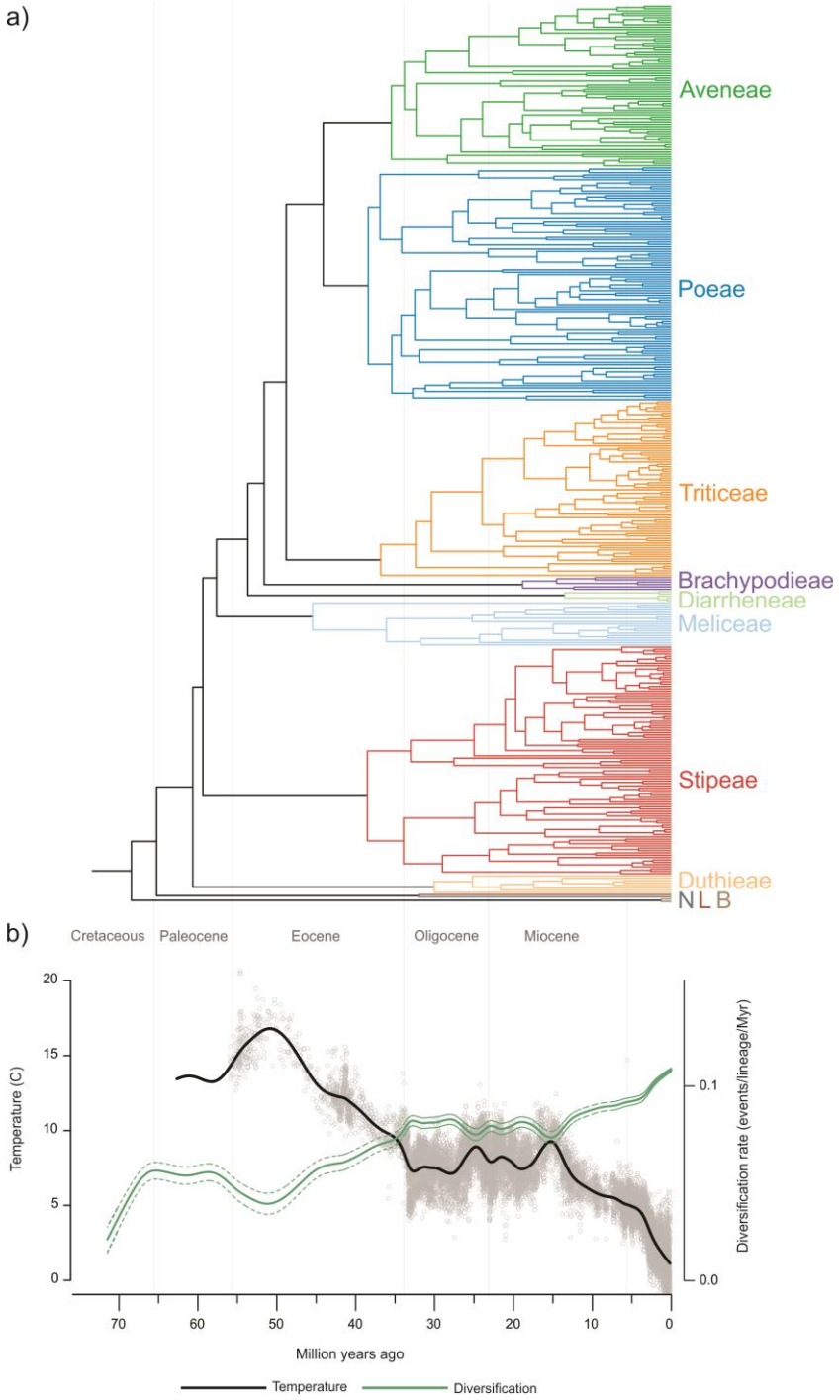

Figure 1 Fossil calibrated Pooideae phylogeny and historic diversification rates. a) Time-tree for Pooideae based on cpDNA sequences (*matK*, *ndhF*, *rbcL*) for 396 species, fossil-calibrated at six internal Pooideae nodes. Pooideae tribes are colour-coded and indicated with name. b) Paleotemperature-dependent diversification model: diversification rates in Pooideae (in green) increase with the decreasing global temperatures (in black). The temperature is represented by the global mean temperature curve from the Paleocene to the present, modified from Zachos et al. (2008). The temperature curve should be treated with care since it is computed on the assumption of an ice-free ocean (see Zachos et al. (2008) for details). Dashed green lines represent confidence intervals of the estimated values from 100 trees randomly selected from the posterior distribution.

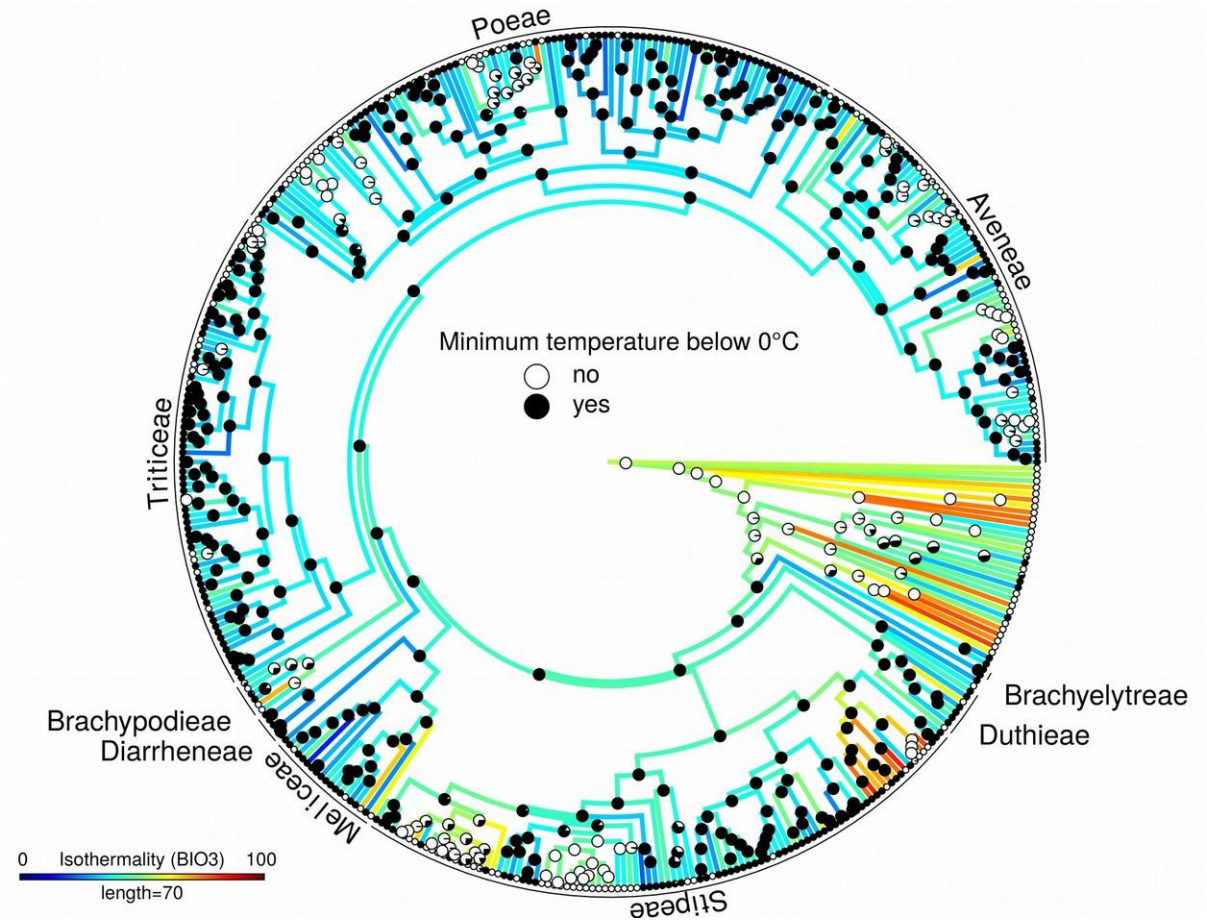

Figure 2 Experience of frost in ancestral Pooideae lineages. The ancestral reconstruction of the minimum temperature of the coldest month (BIO6) as a binary character (below 0°C no/yes) reveals a high probability of frost-experiencing ancestral Pooideae lineages. The posterior probabilities of the ancestral states are plotted as pie chart diagrams onto the dated phylogeny. Branch colours correspond to reconstructed ancestral values for isothermality (BIO11) shown on the scale bar.

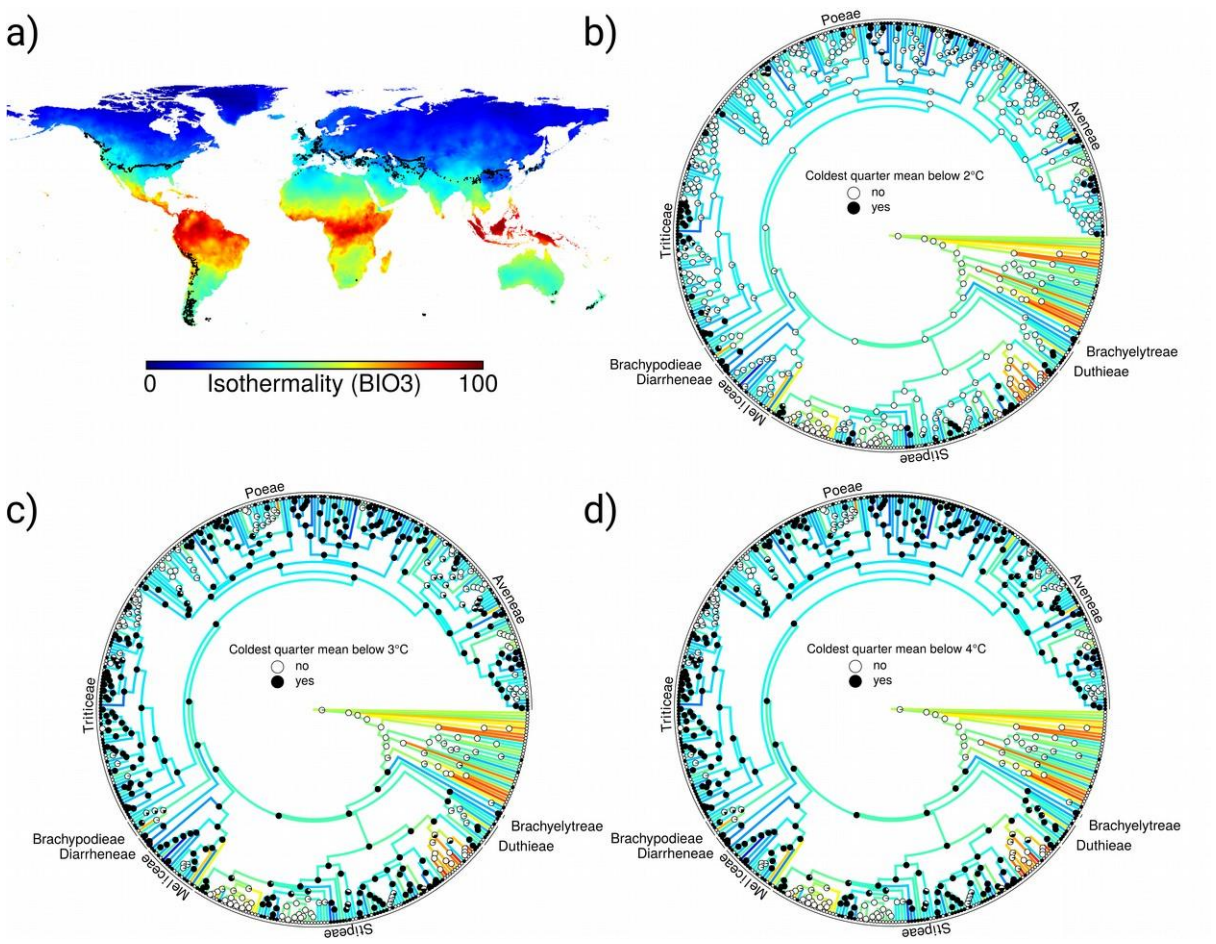

Figure 3 Temperature seasonality and winter severity in ancestral Pooideae lineages. For comparability, global distribution of isothermality values are plotted as color gradient on a contemporary world map a). The scale bar indicates the respective links between color and isothermality value. Black dots in the map indicate coordinates where the mean temperature of the coldest quarter is exactly 2°C. The ancestral reconstructions of the mean temperature of the coldest quarter (BIO11) as three binary characters (below or not below 2°C, 3°C and 4°C shown in b), c) and d) respectively) reveals that Pooideae ancestors likely experienced mild winters with grand mean temperatures below 3°C, but not below 2°C. The posterior probabilities of the binary ancestral states are plotted as pie chart diagrams onto nodes of the dated phylogeny. Branch colors correspond to reconstructed isothermality (BIO3) values.

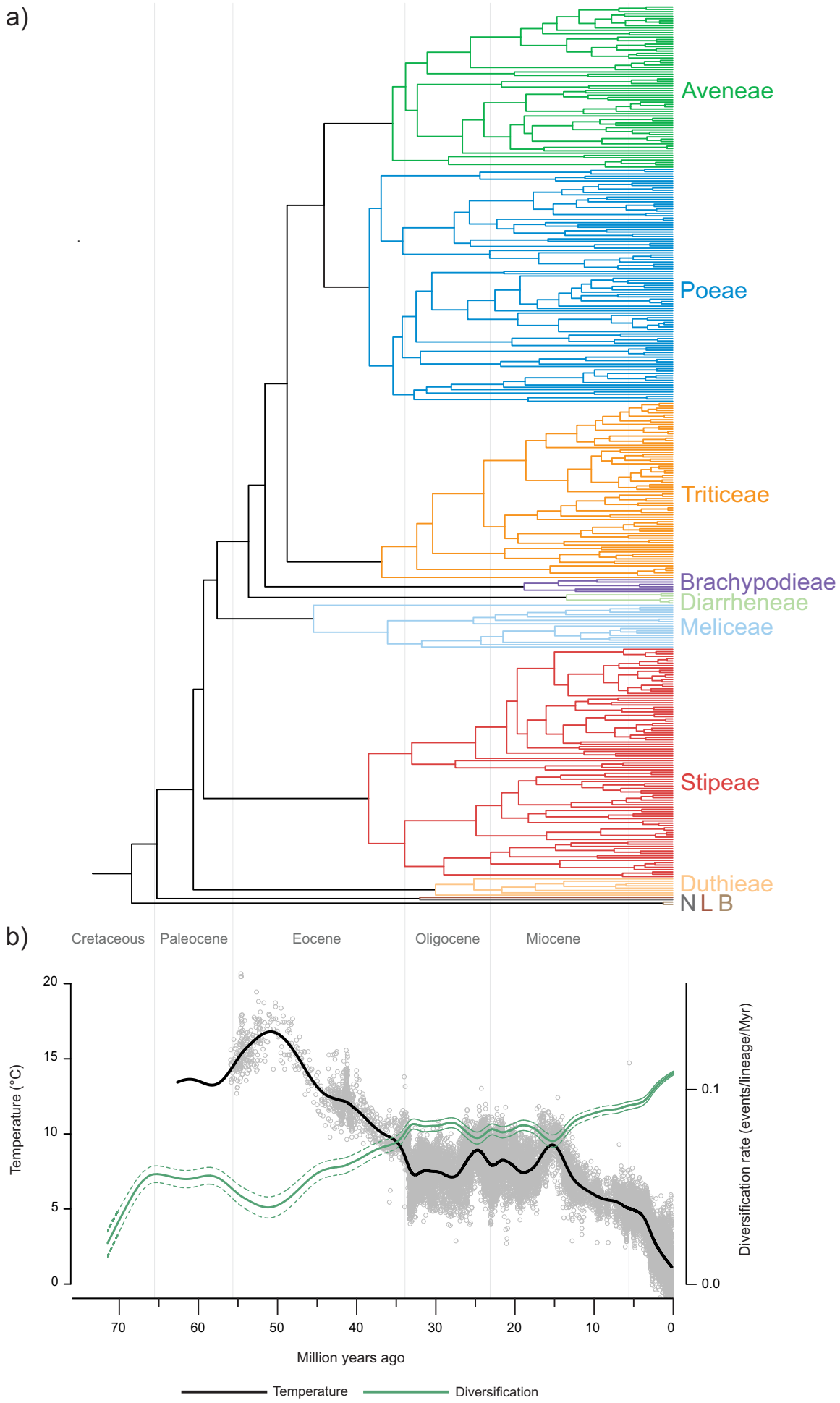
a)
Aveneae
Poeae
Triticeae
Brachypodieae
Diarrheneae
Meliceae
Stipeae
Duthieae
N L B
b)
Cretaceous
Paleocene
Eocene
Oligocene
Miocene
Temperature (°C)
20
15
10
5
0
Diversification rate (events/lineage/Myr)
0.1
0.0
70
60
50
40
30
20
10
0
Million years ago
Temperature
Diversification

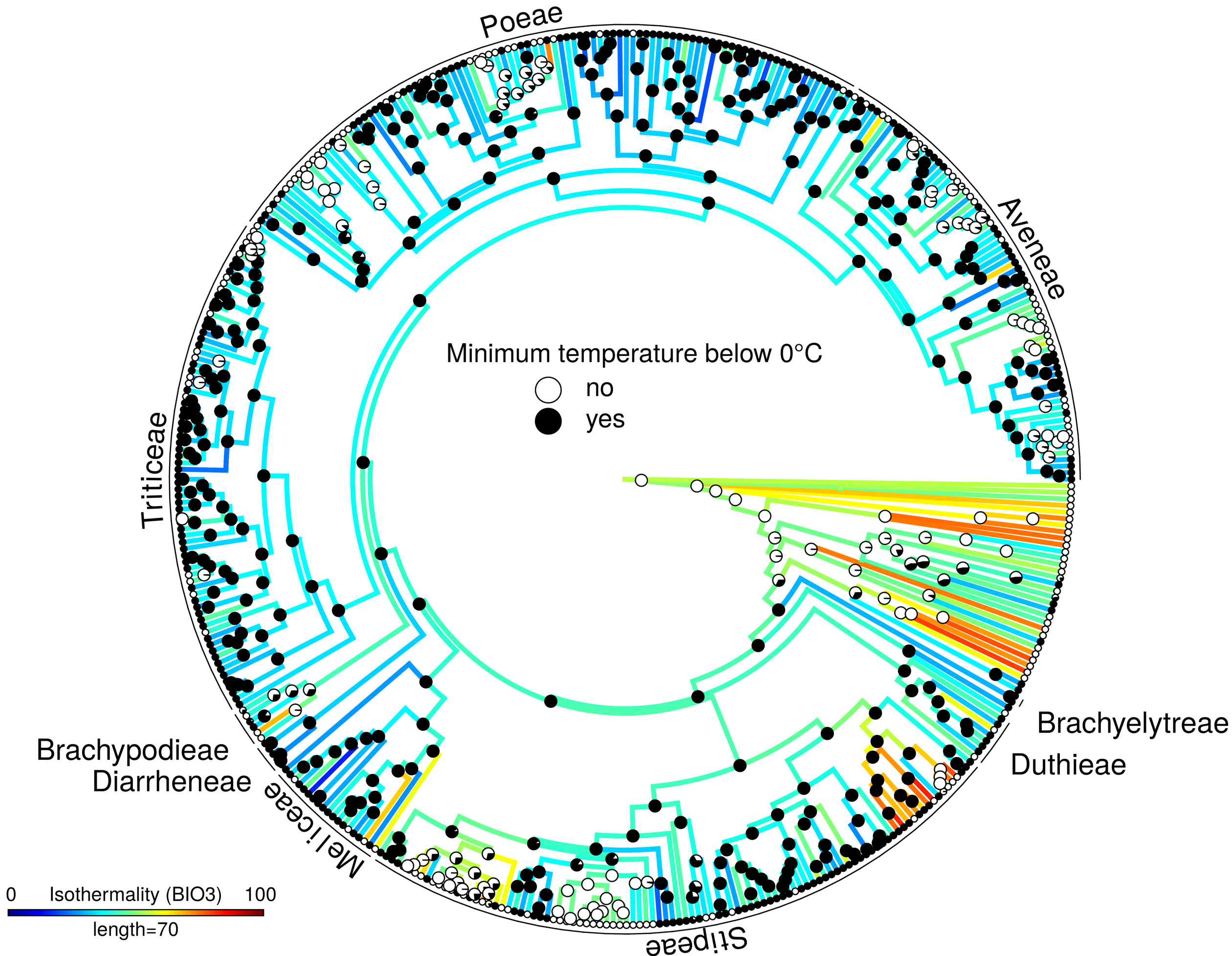
Poeae
Aveneae
Triticeae
Brachypodieae
Diarrheneae
Meliceae
Stipeae
Brachyelytreae
Duthieae
Minimum temperature below 0°C
no
yes
0
Isothermality (BIO3)
100
length=70

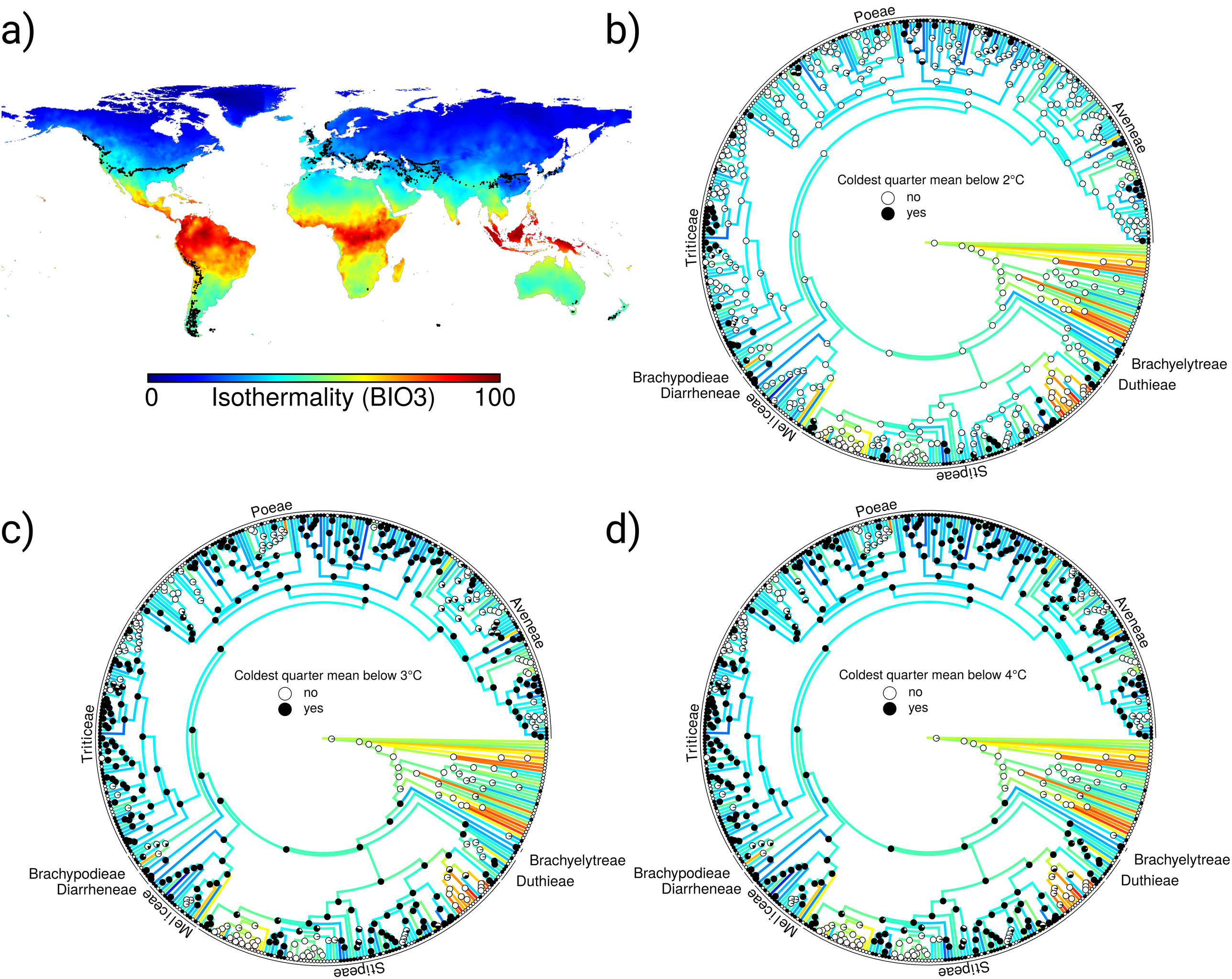
a)
0
Isothermality (BIO3)
100
b)
Poeae
Aveneae
Triticeae
Brachypodieae
Diarrheneae
Meliceae
Stipeae
Brachyelytreae
Duthieae
Coldest quarter mean below 2°C
no
yes
c)
Coldest quarter mean below 3°C
no
yes
d)
Coldest quarter mean below 4°C
no
yes

Appendix 1 – Supporting tables

Table S 1.1 Sampled species, their taxonomic affinities (clade) and GenBank accession numbers for the three chloroplast regions matK, ndhF and rbcL. Clade name abbreviations: AVE = Aveneae; BRA = Brachypodieae; BRY = Brachyelytreae; DIA = Diarrheneae; DUT = Duthieae; LYG = Lygeeae; MEL = Meliceae; NAR = Nardeae; POE = Poeae; STI = Stipeae; TRI = Triticeae; xARI = subfam. Aristidoideae; xARU = subfam. Arundinoideae; xBAM = subfam. Bambusoideae; xCHL = subfam. Chloridioideae; xDAN = subfam. Danthonioideae; xMIC = subfam. Micrairoideae; xORY = subfam. Oryzoideae; xPAN = subfam. Panicoideae; xPUE = subfam. Puelioideae; xPHA = subfam. Pharoideae; xANO = subfam. Anomochlooideae; xECD = Ecdeiocoleaceae; xJOI = Joinvilleaceae; xFLA = Flagellariaceae.

Clade	Species	matK	ndhF	rbcL
AVE	*Agrostis canina*	FJ231115	**MH888123***	JN893786
AVE	*Agrostis capillaris*	FJ231112	JX438119	AY395527
AVE	*Agrostis stolonifera*	EF115543	EF115543	EF115543
AVE	*Agrostis tenerrima*	DQ786877	DQ786805	n/a
AVE	*Agrostis vinealis*	FJ231113	n/a	JN893785
AVE	*Ammophila arenaria*	AM234561	JX438118	JN890705
AVE	*Ammophila breviligulata*	KM974730	KM974730	KM974730
AVE	*Amphibromus scabrivalvis*	DQ786882	DQ786810	n/a
AVE	*Anthoxanthum arcticum*	KC474036	n/a	JN965581
AVE	*Anthoxanthum monticola*	KC474042	n/a	JN965577
AVE	*Anthoxanthum nitens*	KM974740	KM974740	KM974740
AVE	*Anthoxanthum nivale*	LN906649	LN908047	LN907884
AVE	*Anthoxanthum odoratum*	KM974732	KM974732	KM974732
AVE	*Arrhenatherum elatius*	**MH888098**	**MH888124**	**MH888150**
AVE	*Avellinia michelii*	JX438079	JX438131	n/a
AVE	*Avena barbata*	GU367267	KJ529441	HM849803
AVE	*Avena canariensis*	EU833843	n/a	n/a
AVE	*Avena clauda*	EU833844	n/a	n/a
AVE	*Avena fatua*	GU367282	AFU71018	AJ746257
AVE	*Avena sativa*	KM974733	KM974733	KM974733
AVE	*Avena sterilis*	EU833858	JX438124	HE963347
AVE	*Briza maxima*	KM974736	KM974736	KM974736
AVE	*Briza media*	AM234610	n/a	AJ746285
AVE	*Briza minor*	DQ786892	DQ786820	HQ600461
AVE	*Calamagrostis arundinacea*	DQ786895	DQ786823	HQ600475
AVE	*Calamagrostis canadensis*	DQ786896	DQ786824	JN965311
AVE	*Calamagrostis canescens*	**MH888099**	**MH888125**	**MH888151**
AVE	*Calamagrostis epigeios*	EF137489	KM538738	HQ600473

AVE	*Calamagrostis stricta*	KC474256	n/a	JN965322
AVE	*Calotheca brizoides*	DQ786897	DQ786825	n/a
AVE	*Chascolytrum koelerioides*	DQ786918	DQ786846	n/a
AVE	*Chascolytrum subaristatum*	AM234608	DQ786827	KJ599180
AVE	*Dichelachne crinita*	HE574411	HE573529	HE573309
AVE	*Dichelachne micrantha*	DQ786906	DQ786834	n/a
AVE	*Dichelachne rara*	HE574416	HE573535	KT626691
AVE	*Echinopogon caespitosus*	HE574414	DQ786837	HE573310
AVE	*Echinopogon ovatus*	HE574419	HE573533	HE573312
AVE	*Gastridium ventricosum*	FN908056	DQ786842	FN870392
AVE	*Gaudinia coarctata*	FN908057	HE575741	FN870393
AVE	*Gaudinia fragilis*	DQ786915	DQ786843	HM850023
AVE	*Gaudinia hispanica*	DQ786916	DQ786844	n/a
AVE	*Graphephorum wolfii*	DQ786917	DQ786845	n/a
AVE	*Helictotrichon bromoides*	JX438087	JX438142	n/a
AVE	*Helictotrichon convolutum*	AM234557	DQ786847	n/a
AVE	*Helictotrichon longifolium*	AM234565	JX438127	n/a
AVE	*Helictotrichon mortonianum*	DQ786920	DQ786848	n/a
AVE	*Koeleria albida*	DQ786930	DQ786858	n/a
AVE	*Koeleria macrantha*	**MH888100**	**MH888126**	**MH888152**
AVE	*Koeleria vallesiana*	JX438077	JX438129	KF997263
AVE	*Lachnagrostis filiformis*	HE574415	HE573534	HE573287
AVE	*Lagurus ovatus*	FN908059	HE575743	FN870395
AVE	*Phalaris arundinacea*	KM974746	KM974746	KM974746
AVE	*Phalaris brachystachys*	HM850514	n/a	HM850250
AVE	*Phalaris canariensis*	JX438068	JX438117	n/a
AVE	*Phalaris coerulescens*	FN908066	HE575745	FN870402
AVE	*Podagrostis thurberiana*	DQ786936	DQ786864	n/a
AVE	*Polypogon fugax*	HE586077	HE575766	HE575815
AVE	*Polypogon maritimus*	JX438071	JX438122	n/a
AVE	*Polypogon monspeliensis*	DQ146822	DQ786865	HM850275
AVE	*Polypogon viridis*	DQ146824	**MH888127**	HM850276
AVE	*Rostraria azorica*	FN908070	HE575748	FN870406
AVE	*Rostraria cristata*	AM234670	JX438130	HM850311
AVE	*Rostraria pubescens*	DQ786939	DQ786867	n/a
AVE	*Torreyochloa pallida*	KM974752	KM974752	KM974752
AVE	*Triplachne nitens*	DQ786945	DQ786873	n/a
AVE	*Trisetum bifidum*	KF713172	KM538774	HQ600451

AVE	*Trisetum cernuum*	KM974753	KM974753	KM974753
AVE	*Trisetum flavescens*	**MH888101**	**MH888128**	**MH888153**
AVE	*Trisetum loeflingianum*	JX438076	JX438128	n/a
AVE	*Trisetum spicatum*	KC476082	n/a	JN966054
BRA	*Brachypodium boissieri*	JX438065	JX438113	n/a
BRA	*Brachypodium distachyon*	EU325680	EU325680	EU325680
BRA	*Brachypodium madagascariense*	LN906667	LN908065	LN907902
BRA	*Brachypodium mexicanum*	n/a	U71044	n/a
BRA	*Brachypodium pinnatum*	HE573928	AM849133	AM849347
BRA	*Brachypodium stacei*	KJ529317	KJ529429	n/a
BRY	*Brachyelytrum aristosum*	KM974735	KM974735	KM974735
BRY	*Brachyelytrum erectum*	AM234584	GU222731	AY622888
DIA	*Diarrhena americana*	KX601226	**MH888129**	n/a
DIA	*Diarrhena fauriei*	FR694881	JF697879	HQ600429
DIA	*Diarrhena japonica*	FR694882	JF697880	HQ600431
DIA	*Diarrhena mandshurica*	FR694883	n/a	HQ600452
DIA	*Diarrhena obovata*	KM974739	KM974739	KM974739
DUT	*Anisopogon avenaceus*	HE574413	GU222736	HE573296
DUT	*Danthoniastrum compactum*	AM234544	GU254779	n/a
DUT	*Duthiea brachypodium*	AM234547	GU222737	**MH888154**
DUT	*Metcalfia mexicana*	FR694893	JF697884	n/a
DUT	*Phaenosperma globosum*	KM974745	KM974745	KM974745
DUT	*Pseudodanthonia trigyna*	FR694886	GU222735	KP769115
DUT	*Stephanachne nigrescens*	FR694888	JF697899	n/a
DUT	*Stephanachne pappophorea*	FR694889	JF697900	n/a
LYG	*Lygeum spartum*	HE573932	GU222732	EF125146
MEL	*Brylkinia caudata*	FM253121	GU254780	n/a
MEL	*Glyceria declinata*	JN895984	U71048	HM850032
MEL	*Glyceria fluitans*	**MH888102**	n/a	**MH888155**
MEL	*Glyceria grandis*	HQ593315	AY622314	AY632364
MEL	*Glyceria maxima*	JN895612	n/a	JN891215
MEL	*Glyceria obtusa*	HF558505	HF558471	n/a
MEL	*Glyceria occidentalis*	**MH888103**	**MH888130**	**MH888156**
MEL	*Lycochloa avenacea*	FR694895	n/a	n/a
MEL	*Melica cupanii*	n/a	AY622315	AY632365
MEL	*Melica minuta*	KJ529313	KJ529426	n/a
MEL	*Melica mutica*	KM974742	KM974742	KM974742
MEL	*Melica nutans*	**MH888104**	**MH888131**	**MH888157**

MEL	*Melica subulata*	KM974743	KM974743	KM974743
MEL	*Melica uniflora*	HE573933	AM849165	AJ746263
MEL	*Pleuropogon refractus*	n/a	GU222749	n/a
MEL	*Pleuropogon sabinei*	KC475304	KJ913012	KC483463
MEL	*Schizachne purpurascens*	FM253126	GU222748	HQ590262
MEL	*Streblochaete longiarista*	FR694890	n/a	n/a
MEL	*Triniochloa stipoides*	FR694892	JF697911	n/a
NAR	*Nardus stricta*	AM234573	GU222733	AM849379
POE	*Aira caryophyllea*	DQ786878	DQ786806	AM849361
POE	*Aira cupaniana*	DQ786879	DQ786807	n/a
POE	*Aira praecox*	AM234540	n/a	AJ746255
POE	*Alopecurus geniculatus*	**MH888105**	**MH888132**	**MH888158**
POE	*Alopecurus magellanicus*	DQ786880	DQ786808	KC481898
POE	*Alopecurus myosuroides*	FN908046	HE575735	FN870382
POE	*Alopecurus pratensis*	**MH888106**	**MH888133**	**MH888159**
POE	*Alopecurus textilis*	DQ786881	DQ786809	n/a
POE	*Aniselytron treutleri*	DQ786883	DQ786811	n/a
POE	*Antinoria agrostidea*	KJ529360	KJ529464	n/a
POE	*Arctagrostis latifolia*	**MH888107**	**MH888134**	**MH888160**
POE	*Arctophila fulva*	AM234606	n/a	JN965260
POE	*Arctopoa eminens*	FN668469	n/a	n/a
POE	*Arctopoa tibetica*	KM523850	n/a	KX513085
POE	*Avenella flexuosa*	DQ786887	DQ786815	JN892161
POE	*Beckmannia syzigachne*	DQ786889	DQ786817	EF125142
POE	*Bellardiochloa variegata*	DQ786890	DQ786818	n/a
POE	*Castellia tuberculosa*	EF137492	n/a	EF125149
POE	*Catabrosa aquatica*	AM234589	DQ786826	FN870781
POE	*Catapodium marinum*	HE646574	n/a	JN892800
POE	*Corynephorus canescens*	JX438082	JX438136	FN870793
POE	*Cutandia memphitica*	DQ786900	DQ786828	n/a
POE	*Cynosurus cristatus*	**MH888108**	**MH888135**	**MH888161**
POE	*Cynosurus echinatus*	HM850530	KJ529465	HM849933
POE	*Dactylis glomerata*	KM974738	KM974738	KM974738
POE	*Deschampsia antarctica*	KF887484	KF887484	KF887484
POE	*Deschampsia cespitosa*	**MH888109**	**MH888136**	**MH888162**
POE	*Deschampsia foliosa*	FN908052	HE575738	FN870388
POE	*Deschampsia setacea*	JN895038	n/a	JN892159
POE	*Desmazeria rigida*	EF137491	JX438141	EF125150

POE	*Desmazeria sicula*	HE646576	DQ786832	n/a
POE	*Dielsiochloa floribunda*	DQ786907	DQ786835	n/a
POE	*Dryopoa dives*	KJ599286	n/a	KJ599175
POE	*Dupontia fisheri*	AM234602	DQ786836	JN965499
POE	*Echinaria capitata*	AM234599	JX438138	n/a
POE	*Festuca altissima*	JX871939	JX871939	JX871939
POE	*Festuca arundinacea*	KM974751	KM974751	KM974751
POE	*Festuca eskia*	JX438100	JX438158	n/a
POE	*Festuca ovina*	JX871940	JX871940	JX871940
POE	*Festuca petraea*	**MH888110**	**MH888137**	**MH888163**
POE	*Festuca pratensis*	**MH888111**	**MH888138**	**MH888164**
POE	*Festuca pulchella*	KJ529399	KJ529510	n/a
POE	*Festuca rubra*	**MH888112**	**MH888139**	**MH888165**
POE	*Festuca subverticillata*	DQ786912	DQ786840	KJ593413
POE	*Helictochloa hookeri*	KM974734	KM974734	KM974734
POE	*Helictochloa pratensis*	JN894523	n/a	JN893219
POE	*Helictotrichon pubescens*	JN894522	n/a	JN891447
POE	*Holcus annuus*	DQ786921	DQ786849	n/a
POE	*Holcus azoricus*	HM850539	n/a	HM850052
POE	*Holcus lanatus*	**MH888113**	**MH888140**	**MH888166**
POE	*Holcus mollis*	AM234554	n/a	JN892525
POE	*Holcus rigidus*	HM850541	n/a	HM850054
POE	*Hookerochloa eriopoda*	DQ786913	DQ786841	n/a
POE	*Hookerochloa hookeriana*	HE646579	DQ786850	KJ599181
POE	*Lamarckia aurea*	JX438085	JX438140	AJ784834
POE	*Leucopoa kingii*	DQ786923	DQ786851	n/a
POE	*Lolium multiflorum*	JX871942	JX871942	JX871942
POE	*Lolium perenne*	AM777385	AM777385	AM777385
POE	*Lolium rigidum*	DQ786926	DQ786854	HM850133
POE	*Lolium temulentum*	JN895696	KM538758	JN893065
POE	*Mibora minima*	FR694894	DQ786855	JN893662
POE	*Micropyropsis tuberosa*	JX438094	JX438152	n/a
POE	*Milium effusum*	AM234598	KM538761	HQ600468
POE	*Milium vernale*	DQ786928	DQ786856	n/a
POE	*Molineriella laevis*	DQ786929	DQ786857	n/a
POE	*Narduroides salzmannii*	HE646583	JX438160	n/a
POE	*Parapholis cylindrica*	FN908058	HE575742	EF125153
POE	*Parapholis incurva*	AM234583	DQ786859	EF125154

POE	*Parapholis strigosa*	JN896014	n/a	JN893607
POE	*Periballia involucrata*	KJ529353	KJ529460	n/a
POE	*Phippsia algida*	AM234603	n/a	KC483421
POE	*Phleum alpinum*	KM974747	KM974747	KM974747
POE	*Phleum arenarium*	JN895255	n/a	JN893617
POE	*Phleum pratense*	**MH888114**	**MH888141**	**MH888167**
POE	*Poa alpina*	**MH888115**	**MH888142**	**MH888168**
POE	*Poa alsodes*	HQ593386	n/a	HQ590210
POE	*Poa annua*	FN908068	HE575747	FN870404
POE	*Poa autumnalis*	KM523889	n/a	n/a
POE	*Poa billardierei*	DQ786935	DQ786863	JQ933231
POE	*Poa palustris*	KM974749	KM974749	KM974749
POE	*Poa pratensis*	**MH888116**	**MH888143**	**MH888169**
POE	*Poa secunda*	HF558518	HF558485	n/a
POE	*Psilurus incurvus*	HE646587	JX438159	EF125155
POE	*Puccinellia distans*	HE586075	DQ786866	L14621
POE	*Puccinellia fasciculata*	AM234588	n/a	JN892615
POE	*Puccinellia maritima*	JN895281	n/a	JN892617
POE	*Puccinellia nuttalliana*	KM974750	KM974750	KM974750
POE	*Puccinellia phryganodes*	KC475595	n/a	JN965789
POE	*Puccinellia tenella*	KC475620	n/a	JN965784
POE	*Sclerochloa dura*	AM234587	DQ786869	KJ599164
POE	*Scolochloa festucacea*	AM234600	KJ913040	n/a
POE	*Sesleria autumnalis*	HE966993	n/a	HE963664
POE	*Sesleria caerulea*	DQ786942	DQ786870	EF125156
POE	*Sphenopus divaricatus*	HE646589	DQ786871	n/a
POE	*Vahlodea atropurpurea*	AM234549	DQ786875	n/a
POE	*Vulpia bromoides*	JN894508	LN908194,KJ529497	HM850470
POE	*Vulpia ciliata*	JN894723	KJ529487	EF125157
POE	*Vulpia fasciculata*	JN894722	JX438163	JN892996
POE	*Vulpia microstachys*	DQ786948	DQ786876	n/a
POE	*Vulpia myuros*	FN908075	HE575749	FN870411
POE	*Wangenheimia lima*	JX438103	JX438165	n/a
STI	*Achnatherum bromoides*	FN434251	GU254734	n/a
STI	*Achnatherum calamagrostis*	JX438064	GU254743	JQ933203
STI	*Achnatherum Eriocoma aridum*	EU489170	JF697847	n/a
STI	*Achnatherum Eriocoma hymenoides*	KM974729	KM974729	KM974729
STI	*Achnatherum Eriocoma occidentale*	FN434256	GU222739	n/a

STI	*Achnatherum Eriocoma robustum*	GU254715	GU254755	n/a
STI	*Achnatherum inebrians*	GU254695,FN434206	GU254750	n/a
STI	*Achnatherum jacquemontii*	JF697799	JF697855	n/a
STI	*Achnatherum Neotrinia splendens*	GU254687,FN434208	GU254787	n/a
STI	*Achnatherum pekinense*	FN434277	JF697861	HQ600430
STI	*Achnatherum Pseudoeriocoma acutum*	JF697791	JF697846	n/a
STI	*Achnatherum Pseudoeriocoma constrictum*	JF697794	JF697849	n/a
STI	*Achnatherum Pseudoeriocoma eminens*	JF697797	JF697853	n/a
STI	*Achnatherum Pseudoeriocoma multinode*	JF697804	JF697860	n/a
STI	*Achnatherum sibiricum*	LN554420	GU254741	n/a
STI	*Achnatherum Stillmania stillmanii*	JF697810	JF697867	n/a
STI	*Achnatherum Timouria caragana*	FN434210	GU254732	n/a
STI	*Achnatherum Timouria pelliotii*	FN434234	JF697898	n/a
STI	*Achnatherum Timouria saposhnikovii*	GU254692	GU222738	n/a
STI	*Aciachne acicularis*	GU254673	GU254806	n/a
STI	*Aciachne flagellifera*	GU254672	GU254805	n/a
STI	*Amelichloa caudata*	EU489175	GU254764	n/a
STI	*Amelichloa clandestina*	GU254717	GU254765	n/a
STI	*Ampelodesmos mauritanicus*	KM974731	KM974731	KM974731
STI	*Anatherostipa hansmeyeri*	EU489176	GU254804	n/a
STI	*Anatherostipa mucronata*	GU254697	GU254803	n/a
STI	*Anatherostipa obtusa*	JF697813	GU254800	n/a
STI	*Anatherostipa rigidiseta*	GU254699	GU254809	n/a
STI	*Anatherostipa rosea*	GU254671	GU254795	n/a
STI	*Anatherostipa venusta*	GU254680	GU254801	n/a
STI	*Anemanthele lessoniana*	FR832726	JF697870	EF125158
STI	*Austrostipa compressa*	EU489179	n/a	JF769144
STI	*Austrostipa geoffreyi*	JF769107	KF445689	JF769155
STI	*Austrostipa juncifolia*	JF769110	JF697873	JQ886569
STI	*Austrostipa macalpinei*	JF769111	JF697874	KC129565
STI	*Austrostipa nitida*	KC129510	JF697875	KC129573
STI	*Austrostipa pubescens*	n/a	KF445690	JQ886573
STI	*Austrostipa pubinodis*	JF769123	KF445691	JQ886574
STI	*Austrostipa rudis*	n/a	KF445692	JQ886576

STI	*Austrostipa scabra*	FN434337	GU254738	JF769178
STI	*Austrostipa semibarbata*	GU254693	GU254736	FN870770
STI	*Austrostipa tenuifolia*	KC129524	GU254739	JQ886580
STI	*Austrostipa trichophylla*	JF769128	JF697878	JF769183
STI	*Celtica gigantea*	FN434281	GU222740	n/a
STI	*Hesperostipa comata*	EU489185	GU222744	n/a
STI	*Hesperostipa neomexicana*	EU489186	GU254808	n/a
STI	*Hesperostipa spartea*	FN434340	GU254745	n/a
STI	*Jarava annua*	JF697822	JF697882	n/a
STI	*Jarava castellanosii*	EU489191	GU254770	n/a
STI	*Jarava ichu*	EU489202	GU254763	n/a
STI	*Jarava media*	EU489205	GU254758	n/a
STI	*Jarava plumosula*	EU489207	GU254757	n/a
STI	*Jarava pseudoichu*	EU489209	GU254762	n/a
STI	*Jarava scabrifolia*	EU489210	GU254760	n/a
STI	*Macrochloa tenacissima*	**MH888117**	**MH888144**	**MH888170**
STI	*Nassella clarazii*	EU489221,KC129528	GU254766	n/a
STI	*Nassella filiculmis*	EU489224	GU254768	n/a
STI	*Nassella tenuissima*	HF558510	HF558476	JQ886583
STI	*Nassella viridula*	HE573935	HE573457	AY622896
STI	*Oloptum miliaceum*	FN908067	AY622317	FN870403
STI	*Ortachne breviseta*	GU254674	GU254810	n/a
STI	*Ortachne rariflora*	GU254675	GU254771	n/a
STI	*Orthoraphium roylei*	FN434333	GU254753	n/a
STI	*Oryzopsis asperifolia*	KM974744	KM974744	KM974744
STI	*Pappostipa chrysophylla*	EU489192	GU254781	n/a
STI	*Pappostipa hieronymusii*	EU489197	JF697886	n/a
STI	*Pappostipa major*	EU489212	GU254798	n/a
STI	*Patis coreana*	JF697795,KM538799	KF445698	n/a
STI	*Patis kuoi*	JF697828	JF697891	n/a
STI	*Patis racemosa*	n/a	U21924	n/a
STI	*Piptatheropsis canadensis*	JF697825	JF697888	n/a
STI	*Piptatheropsis exigua*	GU254677	GU254752	n/a
STI	*Piptatheropsis micrantha*	KX601236	KX601263	n/a
STI	*Piptatheropsis pungens*	JF697831	JF697894	n/a
STI	*Piptatheropsis shoshoneana*	GU254688	GU254814	n/a
STI	*Piptatherum aequiglume*	FN434213	JF697887	n/a
STI	*Piptatherum coerulescens*	FN434218	GU254789	n/a

STI	*Piptatherum holciforme*	FN434222	GU254817	n/a
STI	*Piptatherum laterale*	FN434223	JF754709	n/a
STI	*Piptochaetium avenaceum*	KM974748	KM974748	KM974748
STI	*Piptochaetium brachyspermum*	EU489233	GU254802	n/a
STI	*Piptochaetium featherstonei*	GU254704	GU254796	n/a
STI	*Piptochaetium montevidense*	JF697833	JF697897	n/a
STI	*Piptochaetium panicoides*	EU489234	GU254794	n/a
STI	*Psammochloa villosa*	AM234607	GU254786	n/a
STI	*Ptilagrostis dichotoma*	FN434229	GU254749	n/a
STI	*Ptilagrostis junatovii*	GU254701	GU254748	n/a
STI	*Ptilagrostis kingii*	GU254712	GU254813	n/a
STI	*Ptilagrostis mongholica*	FN434233	GU254746	n/a
STI	*Stipa barbata*	**MH888118**	**MH888145**	**MH888171**
STI	*Stipa juncea*	HE573937	HE573458	HE573441
STI	*Stipa lagascae*	**MH888119**	**MH888146**	**MH888172**
STI	*Stipa lipskyi*	KT692644	KT692644	KT692644
STI	*Stipa pennata*	LN554456	MG052611	**MH888173**
STI	*Stipa purpurea*	KT983629	KT983629	KT983629
STI	*Stipellula capensis*	AM234576	GU254773	n/a
STI	*Stipellula parviflora*	GU254719	GU254774	n/a
STI	*Trikeraia hookeri*	FR694896	GU254785	n/a
STI	*Trikeraia pappiformis*	FR694891	GU222747	n/a
TRI	*Aegilops comosa*	FJ897859	DQ247906	AY836161
TRI	*Aegilops cylindrica*	KF534489	KF534489	KF534489
TRI	*Aegilops geniculata*	KF534490	KF534490	KF534490
TRI	*Aegilops mutica*	EU012996	DQ247876	AY836157
TRI	*Aegilops sharonensis*	FJ897865	DQ247913	n/a
TRI	*Aegilops speltoides*	JQ740834	JQ740834	JQ740834
TRI	*Aegilops tauschii*	JQ754651	JQ754651	JQ754651
TRI	*Aegilops uniaristata*	FJ897866	DQ247910	n/a
TRI	*Agropyron cristatum*	JX438066	DQ247875	AY836156
TRI	*Agropyron desertorum*	HQ652642	n/a	HQ652721
TRI	*Agropyron mongolicum*	HM540004	AF267661	n/a
TRI	*Australopyrum pectinatum*	HM770815	DQ247877	AY836158
TRI	*Australopyrum retrofractum*	HM540009	AF267662	AY836159
TRI	*Australopyrum velutinum*	HM770817	DQ247878	AY836160
TRI	*Boissiera squarrosa*	EF137488	HE575764	HE575813
TRI	*Bromus benekenii*	**MH888120**	**MH888147**	**MH888174**

TRI	*Bromus catharticus*	FN908049	HE575737	FN870385
TRI	*Bromus hordeaceus*	HE573929	AM849134	AY395531
TRI	*Bromus inermis*	HF558526	DQ786821	HQ600445
TRI	*Bromus ramosus*	HE586076	HE575765	HE575814
TRI	*Bromus tectorum*	HF558493	HF558459	HQ600441
TRI	*Bromus vulgaris*	KM974737	KM974737	KM974737
TRI	*Crithopsis delileana*	HM770829	DQ247895	AY836177
TRI	*Dasypyrum villosum*	HM540011	DQ247881	AY836163
TRI	*Elymus caucasicus*	HQ652701	AF267667	HM770839
TRI	*Elymus elongatus*	HQ652645	DQ247892	HQ652724
TRI	*Elymus farctus*	HE573930	AM849122	AM849350
TRI	*Elymus repens*	HF558527	AF267682	HQ600453
TRI	*Elymus sibiricus*	**MH888121**	**MH888148**	**MH888175**
TRI	*Elymus trachycaulus*	DQ786910	DQ786838	JN965510
TRI	*Eremopyrum bonaepartis*	HM540012	n/a	EF125162
TRI	*Eremopyrum distans*	HM770821	DQ247882	AY836164
TRI	*Eremopyrum triticeum*	HM540014	DQ247883	AY836165
TRI	*Festucopsis serpentini*	HM770823	DQ247884	AY836166
TRI	*Henrardia persica*	HM540017	DQ247885	AY836167
TRI	*Heteranthelium piliferum*	HM540018	DQ247886	AY836168
TRI	*Hordelymus europaeus*	AM234596	EU376152	EU376154
TRI	*Hordeum brachyantherum*	**MH888122**	**MH888149**	**MH888176**
TRI	*Hordeum bulbosum*	KY636105	KY636105	KY636105
TRI	*Hordeum erectifolium*	AB078100	DQ247888	AY836170
TRI	*Hordeum jubatum*	KM974741	KM974741	KM974741
TRI	*Hordeum marinum*	FJ897873	DQ247889	AY836171
TRI	*Hordeum murinum*	HF558528	DQ247890	AY836172
TRI	*Hordeum vulgare*	KC912688	KC912688	KC912688
TRI	*Kengyilia melanthera*	HQ652688	n/a	KC237159
TRI	*Kengyilia mutica*	HQ652664	n/a	HQ652743
TRI	*Kengyilia rigidula*	HQ652693	n/a	HQ652772
TRI	*Kengyilia stenachyra*	HQ652677	n/a	HQ652756
TRI	*Kengyilia thoroldiana*	HQ652663	n/a	HQ652742
TRI	*Leymus angustus*	AF164404	n/a	GU140024
TRI	*Leymus arenarius*	JN894789	n/a	GU140017
TRI	*Leymus mollis*	KF713122	n/a	EU636666
TRI	*Leymus salinus*	n/a	AF108030	GU140018
TRI	*Leymus triticoides*	n/a	AF267694	GU140016

TRI	*Littledalea tibetica*	AM234572	DQ786852	n/a
TRI	*Peridictyon sanctum*	HM770828	DQ247894	AY836176
TRI	*Psathyrostachys fragilis*	HQ619280	DQ247896	AY836178
TRI	*Psathyrostachys juncea*	AB078140	AF267707	AY607050
TRI	*Psathyrostachys stoloniformis*	HQ619281	DQ247898	AY836180
TRI	*Pseudoroegneria spicata*	HM540026	DQ247900	AY836182
TRI	*Pseudoroegneria stipifolia*	HQ652695	n/a	KC237126
TRI	*Pseudoroegneria strigosa*	HQ652698	AF267712	KC237129
TRI	*Pseudoroegneria tauri*	HM540025	n/a	KC237161
TRI	*Secale cereale*	KC912691	KC912691	KC912691
TRI	*Secale strictum*	HM770833	DQ247899	AY836181
TRI	*Secale sylvestre*	AM234581	n/a	n/a
TRI	*Stenostachys gracilis*	HM770810	HM770849	HM770843
TRI	*Taeniatherum caputmedusae*	EF137512	DQ247902	EF125164
TRI	*Thinopyrum bessarabicum*	HQ652644	DQ247903	AY836185
TRI	*Thinopyrum distichum*	FR832843	n/a	AM235075
TRI	*Thinopyrum junceum*	JN893896	n/a	JN891931
TRI	*Triticum aestivum*	KC912694	KC912694	KC912694
TRI	*Triticum monococcum*	KC912692	KC912692	KC912692
TRI	*Triticum timopheevii*	EU013193	DQ304678	n/a
TRI	*Triticum turgidum*	EU013199	DQ247920	HQ894421
TRI	*Triticum urartu*	KC912693	KC912693	KC912693
xARI	*Aristida purpurea*	KJ920224	KJ920224	KJ920224
xARU	*Monachather paradoxus*	KJ920235	KJ920235	KJ920235
xARU	*Phragmites australis*	KF730315	KF730315	KF730315
xBAM	*Arundinaria tecta*	KC817463	KC817463	KC817463
xBAM	*Bambusa bambos*	KJ870988	KJ870988	KJ870988
xBAM	*Buergersiochloa bambusoides*	KJ871000	KJ871000	KJ871000
xBAM	*Chusquea spectabilis*	KJ870990	KJ870990	KJ870990
xBAM	*Cryptochloa strictiflora*	JX235348	JX235348	JX235348
xBAM	*Guadua weberbaueri*	KP793062	KP793062	KP793062
xBAM	*Phyllostachys propinqua*	JN415113	JN415113	JN415113
xCHL	*Centropodia glauca*	KT168383	KT168383	KT168383
xCHL	*Chloris barbata*	KT168393	KT168393	KT168393
xCHL	*Hilaria rigida*	KT168396	KT168396	KT168396
xCHL	*Neyraudia reynaudiana*	KF356392	KF356392	KF356392
xDAN	*Danthonia californica*	KJ920229	KJ920229	KJ920229
xMIC	*Micraira sp*	KJ920234	KJ920234	KJ920234

xORY	*Ehrharta erecta*	AY792568	AM887887	LN907926
xORY	*Leersia oryzoides*	FN908060	HE575734	FN870396
xORY	*Oryza sativa*	JN861110	JN861110	JN861110
xORY	*Streptogyna americana*	n/a	GU222721	AY618663
xPAN	*Reynaudia filiformis*	HE574132	JN604704	HE573433
xPAN	*Sorghum bicolor*	NC_008602	NC_008602	NC_008602
xPAN	*Zea mays*	X86563	X86563	X86563
xPUE	*Guaduella densiflora*	KC123409	AF164777	KC123368
xPUE	*Puelia olyriformis*	KC534841	KC534841	KC534841
xPHA	*Leptaspis cochleata*	HF558509	HF558475	LN908032
xPHA	*Pharus lappulaceus*	KC311467	KC311467	KC311467
xPHA	*Pharus latifolius*	JN032131	JN032131	JN032131
xANO	*Anomochloa marantoidea*	GQ329703	GQ329703	GQ329703
xANO	*Streptochaeta angustifolia*	AF164382	U21982	HQ182451
xECD	*Ecdeiocolea monostachya*	DQ257528	AY438617	HQ182426
xJOI	*Joinvillea plicata*	KX035098	KX035098	KX035098
xFLA	*Flagellaria indica*	DQ257515	AY465643	AY465694

*Accessions in bold were obtained *de novo* in this study by PCR and Sanger sequencing using custom Pooideae-specific primers (Table S2). PCR was performed on a Tetrad 2 Thermal Cycler (Bio-Rad, Hercules, CA, USA) and a Mastercycler ep Gradient Thermal Cycler (Eppendorf, Hamburg, Germany) using JumpStart™ REDTaq ReadyMix (Sigma-Aldrich, St. Louis, MO, USA). Amplicons were Sanger-sequenced in both directions using the same primers as for PCR. Chromatograms and sequences were inspected in BioEdit (Hall, 1999).

Table S1.2 Primer sequences and PCR conditions[1].

Region	Direction	Primer name	Primer sequence
matK	forward	*matK_Po_1F*	5'-TGT TCT GAC CAT ATT GCA CTA TG-3'
matK	reverse	*matK_Po_1526R*	5'-ACG CTC ACT GTG TGA TCC AC-3'
ndhF	forward	*ndhF_Po_1F*	5'-CCG ATG CTA TGG ARG GAC CC-3'
ndhF	reverse	*ndhF_Po_652R*	5'-TTT TTC CCC ATA ARG ATA TTG AA-3'
rbcL	forward	*rbcL_Po_1F*	5'-ACC ACA AAC AGA AAC TAA AGC-3'
rbcL	reverse	*rbcL_Po_590R*	5'-CAT AAA TGG TTG TGA GTT TAC G-3'

[1] 25 µl reactions with 1 µl DNA template and 0.4 µM of both primers. PCR: 120 s at 94°C, 40×(30 s at 94°C, 30 s at 58°C, 120 s at 72°C), 5 min at 72°C and 4°C hold.

Table S1.3 Results for diversification analyses in *TreePar* over 100 trees of the posterior sample, for two rate shifts under two extreme survival probability models where extinction is alternatively set to 1 (100% of the lineages survive to the next time interval) or 0.1 (10% of the lineages survive to the next time interval).

Model	Rate change	logL	LRT	AICc	ΔAIC	AICw	r_1 present	r_2 past	r_3 past	ε_1 present	ε_2 past	ε_3 past	Time shift $_1$	Time shift $_2$	SE logL	SE AICc	SE r1	SE r2	SE r3	SE ε_1	SE ε_2	SE ε_3	SE Time shift $_1$	SE Time shift $_2$
100% survive	0 shift	1354,52	-	2713,07	0,77	0,28	0,08	NA	NA	0,90	NA	NA	NA	NA	2,27	4,55	0,00	NA	NA	0,00	NA	NA	NA	NA
	1 shift	**1351,07**	**0,08**	**2712,30**	**0,00**	**0,41**	**0,13**	**0,09**	**NA**	**0,79**	**0,55**	**NA**	**25,17**	**NA**	**2,28**	**4,56**	**0,01**	**0,01**	**NA**	**0,02**	**0,04**	**NA**	**1,64**	**NA**
	2 shifts	1348,56	0,17	2713,50	1,20	0,23	0,16	0,07	0,03	0,73	0,83	0,49	15,75	35,23	2,29	4,58	0,01	0,02	0,05	0,03	0,02	0,07	1,33	1,34
10% survive	0 shift	**1354,52**	**-**	**2713,07**	**0,00**	**0,89**	**0,08**	**NA**	**NA**	**0,90**	**NA**	**NA**	**NA**	**NA**	**2,27**	**4,55**	**0,00**	**NA**	**NA**	**0,00**	**NA**	**NA**	**NA**	**NA**
	1 shift	1351,00	0,61	2712,17	4,31	0,10	0,13	0,11	NA	0,80	0,90	NA	25,63	NA	2,28	4,56	0,01	0,01	NA	0,02	0,02	NA	1,62	NA
	2 shifts	1348,41	1	2713,20	12,60	0,00	0,14	0,21	0,14	0,77	0,90	0,94	15,82	36,80	2,29	4,57	0,01	0,04	0,01	0,03	0,02	0,02	1,28	1,11

Bold font marks the model with the best fit. *LogL*, log likelihood value; AICc, small-sample-size corrected version of Akaike information criterion (AIC); ΔAIC, deltaAIC; difference between the AIC of several models, the best model has a ΔAIC of 0 and a difference bigger than 2 in ΔAIC values is generally considered significant; AICw, AIC weights; ε_i: extinction fraction, or turnover rate (extinction/speciation) estimated for the successive time intervals as we move from the present to the past; r_i, diversification rate (speciation minus extinction) estimates for the same intervals; Time shift *i*, shift times detected by the model in million years; SE, the standard error for the different parameters.

Table S1.4 Results for the paleoenvironment-dependent diversification model in RPANDA for the posterior sample of tree.

Models	#p	logL	AICc	ΔAIC	AICw	λ	α	μ	β	SE logL	SE AICc	SE λ	SE α	SE μ	SE β
Birth.cst-Death.cst	2	-1354,52	**2713,07**	**0,00**	**0,35**	0,81	NA	0,72	NA	2,27	4,55	0,01	NA	0,01	NA
Birth. Time.var-Death.cst	3	-1373,66	2753,38	40,30	0,00	0,40	-0,04	0,13	NA	2,41	4,83	0,02	0,00	0,03	NA
Birth.cst-Death. Time.var	3	-1353,99	**2714,05**	**0,98**	**0,21**	0,77	NA	0,68	0,001	2,28	4,57	0,01	NA	0,01	0,00
Birth. Time.var-Death- Time.var	4	-1353,99	2716,09	3,02	0,08	0,76	-0,01	0,66	-0,007	2,29	4,58	0,01	0,00	0,01	0,00
Birth.Env.var-Death.cst	3	-1355,71	2717,48	4,41	0,04	0,71	-0,10	0,36	NA	2,24	4,48	0,01	0,01	0,03	NA
Birth.cst-Death.Env.var	3	-1353,83	**2713,73**	**0,66**	**0,25**	0,75	NA	0,63	0,007	2,28	4,56	0,01	NA	0,01	0,00
Birth.Env.var-Death-Env.var	4	-1354,13	2716,36	3,28	0,07	0,76	-0,05	0,56	-0,151	2,29	4,58	0,01	0,01	0,02	0,10

Bold font marks the models with the best fit. Birth.cst-Death.cst, birth-death model with constant diversification rates; Birth. Time.var-Death.cst, speciation rate varies through time, while extinction rate remains constant; Birth.cst-Death. Time.var, speciation rate remains constant, while extinction rate varies through time; Birth. Time.var-Death- Time.var, both speciation and extinction rate vary through time; Birth.Env.var-Death.cst, speciation rate varies according to temperature, while extinction remains constant; Birth.cst-Death.Env.var, extinction varies with temperature but speciation remains constant; Birth.Env.var-Death.Env.Var, both speciation and extinction rates vary according to the temperature; #p, the number of parameters; logL, log likelihood; AICc, small-sample-size corrected version of Akaike information criterion (AIC); ΔAIC, deltaAIC; difference between the AIC of several models, the best model has a ΔAIC of 0 and a difference bigger than 2 in ΔAIC values is generally considered significant; AICw, AIC weights; λ, value for speciation rate; μ, value for extinction rate; α and β, correlation parameters between time or paleoenvironmental (temperature) data and speciation and extinction rates, respectively; SE, the standard error for the different parameters.

Tables S1.5 Phylogenetic signal for binary characters

Discrete characters	Fritz and Purvis' D	p-value, character not distributed randomly	p-value, character not distributed according Brownian motion
BIO6 below 0°C (no/yes)	0.42789	0.000	0.000
BIO11 below 2°C (no/yes)	0.57755	0.000	0.000
BIO11 below 3°C (no/yes)	0.51743	0.000	0.000
BIO11 below 4°C (no/yes)	0.48982	0.000	0.000

Tables S1.6 Fit of symmetrical and asymmetrical models for binary character evolution.

Discrete characters	AIC for symmetrical model	AIC for asymmetrical model (all rates different)	Difference
BIO6 below 0°C (no/yes)	483.25	**481.48**	1.77
BIO11 below 2°C (no/yes)	491.45	**482.23**	9.21
BIO11 below 3°C (no/yes)	**491.91**	493.55	1.64
BIO11 below 4°C (no/yes)	**489.83**	491.51	1.69

Bold font marks the model with the best fit.

Table S1.7 Pagels lambda for BIOCLIM and geographic coordinates.

Parameter	Pagel's λ	p value, λ ≠ 0	p value, λ ≠ 1	Description
BIO1	0.8218	2.238E-30	8.071E-37	Annual Mean Temperature
BIO2	0.5685	9.28E-26	1.022E-47	Mean Diurnal Range (Mean of monthly (max temp - min temp))
BIO3	**0.9507**	6.425E-57	7.399E-14	Isothermality (BIO2/BIO7) (* 100)
BIO4	**0.912**	1.722E-33	9.975E-29	Temperature Seasonality (standard deviation *100)
BIO5	0.6582	5.259E-17	4.351E-35	Max Temperature of Warmest Month
BIO6	**0.8618**	3.83E-31	8.772E-38	Min Temperature of Coldest Month
BIO7	0.8513	1.783E-27	4.175E-38	Temperature Annual Range (BIO5-BIO6)
BIO8	0.6826	2.11E-27	2.739E-47	Mean Temperature of Wettest Quarter
BIO9	0.7467	2.569E-15	7.771E-36	Mean Temperature of Driest Quarter
BIO10	0.7006	1.967E-19	1.799E-34	Mean Temperature of Warmest Quarter
BIO11	**0.872**	1.078E-34	1.358E-38	Mean Temperature of Coldest Quarter
BIO12	0.8034	4.864E-32	6.252E-45	Annual Precipitation
BIO13	0.8281	2.36E-32	3.808E-37	Precipitation of Wettest Month
BIO14	0.5782	5.01E-13	4.849E-44	Precipitation of Driest Month
BIO15	0.3381	2.646E-12	1.697E-54	Precipitation Seasonality (Coefficient of Variation)
BIO16	0.8194	8.723E-31	1.037E-38	Precipitation of Wettest Quarter
BIO17	0.5952	6.318E-14	4.523E-42	Precipitation of Driest Quarter
BIO18	0.7886	5.301E-25	4.033E-31	Precipitation of Warmest Quarter
BIO19	0.6582	1.219E-10	6.733E-49	Precipitation of Coldest Quarter
Longitude	0.9177	1.205E-25	1.789E-12	Longitude
Latitude	0.9488	3.879E-36	6.929E-08	Latitude

Bold font marks the vartiables with Pagels lambda >0.86.

Appendix 2 – Supporting methods

Justification for use of Poaceae fossils for calibration

(1) Fossil ***Paleoeriocoma hitchcockii*** **(Pooideae: Stipeae)**, from the Late Miocene Ash Hollow Formation (8–12 Ma) of Nebraska (Thomasson, 1988), is interpreted as an early representative of extant *Piptatheropsis* (*Oryzopsis* sect. *Oryzopsis* in Thomasson, 1980). The karyopsis fossil has a lemma epidermal pattern (LEP) similar to several extant species (*P. canadensis*, *P. exigua*, *P. pungens*), i.e. in having regular to irregularly shaped long cells, prominent hooks, and hairs that are generally aligned in regular rows (Thomasson, 1988).

(2) The contemporary genus ***Nassella*** **(Pooideae: Stipeae)** is represented by three fossil morphospecies from the same geological formation (8–12 Ma) as *Paleoeriocoma* (Thomasson, 1980). The karyopsis of *Nassella* is readily distinguishable by the ladder-like LEP pattern consisting of compressed and undifferentiated fundamental and silica cells in alternation (Romaschenko et al., 2012; Thomasson, 1978).

(3) Fossil ***Berriochloa*** **(Pooideae: Stipeae)** with 22 karyopsis morphospecies from various fossil deposits in continental North America (Thomasson, 1988) are interpreted as early representatives of extant *Hesperostipa* (Romaschenko et al., 2012). Some fossil *Berriochloa* (*B. minuta*, *B. maxima*) have LEPs similar to those of extant species (*H. comata*, *H. neomexicana*, *H. spartea*), i.e. in consisting of only fundamental cells with deeply sinuous sides and end-walls, lacking silica cells and cork cells (Romaschenko et al., 2012; Thomasson, 1978). The included data points representing *Berriochloa* fossils are from the Hemphillian (4.75–9 Ma), Miocene (5.3–23 Ma), Early to Middle Hemphillian (7–9 Ma) (Thomasson, 2005), Clarendonian (10.3–13.6 Ma), earliest Middle Miocene (16–23 Ma), Early Miocene / Late Hemingfordian (16.3–20.6 Ma) (Thomasson, 1982), Late Oligocene to Early Miocene (23–33.9 Ma) (Thomasson, 1985), and Middle Miocene (26–33.9 Ma).

(4) Fossil **"*Festuca* cf. *capillata*" (Pooideae: Poeae)**, from the Turów Lignite Mine of the Lower Miocene (16–23 Ma) of Poland (Juchniewicz, 1975), is interpreted as belonging to the narrow-leaved Loliineae based on cuticular similarity to contemporary taxa (Minaya, 2015).

(5) The contemporary, monotypic ***Lygeum*** **(Pooideae: Lygeeae)** has a pollen fossil record from the Miocene and Pliocene of Spain (Jiménez-Moreno, Fauquette, & Suc, 2010; Jiménez-Moreno & Suc, 2007). Pollen grains of *Lygeum* are distinguished by their more or less elongated shape, versus generally spheroidal in the rest of the family (Abdeddaim-Boughanmi & Kaid-Harche, 2009; Kellogg, 2015; Mander, Li, Mio, Fowlkes, & Punyasena, 2013). The included data points for fossil *Lygeum* are from Earliest Langhian (16 Ma), Earliest Serravallian (13.8 Ma), Serravallian (11.6–13.8 Ma), and Burdigalian-Langhian (13.8–20.4 Ma). *Lygeum* was included in the PyRate analysis only in order to help optimise the estimation of fossilisation probability.

(6) Fossil ***Stipa florissantii*** **(Pooideae: Stipeae)**, a karyopsis from the Eocene Florissant Formation (34.07–36.70 Ma) of Colorado (MacGinitie, 1953; Manchester, 2001), represents the oldest known fossil assignable to tribe Stipeae. The fossil has not been assigned to extant Stipeae lineages and therefore may serve to calibrate the stem node of the tribe to >34 Ma (Iles, Smith, Gandolfo, & Graham, 2015).

(7) Fossil **"Bambusoideae cf. *Chusquea*" (Bambusoideae)**, a phytolith from the Late Eocene (33.9–41.2 Ma) of North America (Strömberg, 2005), calibrates the stem node of *Chusquea* (Prasad et al., 2011) to >33.9 Ma.

(8) Fossil ***Leersia seifhennersdorfensis*** **(Oryzoideae)**, the distal end of an inflorescence from the Oligocene (30.7 Ma) of the Seifhennersdorf locality of Saxony, Germany (H Walther, 1974; Walther

& Kvaček, 2007), is assignable to extant *Leersia* (Oryzoideae) and may serve to calibrate its stem node to >30.7 Ma (Iles et al., 2015).

(9) Fossil ***Changii indicum*** **(Oryzoideae: Oryzeae)**, epidermal fragments containing phytoliths from the Maastrichtian-Danian (66 Ma) Deccan beds of India (Prasad, Strömberg, Alimohammadian, & Sahni, 2005), has been assigned to Oryzeae (Prasad et al., 2011) and may be used to calibrate the stem node of Oryzeae (=crown node of Oryzoideae) to >66 Ma (Iles et al., 2015).

(10) Fossil ***Pharus primuncinatus*** **(Pharoideae)**, a spikelet attached to mammalian hair recovered from Dominican amber (15–20 Ma), is assignable to *Pharus* and may be used to calibrate its stem node to >15 Ma (Iles et al., 2015 and references therein).

(11) Fossil **Poaceae**, epidermal pieces with phytoliths from Early Cretaceous (Albian; 101–113 Ma) of China extracted from dental structures of a hadrosauroid dinosaur *Equijubus normani*, is assignable to the crown node of Poaceae based on several diagnostic characters (Wu, You & Li, 2018) and may therefore serve to calibrate this node to >101 Ma. (It may be noted that this fossil is only marginally older than another convincing fossil, a grass spikelet infected by a *Claviceps*-like fungal sclerotium (*Palaeoclaviceps parasiticus*; Poinar Jr., Alderman, & Wunderlich, 2015) trapped in Myanmar amber from the Early Cretaceous (98.2–99.4 Ma; Shi et al., 2012) and which may be used to calibrate the stem node of Poaceae to >98 Ma.)

References

Abdeddaim-Boughanmi, K., & Kaid-Harche, M. (2009). Structure, ultrastructure of the anther, pollen microsporogenesis and morphology of pollen grains of two populations of *Lygeum spartum* L. in Algeria. *American Journal of Agricultural and Biological Sciences*, *4*(3), 201–205.

Iles, W. J. D., Smith, S. Y., Gandolfo, M. A., & Graham, S. W. (2015). Monocot fossils suitable for molecular dating analyses. *Botanical Journal of the Linnean Society*, *178*(3), 346–374.

Jiménez-Moreno, G., Fauquette, S., & Suc, J. P. (2010). Miocene to Pliocene vegetation reconstruction and climate estimates in the Iberian Peninsula from pollen data. *Review of Palaeobotany and Palynology*, *162*(3), 403–415.

Jiménez-Moreno, G., & Suc, J.-P. (2007). Middle Miocene latitudinal climatic gradient in Western Europe: Evidence from pollen records. *Palaeogeography, Palaeoclimatology, Palaeoecology*, *253*(1–2), 208–225.

Juchniewicz, K. (1975). Flora kopalna Turowa koło Bogatyni w świetle analizy nabłonkowej. *Prace Muzeum Ziemi*, *24*, 65–132.

Kellogg, E. A. (2015). Fossil record and rates of diversification. In *The families and genera of vascular plants, vol 13. flowering plants monocots* (pp. 103–107). Cham: Springer International Publishing.

Manchester, S. (2001). Update on the megafossil flora of Florissant, Colorado. In E. Evanoff, K. Gregory-Wodzicki, & K. Johnson (Eds.), *Proceedings of the Denver Museum of Nature and Science Series* (pp. 137–161). Denver, CO: Denver Museum of Nature and Science.

Mander, L., Li, M., Mio, W., Fowlkes, C. C., & Punyasena, S. W. (2013). Classification of grass pollen through the quantitative analysis of surface ornamentation and texture. *Proceedings of the Royal Society B: Biological Sciences*, *280*(1770), 20131905.

Minaya, M. Á. (2015). *A multigenomic approach to the phylogeny, evolution and biogeography of the grass subfamily Pooideae with an emphasis on the subtribe Loliinae*. Universidad de Zaragoza.

Poinar Jr., G. O., Alderman, S., & Wunderlich, J. (2015). One hundred million year old ergot : psychotropic compounds in the Cretaceous ? *Paleodiversity*, *8*(December), 13–19.

Prasad, V., Strömberg, C. A. E., Alimohammadian, H., & Sahni, A. (2005). Dinosaur coprolites and the early evolution of grasses and grazers. *Science*, *310*(5751), 1177–1180.

Prasad, V., Strömberg, C. A. E., Leaché, A. D., Samant, B., Patnaik, R., Tang, L., … Sahni, A. (2011). Late Cretaceous origin of the rice tribe provides evidence for early diversification in Poaceae. *Nature Communications*, (2), 480.

Romaschenko, K., Peterson, P. M., Soreng, R. J., Garcia-Jacas, N., Futorna, O., & Susanna, A. (2012). Systematics and evolution of the needle grasses (Poaceae: Pooideae: Stipeae) based on analysis of multiple chloroplast loci, ITS, and lemma micromorphology. *Taxon*, *61*(1), 18–44.

Shi, G., Grimaldi, D. A., Harlow, G. E., Wang, J. J., Wang, J. J., Yang, M., … Li, X. (2012). Age constraint on Burmese amber based on U-Pb dating of zircons. *Cretaceous Research*, *37*, 155–163.

Strömberg, C. A. E. (2005). Decoupled taxonomic radiation and ecological expansion of open-habitat grasses in the Cenozoic of North America. *Proceedings of the National Academy of Sciences*, *102*(34), 11980–11984.

Thomasson, J. R. (1978). Epidermal patterns of the lemma in some fossil and living grasses and their phylogenetic significance. *Science*, *199*(4332), 975–977.

Thomasson, J. R. (1982). Fossil grass anthoecia and other plant fossils from arthropod burrows in the Miocene of western Nebraska. *Journal of Paleontology*, *56*, 1011–1017.

Thomasson, J. R. (1985). Miocene fossil grasses: possible adaptation in reproductive bracts (lemma and palea). *Annals of the Missouri Botanical Garden*, *72*(4), 843–851.

Thomasson, J. R. (1988). Fossil grasses: 1820–1986 and beyond. In *International Symposium on Grass Systematics and Evolution, Washington, DC (USA), 27–31 Jul 1986*.

Thomasson, J. R. (2005). *Berriochloa gabeli* and *Berriochloa huletti* (Gramineae: Stipeae), two new grass species from the late Miocene Ash Hollow formation of Nebraska and Kansas. *Journal of Paleontology*, *79*(1), 185–199.

Walther, H. (1974). Ergänzungen zur Flora von Seifhennersdorf (Sachsen), II. Teil. *Abhandlungen Des Staatlichen Museums Für Mineralogie Und Geologie Zu Dresden*, *21*, 143–185.

Walther, H., & Kvaček, Z. (2007). Early Oligocene flora of Seifhennersdorf (Saxony). *Acta Musei Nationalis Pragae*, *63*(2), 85–174.

Wu, Y., You, H. L., & Li, X. Q. (2018). Dinosaur-associated Poaceae epidermis and phytoliths from the Early Cretaceous of China. *National Science Review*, *5*(5), 721–727.

Appendix 3 – Supporting figures

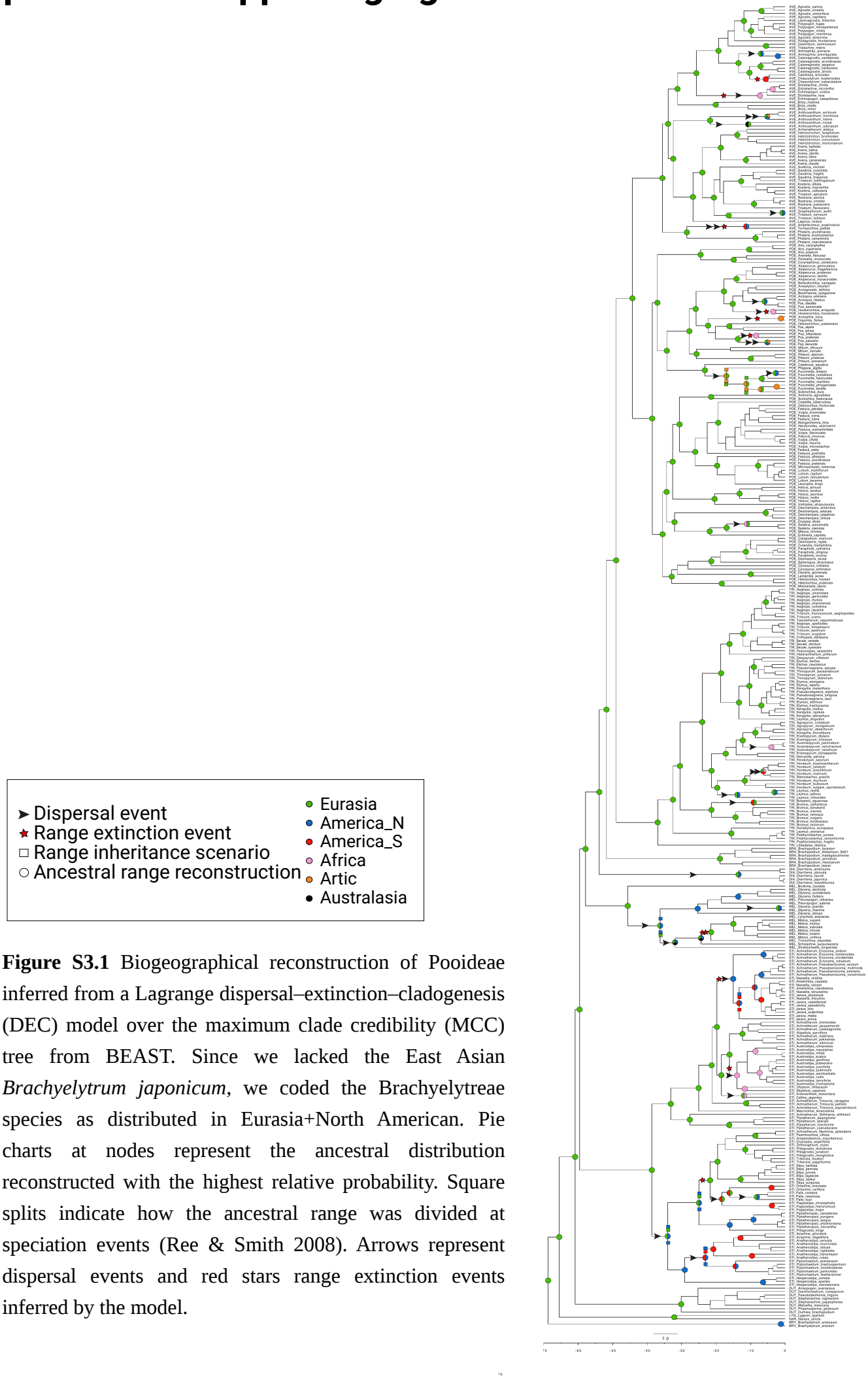

Figure S3.1 Biogeographical reconstruction of Pooideae inferred from a Lagrange dispersal–extinction–cladogenesis (DEC) model over the maximum clade credibility (MCC) tree from BEAST. Since we lacked the East Asian *Brachyelytrum japonicum*, we coded the Brachyelytreae species as distributed in Eurasia+North American. Pie charts at nodes represent the ancestral distribution reconstructed with the highest relative probability. Square splits indicate how the ancestral range was divided at speciation events (Ree & Smith 2008). Arrows represent dispersal events and red stars range extinction events inferred by the model.

Appendix 4 Results from Lagrange dispersal–extinction–cladogenesis model biogeographic analyses

Section 4.1 Phylogenetic tree in Newick format with nodelables being numbered according to nodes in section 4.2

((((((((((((((((((AVE_Agrostis_canina:3.38745,AVE_Agrostis_vinealis:3.38745)1:3.45468,AVE_Agrostis_stolonifera:6.84213)2:5.07204,(((AVE_Agrostis_capillaris:6.12585,AVE_Lachnagrostis_filiformis:6.12585)3:1.6478,((AVE_Polypogon_fugax:3.41093,(AVE_Polypogon_monspeliensis:1.67197,AVE_Polypogon_viridis:1.67197)4:1.73896)5:2.60105,AVE_Polypogon_maritimus:6.01198)6:1.76167)7:2.08227,AVE_Agrostis_tenerrima:9.85592)8:2.05825)9:2.8048,AVE_Podagrostis_thurberiana:14.719)10:1.80437,(AVE_Gastridium_ventricosum:5.5152,AVE_Triplachne_nitens:5.5152)11:11.0081)12:2.77593,(AVE_Ammophila_arenaria:7.00022,(AVE_Ammophila_breviligulata:2.0752,AVE_Calamagrostis_canadensis:2.0752)13:4.92503)14:6.47634,(((AVE_Calamagrostis_arundinacea:3.51673,AVE_Calamagrostis_epigeios:3.51673)15:3.58759,(AVE_Calamagrostis_canescens:2.11695,AVE_Calamagrostis_stricta:2.11695)16:4.98737)17:3.20709,((AVE_Calotheca_brizoides:4.56673,AVE_Chascolytrum_koelerioides:4.56673)18:1.01322,AVE_Chascolytrum_subaristatum:5.57994)19:4.73146)20:3.16515)21:5.82271)22:6.41714,((((AVE_Dichelachne_crinita:1.56658,AVE_Dichelachne_micrantha:1.56658)23:2.02791,AVE_Echinopogon_ovatus:3.59448)24:1.64992,AVE_Dichelachne_rara:5.24441)25:2.06289,AVE_Echinopogon_caespitosus:7.3073)26:18.4091)27:5.47573,(AVE_Briza_maxima:20.1213,(AVE_Briza_media:10.762,AVE_Briza_minor:10.762)28:9.35923)29:11.0709)30:2.74162,((((AVE_Anthoxanthum_arcticum:1.94006,AVE_Anthoxanthum_monticola:1.94006)31:3.3062,AVE_Anthoxanthum_nitens:5.24625)32:16.5069,(AVE_Anthoxanthum_nivale:10.6693,AVE_Anthoxanthum_odoratum:10.6693)33:11.084)34:10.6872,(((((AVE_Arrhenatherum_elatius:11.0785,AVE_Helictotrichon_longifolium:11.0785)35:2.78469,(AVE_Helictotrichon_bromoides:10.7719,(AVE_Helictotrichon_convolutum:8.23503,AVE_Helictotrichon_mortonianum:8.23503)36:2.53685)37:3.09132)38:4.78146,((((AVE_Avena_barbata:4.12667,(AVE_Avena_sativa:1.00649,AVE_Avena_sterilis:1.00649)39:3.12019)40:1.22038,AVE_Avena_fatua:5.34706)41:1.83968,AVE_Avena_canariensis:7.18674)42:4.1528,AVE_Avena_clauda:11.3395)43:7.30513)44:5.33694,((AVE_Avellinia_michelii:18.8713,((((AVE_Gaudinia_coarctata:2.552,AVE_Gaudinia_fragilis:2.552)45:6.71257,(AVE_Gaudinia_hispanica:7.23847,AVE_Trisetum_loeflingianum:7.23847)46:2.02611)47:3.45644,(AVE_Koeleria_albida:8.47048,(AVE_Koeleria_macrantha:5.15276,(AVE_Koeleria_vallesiana:2.93951,AVE_Trisetum_spicatum:2.93951)48:2.21325)49:3.31772)50:4.25054)51:5.12418,((AVE_Rostraria_azorica:3.27768,(AVE_Rostraria_cristata:1.50514,AVE_Rostraria_pubescens:1.50514)52:1.77254)53:5.72514,AVE_Trisetum_flavescens:9.00282)54:8.84238)55:1.02608)56:1.75981,((AVE_Graphephorum_wolfii:0.733237,AVE_Trisetum_cernuum:0.733237)57:15.6212,AVE_Trisetum_bifidum:16.3544)58:4.27665)59:3.35052)60:2.7345,AVE_Lagurus_ovatus:26.7161)61:5.72429)62:1.49335)63:1.645,((AVE_Amphibromus_scabrivalvis:11.2659,AVE_Torreyochloa_pallida:11.2659)64:17.2115,((AVE_Phalaris_arundinacea:6.53549,(AVE_Phalaris_brachystachys:2.1811,AVE_Phalaris_canariensis:2.1811)65:4.35439)66:2.03041,AVE_Phalaris_coerulescens:8.5659)67:19.9116)68:7.10127)69:8.7022,(((((POE_Aira_caryophyllea:3.55661,POE_Aira_cupaniana:3.55661)70:6.85006,POE_Aira_praecox:10.4067)71:14.0863,((POE_Avenella_flexuosa:11.16,POE_Periballia_involucrata:11.16)72:3.72254,POE_Corynephorus_canescens:14.8825)73:9.61042)74:12.5495,(((((((POE_Alopecurus_geniculatus:5.18638,POE_Alopecurus_magellanicus:5.18638)75:4.26499,(POE_Alopecurus_pratensis:2.54508,POE_Alopecurus_textilis:2.54508)76:6.90629)77:1.90482,POE_Alopecurus_myosuroides:11.3562)78:2.73521,POE_Bellardiochloa_variegata:14.0914)79:3.62423,((((POE_Aniselytron_treutleri:8

.36555,POE_Arctagrostis_latifolia:8.36555)80:2.35621,POE_Beckmannia_syzigachne:10.7218)81:1.50446,((POE_Arctopoa_eminens:2.36089,POE_Arctopoa_tibetica:2.36089)82:3.55443,(POE_Poa_alsodes:2.06398,POE_Poa_autumnalis:2.06398)83:3.85135)84:6.31089)85:2.94911,(POE_Hookerochloa_eriopoda:3.4406,POE_Hookerochloa_hookeriana:3.4406)86:11.7347)87:2.5403)88:8.10805,((POE_Arctophila_fulva:1.20026,POE_Dupontia_fisheri:1.20026)89:21.1365,((POE_Helictotrichon_pubescens:16.1753,(POE_Poa_alpina:12.04,POE_Poa_annua:12.04)90:4.1353)91:3.99563,((POE_Poa_billardierei:8.4103,POE_Poa_pratensis:8.4103)92:5.27197,(POE_Poa_palustris:5.11445,POE_Poa_secunda:5.11445)93:8.56782)94:6.48867)95:2.16582)96:3.48692)97:1.93736,((POE_Milium_effusum:15.8545,POE_Milium_vernale:15.8545)98:9.86319,((POE_Phleum_alpinum:2.90062,POE_Phleum_pratense:2.90062)99:7.03036,POE_Phleum_arenarium:9.93098)100:15.7867)101:2.04335)102:6.53523,(POE_Catabrosa_aquatica:23.2511,(POE_Phippsia_algida:17.0304,((((POE_Puccinellia_distans:2.8013,POE_Puccinellia_nuttalliana:2.8013)103:2.22604,POE_Puccinellia_fasciculata:5.02735)104:1.72973,POE_Puccinellia_maritima:6.75708)105:4.4606,((POE_Puccinellia_phryganodes:2.42685,POE_Puccinellia_tenella:2.42685)106:4.55341,POE_Sclerochloa_dura:6.98026)107:4.23742)108:5.81272)109:6.22068)110:11.0452)111:2.74615)112:1.49496,(((((POE_Antinoria_agrostidea:21.4465,POE_Scolochloa_festucacea:21.4465)113:9.15318,(((POE_Castellia_tuberculosa:19.3848,((((((POE_Dielsiochloa_floribunda:7.58013,(POE_Festuca_petraea:5.71985,POE_Vulpia_bromoides:5.71985)114:1.86028)115:2.77137,((POE_Festuca_ovina:3.61001,POE_Festuca_rubra:3.61001)116:4.08248,POE_Wangenheimia_lima:7.6925)117:2.659)118:1.23239,POE_Narduroides_salzmannii:11.5839)119:1.27452,((POE_Festuca_subverticillata:6.98593,POE_Vulpia_fasciculata:6.98593)120:4.64326,(POE_Psilurus_incurvus:2.90371,(POE_Vulpia_ciliata:1.43633,POE_Vulpia_myuros:1.43633)121:1.46737)122:8.72549)123:1.22922)124:1.61265,POE_Vulpia_microstachys:14.4711)125:2.74002,POE_Festuca_eskia:17.2111)126:2.17372)127:3.20386,POE_Festuca_pulchella:22.5887)128:3.45767,(POE_Festuca_altissima:19.686,((POE_Festuca_arundinacea:7.80794,((POE_Festuca_pratensis:3.22942,POE_Micropyropsis_tuberosa:3.22942)129:1.89239,(((POE_Lolium_multiflorum:1.08767,POE_Lolium_rigidum:1.08767)130:0.695093,POE_Lolium_temulentum:1.78276)131:1.4219,POE_Lolium_perenne:3.20466)132:1.91715)133:2.68613)134:6.69359,POE_Leucopoa_kingii:14.5015)135:5.18452)136:6.36029)137:4.55338)138:2.00634,((POE_Holcus_annuus:6.64851,POE_Holcus_lanatus:6.64851)139:6.53646,((POE_Holcus_azoricus:1.92015,POE_Holcus_mollis:1.92015)140:5.50578,POE_Holcus_rigidus:7.42593)141:5.75904)142:7.25012,POE_Vahlodea_atropurpurea:20.4351)143:12.171)144:1.75669,(((POE_Deschampsia_antarctica:3.36907,POE_Deschampsia_setacea:3.36907)145:2.2266,(POE_Deschampsia_cespitosa:3.64764,POE_Deschampsia_foliosa:3.64764)146:1.94802)147:26.4654,(((POE_Dryopoa_dives:11.0527,(POE_Sesleria_autumnalis:2.03623,POE_Sesleria_caerulea:2.03623)148:9.0165)149:5.89252,POE_Mibora_minima:16.9452)150:4.90811,POE_Echinaria_capitata:21.8534)151:10.2077)152:2.30167)153:1.17096,((((((POE_Catapodium_marinum:2.03008,POE_Desmazeria_rigida:2.03008)154:7.90719,(POE_Cutandia_memphitica:8.25452,((POE_Parapholis_cylindrica:2.15483,POE_Parapholis_strigosa:2.15483)155:1.30282,POE_Parapholis_incurva:3.45765)156:4.79687)157:1.68275)158:1.42233,POE_Desmazeria_sicula:11.3596)159:7.40516,POE_Sphenopus_divaricatus:18.7648)160:2.71728,POE_Cynosurus_cristatus:21.4821)161:6.64893,POE_Cynosurus_echinatus:28.131)162:3.13595,(POE_Dactylis_glomerata:9.94862,POE_Lamarckia_aurea:9.94862)163:21.3183)164:1.60804,((POE_Helictochloa_hookeri:3.33488,POE_Helictochloa_pratensis:3.33488)165:15.0359,POE_Molineriella_laevis:18.3707)166:14.5042)167:2.65874)168:3.00365)169:5.74358)170:4.71629,((((((((((((TRI_Aegilops_comosa:1.71633,TRI_Aegilops_uniaristata:1.71633)171:2.19655,((TRI_Aegilops_geniculata:2.07059,TRI_Aegilops_muticа:2.07059)172:1.0728,TRI_Aegilops_sharonensis:3.1434)173:0.769485)174:1.61876,(TRI_Aegilops_cylindrica:1.1023,TRI_Aegilops_tauschii:1.1023)175:4.42935)176:1.15143,(TRI_Triticum_monococcum_aegilopoides:2.81588,TRI_Triticum_urartu:2.81588)177:3.8672)178:2.20557,TRI_Taeniatherum_caputmedusae:8.88865)179:0.921178,((TRI_Aegilops_speltoides:1.75748,TRI_Triticum_timopheevii:1.75748)180:1.94926,(TRI_Triticum_aestivum:0.622451,TRI_Triticum_turgidum:0.622451)181:3.0842

9)182:6.10309)183:2.36929,((TRI_Crithopsis_delileana:8.0176,((TRI_Secale_cereale:0.889106,TRI_Se
cale_strictum:0.889106)184:2.85524,TRI_Secale_sylvestre:3.74435)185:4.27325)186:1.9014,TRI_Fes
tucopsis_serpentini:9.919)187:2.26012)188:3.92495,TRI_Heteranthelium_piliferum:16.1041)189:2.5
47,((((TRI_Dasypyrum_villosum:6.67498,TRI_Elymus_farctus:6.67498)190:2.40027,(((TRI_Elymus_ca
ucasicus:3.76519,TRI_Pseudoroegneria_spicata:3.76519)191:2.29473,(TRI_Thinopyrum_bessarabicu
m:2.85861,TRI_Thinopyrum_junceum:2.85861)192:3.20131)193:1.66034,TRI_Thinopyrum_distichu
m:7.72026)194:1.35499)195:1.26644,(((((TRI_Elymus_elongatus:1.74021,TRI_Elymus_repens:1.7402
1)196:1.015,(TRI_Kengyilia_melanthera:1.03528,TRI_Pseudoroegneria_stipifolia:1.03528)197:1.7199
3)198:1.2685,(TRI_Pseudoroegneria_strigosa:1.26217,TRI_Pseudoroegneria_tauri:1.26217)199:2.76
155)200:1.31372,(TRI_Elymus_sibiricus:1.37106,TRI_Elymus_trachycaulus:1.37106)201:3.96638)202
:1.52984,((TRI_Kengyilia_mutica:2.92919,TRI_Kengyilia_rigidula:2.92919)203:1.63803,TRI_Kengyilia_
stenachyra:4.56721)204:2.30007)205:3.47441)206:3.01158,TRI_Leymus_angustus:13.3533)207:5.29
78)208:5.36871,(((((((TRI_Agropyron_cristatum:1.28406,TRI_Agropyron_mongolicum:1.28406)209:5
.50797,(TRI_Agropyron_desertorum:3.39561,TRI_Kengyilia_thoroldiana:3.39561)210:3.39641)211:1.
82297,(TRI_Eremopyrum_distans:4.41869,TRI_Eremopyrum_triticeum:4.41869)212:4.1963)213:3.61
792,((TRI_Australopyrum_pectinatum:0.602823,TRI_Australopyrum_retrofractum:0.602823)214:3.3
871,TRI_Australopyrum_velutinum:3.98993)215:8.24299)216:1.96803,(TRI_Eremopyrum_bonaepart
is:7.95624,TRI_Henrardia_persica:7.95624)217:6.24471)218:2.99322,TRI_Peridictyon_sanctum:17.1
942)219:4.13406,((((((TRI_Hordeum_brachyantherum:1.96495,TRI_Hordeum_jubatum:1.96495)220:
2.94012,TRI_Hordeum_erectifolium:4.90507)221:1.35718,(TRI_Hordeum_marinum:4.20971,TRI_Ste
nostachys_gracilis:4.20971)222:2.05254)223:3.92098,TRI_Hordeum_murinum:10.1832)224:1.48968,
(TRI_Hordeum_bulbosum:5.63964,TRI_Hordeum_vulgare_spontaneum:5.63964)225:6.03327)226:7.
98696,((TRI_Leymus_mollis:3.03586,TRI_Leymus_salinus:3.03586)227:10.7797,TRI_Leymus_triticoid
es:13.8156)228:5.84428)229:1.66836)230:2.69155)231:6.47193,((TRI_Boissiera_squarrosa:9.08555,
TRI_Bromus_catharticus:9.08555)232:12.2598,((TRI_Bromus_benekenii:9.32265,((TRI_Bromus_iner
mis:5.10271,TRI_Bromus_ramosus:5.10271)233:2.09233,TRI_Bromus_vulgaris:7.19504)234:2.12762
)235:5.04502,(TRI_Bromus_hordeaceus:7.42281,TRI_Bromus_tectorum:7.42281)236:6.94487)237:6.
97765)238:9.14638)239:2.00954,(TRI_Hordelymus_europaeus:15.5836,(((TRI_Leymus_arenarius:0.8
85964,TRI_Psathyrostachys_juncea:0.885964)240:1.46823,TRI_Psathyrostachys_stoloniformis:2.354
2)241:2.13325,TRI_Psathyrostachys_fragilis:4.48745)242:11.0962)243:16.9176)244:4.45319,TRI_Littl
edalea_tibetica:36.9544)245:12.0428)246:2.80643,(((BRA_Brachypodium_boissieri:9.66108,BRA_Br
achypodium_distachyon_Bd21:9.66108)247:4.87307,(BRA_Brachypodium_madagascariense:4.2193
4,BRA_Brachypodium_pinnatum:4.21934)248:10.3148)249:4.34171,(BRA_Brachypodium_mexicanu
m:12.3603,BRA_Brachypodium_stacei:12.3603)250:6.5156)251:32.9278)252:2.08113,((DIA_Diarrhe
na_americana:1.49348,DIA_Diarrhena_obovata:1.49348)253:11.989,(DIA_Diarrhena_fauriei:1.5922,
(DIA_Diarrhena_japonica:0.499907,DIA_Diarrhena_mandshurica:0.499907)254:1.09229)255:11.890
3)256:40.4023)257:3.99266,(MEL_Brylkinia_caudata:45.6359,(((((((MEL_Glyceria_declinata:4.18623,
MEL_Glyceria_occidentalis:4.18623)258:3.78802,MEL_Glyceria_fluitans:7.97425)259:5.63014,MEL_
Pleuropogon_refractus:13.6044)260:4.86632,MEL_Pleuropogon_sabinei:18.4707)261:4.05986,(MEL
_Glyceria_grandis:1.7805,MEL_Glyceria_maxima:1.7805)262:20.7501)263:2.79053,MEL_Glyceria_ob
tusa:25.3211)264:10.9043,((((MEL_Lycochloa_avenacea:14.9769,(((MEL_Melica_cupanii:6.60756,(M
EL_Melica_mutica:4.56801,MEL_Melica_subulata:4.56801)265:2.03955)266:1.36018,MEL_Melica_
minuta:7.96773)267:3.7542,(MEL_Melica_nutans:8.03832,MEL_Melica_uniflora:8.03832)268:3.683
62)269:3.25497)270:6.58934,MEL_Triniochloa_stipoides:21.5662)271:2.79565,MEL_Schizachne_pur
purascens:24.3619)272:7.53123,MEL_Streblochaete_longiarista:31.8931)273:4.33225)274:9.41052)
275:12.2416)276:1.73716,(((((((STI_Achnatherum_Eriocoma_aridum:6.23827,((STI_Achnatherum_Er
iocoma_hymenoides:2.14301,STI_Achnatherum_Eriocoma_occidentale:2.14301)277:1.33577,STI_Ac
hnatherum_Eriocoma_robustum:3.47878)278:2.75949)279:8.79373,((((((STI_Achnatherum_Pseudoe

riocoma_acutum:0.722502,STI_Achnatherum_Pseudoeriocoma_multinode:0.722502)280:1.16218,STI_Achnatherum_Pseudoeriocoma_eminens:1.88468)281:2.32465,STI_Achnatherum_Pseudoeriocoma_constrictum:4.20933)282:2.63191,STI_Nassella_viridula:6.84124)283:1.94749,(((STI_Amelichloa_caudata:1.67127,STI_Nassella_clarazii:1.67127)284:2.78342,((STI_Amelichloa_clandestina:0.947315,STI_Nassella_tenuissima:0.947315)285:1.67378,(STI_Jarava_plumosula:1.38771,STI_Nassella_filiculmis:1.38771)286:1.23339)287:1.8336)288:2.42923,(((STI_Jarava_castellanosii:1.27894,STI_Jarava_pseudoichu:1.27894)289:2.69266,(STI_Jarava_ichu:2.76504,STI_Jarava_scabrifolia:2.76504)290:1.20656)291:1.74913,STI_Jarava_media:5.72073)292:1.16319)293:1.90481)294:4.50083,STI_Jarava_annua:13.2896)295:1.74245)296:4.73193,(((((STI_Achnatherum_bromoides:6.96943,STI_Achnatherum_jacquemontii:6.96943)297:3.75318,(STI_Achnatherum_calamagrostis:7.78416,STI_Stipellula_parviflora:7.78416)298:2.93845)299:1.6322,((STI_Achnatherum_inebrians:2.41668,STI_Achnatherum_pekinense:2.41668)300:4.05308,STI_Achnatherum_sibiricum:6.46977)301:5.88504)302:3.74428,((((STI_Austrostipa_compressa:2.35679,STI_Austrostipa_macalpinei:2.35679)303:6.23266,(STI_Austrostipa_nitida:0.918399,STI_Austrostipa_scabra:0.918399)304:7.67105)305:2.39974,(((STI_Austrostipa_geoffreyi:2.56689,STI_Austrostipa_pubescens:2.56689)306:2.04444,((STI_Austrostipa_juncifolia:2.66697,STI_Austrostipa_pubinodis:2.66697)307:0.97284,STI_Austrostipa_semibarbata:3.63981)308:0.971523)309:2.74513,(STI_Austrostipa_rudis:5.3671,(STI_Austrostipa_tenuifolia:3.44451,STI_Austrostipa_trichophylla:3.44451)310:1.9226)311:1.98936)312:3.63273)313:2.91633,(STI_Oloptum_miliaceum:11.7082,STI_Stipellula_capensis:11.7082)314:2.19736)315:2.19357)316:2.37977,(STI_Anemanthele_lessoniana:11.8864,STI_Celtica_gigantea:11.8864)317:6.59248)318:1.28507)319:1.33223,(STI_Achnatherum_Timouria_caragana:11.2678,(STI_Achnatherum_Timouria_pelliotii:7.25078,STI_Achnatherum_Timouria_saposhnikovii:7.25078)320:4.01703)321:9.82835)322:3.96032,STI_Macrochloa_tenacissima:25.0565)323:8.08685,(STI_Achnatherum_Stillmania_stillmanii:27.6183,(((STI_Piptatherum_aequiglume:6.33067,STI_Piptatherum_laterale:6.33067)324:2.66586,STI_Piptatherum_holciforme:8.99653)325:7.20415,STI_Piptatherum_coerulescens:16.2007)326:11.4176)327:5.52504)328:5.50015,(((((((STI_Achnatherum_Neotrinia_splendens:2.72417,STI_Psammochloa_villosa:2.72417)329:5.89349,STI_Ampelodesmos_mauritanicus:8.61766)330:5.60593,STI_Oryzopsis_asperifolia:14.2236)331:3.10432,(STI_Orthoraphium_roylei:11.536,((STI_Ptilagrostis_dichotoma:3.57072,STI_Ptilagrostis_junatovii:3.57072)332:5.27955,(STI_Ptilagrostis_mongholica:6.59296,(STI_Trikeraia_hookeri:4.01809,STI_Trikeraia_pappiformis:4.01809)333:2.57487)334:2.2573)335:2.68577)336:5.79188)337:2.24797,(((((STI_Stipa_barbata:2.52222,STI_Stipa_pennata:2.52222)338:1.48254,STI_Stipa_juncea:4.00476)339:1.89655,STI_Stipa_lagascae:5.90131)340:1.78923,STI_Stipa_lipskyi:7.69054)341:5.20759,STI_Stipa_purpurea:12.8981)342:6.67775)343:2.1661,(((STI_Ortachne_breviseta:3.92643,STI_Ortachne_rariflora:3.92643)344:12.187,((STI_Patis_coreana:5.02485,STI_Patis_racemosa:5.02485)345:3.13535,STI_Patis_kuoi:8.1602)346:7.95327)347:2.22477,(STI_Pappostipa_chrysophylla:3.79915,(STI_Pappostipa_hieronymusii:1.79621,STI_Pappostipa_major:1.79621)348:2.00294)349:14.5391)350:3.40373)351:3.23901,(((STI_Piptatheropsis_canadensis:1.07516,STI_Piptatheropsis_pungens:1.07516)352:8.07896,((STI_Piptatheropsis_exigua:0.796618,STI_Piptatheropsis_shoshoneana:0.796618)353:1.40825,STI_Piptatheropsis_micrantha:2.20487)354:6.94925)355:6.87911,STI_Ptilagrostis_kingii:16.0332)356:8.94775)357:9.07177,((((((STI_Aciachne_acicularis:5.73835,STI_Aciachne_flagellifera:5.73835)358:7.18322,STI_Anatherostipa_venusta:12.9216)359:1.96116,(STI_Anatherostipa_mucronata:7.4577,(STI_Anatherostipa_obtusa:4.10215,STI_Anatherostipa_rigidiseta:4.10215)360:3.35554)361:7.42503)362:5.84594,(STI_Anatherostipa_hansmeyeri:9.57977,STI_Anatherostipa_rosea:9.57977)363:11.1489)364:2.40201,(STI_Piptochaetium_avenaceum:14.341,(((STI_Piptochaetium_brachyspermum:2.2848,STI_Piptochaetium_montevidense:2.2848)365:1.23841,STI_Piptochaetium_panicoides:3.52321)366:1.37055,STI_Piptochaetium_featherstonei:4.89376)367:9.44723)368:8.78969)369:5.95026,((STI_Hesperostipa_comata:2.56336,STI_Hesperostipa_spartea:2.56336)370:3.81784,STI_Hesperostipa_neomexicana:6.38121)371:22.6997)372:4.97182)373:4.59071)374:20.9712)375:1.28535,((DUT_Anisopogon_avenace

us:25.2607,(((DUT_Danthoniastrum_compactum:13.8393,((DUT_Pseudodanthonia_trigyna:5.93337,DUT_Stephanachne_nigrescens:5.93337)376:1.29993,DUT_Stephanachne_pappophorea:7.2333)377:6.60601)378:3.61875,DUT_Metcalfia_mexicana:17.4581)379:4.25447,DUT_Phaenosperma_globosum:21.7125)380:3.54819)381:4.87122,DUT_Duthiea_brachypodium:30.1319)382:30.768)383:4.62154,(LYG_Lygeum_spartum:32.1295,NAR_Nardus_stricta:32.1295)384:33.392)385:3.20537,(BRY_Brachyelytrum_aristosum:1.22617,BRY_Brachyelytrum_erectum:1.22617)386:67.5007)387;

Section 4.2. Biogeographical reconstruction of Pooideae inferred from a DEC model with Brachyelytreae species coded with a Nort American + Eurasian distribution, due to the asian *Brachyelytrum japonicum* missing in the phylogeny.

Relative probabilities for each ancestral scenario are indicated. Ancestral scenarios are indicated with letters that correspond with our six operational areas: Africa (a), North America (b), SouthAmerica (c), the Arctic (d), Australasia (e) and Eurasia (f). Respective node numbers are indicated on the tree file supplied in Section 4.1 Appendix 4.

```
initial -ln likelihood: 712.709
Optimizing (simplex) -ln likelihood.
dis: 0.0040997 ext: 0.016548
final -ln likelihood: 654.891
Ancestral splits for:	1
	f|f	0.882711	(655.015)
Ancestral splits for:	2
	f|f	0.88197	(655.016)
Ancestral splits for:	3
	f|f	0.971479	(654.919)
Ancestral splits for:	4
	f|f	0.990281	(654.9)
Ancestral splits for:	5
	f|f	0.9855	(654.905)
Ancestral splits for:	6
	f|f	0.996612	(654.894)
Ancestral splits for:	7
	f|f	0.983467	(654.907)
Ancestral splits for:	8
	f|f	0.990566	(654.9)
Ancestral splits for:	9
	f|f	0.923416	(654.97)
Ancestral splits for:	10
	f|f	0.703474	(655.242)
	f|b	0.179728	(656.607)
Ancestral splits for:	11
	f|f	0.955697	(654.936)
Ancestral splits for:	12
	f|f	0.905158	(654.99)
Ancestral splits for:	13
	b|b	0.959426	(654.932)
```

```
Ancestral splits for:	14
	f|b	0.691479	(655.259)
	f|f	0.144886	(656.822)
Ancestral splits for:	15
	f|f	0.99748	(654.893)
Ancestral splits for:	16
	f|f	0.391513	(655.828)
	f|b_d_f0.258808	(656.242)
	f|b_f	0.173455	(656.642)
	f|d_f	0.167011	(656.68)
Ancestral splits for:	17
	f|f	0.840607	(655.064)
Ancestral splits for:	18
	c|c	0.96604	(654.925)
Ancestral splits for:	19
	c|c	0.491362	(655.601)
	c|f	0.38902	(655.835)
Ancestral splits for:	20
	f|f	0.493261	(655.597)
	f|c	0.307042	(656.071)
	f|c_f	0.0745332	(657.487)
Ancestral splits for:	21
	f|f	0.733916	(655.2)
Ancestral splits for:	22
	f|f	0.896921	(654.999)
Ancestral splits for:	23
	e|e	0.999461	(654.891)
Ancestral splits for:	24
	e|e	0.997625	(654.893)
Ancestral splits for:	25
	e|e	0.985509	(654.905)
Ancestral splits for:	26
	e|e	0.886912	(655.011)
Ancestral splits for:	27
	f|f	0.646842	(655.326)
	f|e	0.20827	(656.459)
Ancestral splits for:	28
	f|f	0.989388	(654.901)
Ancestral splits for:	29
	f|f	0.983834	(654.907)
Ancestral splits for:	30
	f|f	0.962847	(654.928)
Ancestral splits for:	31
	b|d	0.887618	(655.01)
Ancestral splits for:	32
	d|b_d_f	0.283185	(656.152)
	b|b_f	0.157128	(656.741)
	d|d_f	0.156992	(656.742)
Ancestral splits for:	33
	a|f	0.524915	(655.535)
	f|f	0.245619	(656.295)
```

```
        a_f|f    0.0805661      (657.409)
        a|a_f    0.0805661      (657.409)
Ancestral splits for:     34
        f|f      0.723435       (655.214)
Ancestral splits for:     35
        f|f      0.94759        (654.944)
Ancestral splits for:     36
        f|f      0.985164       (654.906)
Ancestral splits for:     37
        f|f      0.993327       (654.897)
Ancestral splits for:     38
        f|f      0.968984       (654.922)
Ancestral splits for:     39
        f|f      0.988271       (654.902)
Ancestral splits for:     40
        f|f      0.998056       (654.893)
Ancestral splits for:     41
        f|f      0.989297       (654.901)
Ancestral splits for:     42
        f|f      0.994247       (654.896)
Ancestral splits for:     43
        f|f      0.99281        (654.898)
Ancestral splits for:     44
        f|f      0.990735       (654.9)
Ancestral splits for:     45
        f|f      0.99812        (654.892)
Ancestral splits for:     46
        f|f      0.998023       (654.893)
Ancestral splits for:     47
        f|f      0.997459       (654.893)
Ancestral splits for:     48
        f|f      0.988884       (654.902)
Ancestral splits for:     49
        f|f      0.888038       (655.009)
Ancestral splits for:     50
        f|f      0.975771       (654.915)
Ancestral splits for:     51
        f|f      0.993556       (654.897)
Ancestral splits for:     52
        f|f      0.999349       (654.891)
Ancestral splits for:     53
        f|f      0.975502       (654.915)
Ancestral splits for:     54
        f|f      0.989295       (654.901)
Ancestral splits for:     55
        f|f      0.998431       (654.892)
Ancestral splits for:     56
        f|f      0.997243       (654.893)
Ancestral splits for:     57
        b|b_c    0.836112       (655.07)
        b|b      0.129524       (656.934)
```

```
Ancestral splits for:	58
	f|f	0.588161	(655.421)
	b|f	0.130396	(656.928)
	c|f	0.0972372	(657.221)
Ancestral splits for:	59
	f|f	0.939165	(654.953)
Ancestral splits for:	60
	f|f	0.988073	(654.903)
Ancestral splits for:	61
	f|f	0.989183	(654.901)
Ancestral splits for:	62
	f|f	0.986357	(654.904)
Ancestral splits for:	63
	f|f	0.987316	(654.903)
Ancestral splits for:	64
	c|b	0.375047	(655.871)
	b|b	0.0865196	(657.338)
	c_f|b	0.0844711	(657.362)
	c|b_f	0.0844711	(657.362)
	c|b_c	0.0603602	(657.698)
	b_c|b	0.0603602	(657.698)
	c|c	0.0523259	(657.841)
Ancestral splits for:	65
	f|f	0.998498	(654.892)
Ancestral splits for:	66
	f|f	0.485666	(655.613)
	b_d_f|f0.212254	(656.441)
	b_f|f	0.168573	(656.671)
	d_f|f	0.10725	(657.123)
Ancestral splits for:	67
	f|f	0.487698	(655.609)
	b_f|b	0.0678973	(657.58)
	b_f|f	0.0678973	(657.58)
Ancestral splits for:	68
	f|f	0.462051	(655.663)
	b|b_f	0.139362	(656.861)
Ancestral splits for:	69
	f|f	0.859624	(655.042)
Ancestral splits for:	70
	f|f	0.796764	(655.118)
Ancestral splits for:	71
	f|f	0.790425	(655.126)
Ancestral splits for:	72
	f|f	0.972765	(654.918)
Ancestral splits for:	73
	f|f	0.979509	(654.911)
Ancestral splits for:	74
	f|f	0.916483	(654.978)
Ancestral splits for:	75
	f|f	0.951158	(654.941)
Ancestral splits for:	76
```

```
        f|f     0.99799         (654.893)
Ancestral splits for:   77
        f|f     0.982713        (654.908)
Ancestral splits for:   78
        f|f     0.979454        (654.911)
Ancestral splits for:   79
        f|f     0.991193        (654.899)
Ancestral splits for:   80
        f|f     0.487192        (655.61)
        f|d     0.396882        (655.815)
Ancestral splits for:   81
        f|f     0.851241        (655.052)
Ancestral splits for:   82
        b_f|f   0.912041        (654.983)
Ancestral splits for:   83
        b|b     0.995408        (654.895)
Ancestral splits for:   84
        b_f|b   0.84813         (655.055)
Ancestral splits for:   85
        f|f     0.785481        (655.132)
Ancestral splits for:   86
        e|e     0.903233        (654.992)
Ancestral splits for:   87
        f|f     0.542044        (655.503)
        f|e     0.271634        (656.194)
Ancestral splits for:   88
        f|f     0.818639        (655.091)
        f|e_f   0.126098        (656.961)
Ancestral splits for:   89
        d|d     0.97542         (654.915)
Ancestral splits for:   90
        f|f     0.698909        (655.249)
Ancestral splits for:   91
        f|f     0.87712         (655.022)
Ancestral splits for:   92
        e|e     0.522235        (655.54)
        e|f     0.166781        (656.682)
        f|f     0.0931521       (657.264)
Ancestral splits for:   93
        b_d_f|b         0.485257        (655.614)
        b_f|b   0.324468        (656.016)
Ancestral splits for:   94
        f|f     0.253064        (656.265)
        e|f     0.143762        (656.83)
        e|b_f   0.108621        (657.11)
        e|d_f   0.104311        (657.151)
        e_f|f   0.0403279       (658.101)
Ancestral splits for:   95
        f|f     0.707625        (655.236)
Ancestral splits for:   96
        f|f     0.597334        (655.406)
```

```
        d|d_f   0.168949        (656.669)
        d|f     0.115172        (657.052)
Ancestral splits for:   97
        f|f     0.922903        (654.971)
Ancestral splits for:   98
        f|f     0.985931        (654.905)
Ancestral splits for:   99
        f|f     0.968187        (654.923)
Ancestral splits for:   100
        f|f     0.980786        (654.91)
Ancestral splits for:   101
        f|f     0.994853        (654.896)
Ancestral splits for:   102
        f|f     0.965406        (654.926)
Ancestral splits for:   103
        f|b     0.816318        (655.094)
Ancestral splits for:   104
        f|f     0.742756        (655.188)
        b_f|b   0.115587        (657.048)
        b_f|f   0.115587        (657.048)
Ancestral splits for:   105
        f|f     0.90529         (654.99)
Ancestral splits for:   106
        d|d     0.975123        (654.916)
Ancestral splits for:   107
        d|f     0.768828        (655.153)
Ancestral splits for:   108
        f|d_f   0.705079        (655.24)
        f|f     0.227158        (656.373)
Ancestral splits for:   109
        d|d_f   0.507018        (655.57)
        d|d     0.19874         (656.506)
        f|f     0.134709        (656.895)
        d|f     0.0927837       (657.268)
Ancestral splits for:   110
        f|f     0.48097         (655.623)
        d_f|d   0.141781        (656.844)
        d|d_f   0.0897946       (657.301)
        f|d_f   0.0897946       (657.301)
Ancestral splits for:   111
        f|f     0.959259        (654.932)
Ancestral splits for:   112
        f|f     0.989796        (654.901)
Ancestral splits for:   113
        f|f     0.856392        (655.046)
Ancestral splits for:   114
        f|f     0.984532        (654.906)
Ancestral splits for:   115
        c|f     0.473318        (655.639)
        f|f     0.435994        (655.721)
Ancestral splits for:   116
```

```
        f|f     0.95438         (654.937)
Ancestral splits for:   117
        f|f     0.983431        (654.907)
Ancestral splits for:   118
        f|f     0.951935        (654.94)
Ancestral splits for:   119
        f|f     0.988715        (654.902)
Ancestral splits for:   120
        b|f     0.614419        (655.378)
        f|f     0.237028        (656.33)
Ancestral splits for:   121
        f|f     0.999545        (654.891)
Ancestral splits for:   122
        f|f     0.997671        (654.893)
Ancestral splits for:   123
        f|f     0.795684        (655.119)
        b_f|f   0.193063        (656.535)
Ancestral splits for:   124
        f|f     0.815045        (655.095)
        f|b_f   0.177377        (656.62)
Ancestral splits for:   125
        f|f     0.577647        (655.439)
        f|b     0.190852        (656.547)
        b_f|b   0.177989        (656.617)
Ancestral splits for:   126
        f|f     0.936755        (654.956)
Ancestral splits for:   127
        f|f     0.982179        (654.909)
Ancestral splits for:   128
        f|f     0.99199         (654.899)
Ancestral splits for:   129
        f|f     0.999001        (654.892)
Ancestral splits for:   130
        f|f     0.99988         (654.891)
Ancestral splits for:   131
        f|f     0.999708        (654.891)
Ancestral splits for:   132
        f|f     0.999201        (654.891)
Ancestral splits for:   133
        f|f     0.998053        (654.893)
Ancestral splits for:   134
        f|f     0.985974        (654.905)
Ancestral splits for:   135
        f|f     0.53036         (655.525)
        f|b     0.331107        (655.996)
Ancestral splits for:   136
        f|f     0.909323        (654.986)
Ancestral splits for:   137
        f|f     0.986338        (654.904)
Ancestral splits for:   138
        f|f     0.991073        (654.9)
```

```
Ancestral splits for:	139
	f|f	0.994805	(654.896)
Ancestral splits for:	140
	f|f	0.998702	(654.892)
Ancestral splits for:	141
	f|f	0.995166	(654.895)
Ancestral splits for:	142
	f|f	0.991536	(654.899)
Ancestral splits for:	143
	f|f	0.944255	(654.948)
Ancestral splits for:	144
	f|f	0.995819	(654.895)
Ancestral splits for:	145
	f|f	0.979014	(654.912)
Ancestral splits for:	146
	f|f	0.97973	(654.911)
Ancestral splits for:	147
	f|f	0.970165	(654.921)
Ancestral splits for:	148
	f|f	0.897362	(654.999)
Ancestral splits for:	149
	e|f	0.413506	(655.774)
	f|f	0.361444	(655.908)
	e|e_f	0.113538	(657.066)
	e_f|f	0.0654528	(657.617)
Ancestral splits for:	150
	f|f	0.894795	(655.002)
Ancestral splits for:	151
	f|f	0.962454	(654.929)
Ancestral splits for:	152
	f|f	0.993756	(654.897)
Ancestral splits for:	153
	f|f	0.998296	(654.892)
Ancestral splits for:	154
	f|f	0.972567	(654.918)
Ancestral splits for:	155
	f|f	0.989258	(654.901)
Ancestral splits for:	156
	f|f	0.976415	(654.914)
Ancestral splits for:	157
	f|f	0.997045	(654.894)
Ancestral splits for:	158
	f|f	0.996775	(654.894)
Ancestral splits for:	159
	f|f	0.993821	(654.897)
Ancestral splits for:	160
	f|f	0.994868	(654.896)
Ancestral splits for:	161
	f|f	0.990957	(654.9)
Ancestral splits for:	162
	f|f	0.993922	(654.897)
```

```
Ancestral splits for:	163
	f|f	0.982782	(654.908)
Ancestral splits for:	164
	f|f	0.996619	(654.894)
Ancestral splits for:	165
	f|f	0.557006	(655.476)
	b_f|f	0.424389	(655.748)
Ancestral splits for:	166
	f|f	0.836899	(655.069)
Ancestral splits for:	167
	f|f	0.989499	(654.901)
Ancestral splits for:	168
	f|f	0.996549	(654.894)
Ancestral splits for:	169
	f|f	0.993491	(654.897)
Ancestral splits for:	170
	f|f	0.982568	(654.908)
Ancestral splits for:	171
	f|f	0.99954	(654.891)
Ancestral splits for:	172
	f|f	0.999719	(654.891)
Ancestral splits for:	173
	f|f	0.999716	(654.891)
Ancestral splits for:	174
	f|f	0.999566	(654.891)
Ancestral splits for:	175
	f|f	0.99946	(654.891)
Ancestral splits for:	176
	f|f	0.999418	(654.891)
Ancestral splits for:	177
	f|f	0.998761	(654.892)
Ancestral splits for:	178
	f|f	0.999098	(654.891)
Ancestral splits for:	179
	f|f	0.999112	(654.891)
Ancestral splits for:	180
	f|f	0.999443	(654.891)
Ancestral splits for:	181
	f|f	0.999728	(654.891)
Ancestral splits for:	182
	f|f	0.998079	(654.892)
Ancestral splits for:	183
	f|f	0.998448	(654.892)
Ancestral splits for:	184
	f|f	0.999659	(654.891)
Ancestral splits for:	185
	f|f	0.998362	(654.892)
Ancestral splits for:	186
	f|f	0.99838	(654.892)
Ancestral splits for:	187
	f|f	0.997937	(654.893)
```

```
Ancestral splits for:	188
	f|f	0.998084	(654.892)
Ancestral splits for:	189
	f|f	0.996404	(654.894)
Ancestral splits for:	190
	f|f	0.998169	(654.892)
Ancestral splits for:	191
	f|b	0.716078	(655.225)
	f|f	0.193269	(656.534)
Ancestral splits for:	192
	f|f	0.998925	(654.892)
Ancestral splits for:	193
	f|f	0.903325	(654.992)
Ancestral splits for:	194
	f|f	0.985715	(654.905)
Ancestral splits for:	195
	f|f	0.996755	(654.894)
Ancestral splits for:	196
	f|f	0.995381	(654.895)
Ancestral splits for:	197
	f|f	0.999777	(654.891)
Ancestral splits for:	198
	f|f	0.998809	(654.892)
Ancestral splits for:	199
	f|f	0.999586	(654.891)
Ancestral splits for:	200
	f|f	0.999322	(654.891)
Ancestral splits for:	201
	b_f|b	0.987906	(654.903)
Ancestral splits for:	202
	f|f	0.916902	(654.977)
Ancestral splits for:	203
	f|f	0.992031	(654.899)
Ancestral splits for:	204
	f|f	0.997269	(654.893)
Ancestral splits for:	205
	f|f	0.974	(654.917)
Ancestral splits for:	206
	f|f	0.99401	(654.897)
Ancestral splits for:	207
	f|f	0.993768	(654.897)
Ancestral splits for:	208
	f|f	0.995536	(654.895)
Ancestral splits for:	209
	f|f	0.979123	(654.912)
Ancestral splits for:	210
	f|f	0.984215	(654.906)
Ancestral splits for:	211
	f|f	0.991868	(654.899)
Ancestral splits for:	212
	f|f	0.849495	(655.054)
```

```
        f|b_f   0.142313        (656.84)
Ancestral splits for:   213
        f|f     0.961905        (654.929)
Ancestral splits for:   214
        e|e     0.996324        (654.894)
Ancestral splits for:   215
        e|e     0.865355        (655.035)
Ancestral splits for:   216
        f|f     0.559508        (655.471)
        f|e     0.344125        (655.957)
Ancestral splits for:   217
        f|f     0.994721        (654.896)
Ancestral splits for:   218
        f|f     0.894317        (655.002)
Ancestral splits for:   219
        f|f     0.974401        (654.916)
Ancestral splits for:   220
        b|b_f   0.921697        (654.972)
Ancestral splits for:   221
        f|c     0.344433        (655.956)
        b_f|c   0.321121        (656.026)
        f|f     0.0980624       (657.213)
Ancestral splits for:   222
        e|e     0.6726  (655.287)
        f|e     0.141338        (656.847)
Ancestral splits for:   223
        c_f|e   0.296942        (656.105)
        f|e     0.143617        (656.831)
        b_f|e   0.120059        (657.01)
        f|f     0.119748        (657.013)
Ancestral splits for:   224
        f|f     0.796337        (655.118)
Ancestral splits for:   225
        f|f     0.995789        (654.895)
Ancestral splits for:   226
        f|f     0.874806        (655.024)
Ancestral splits for:   227
        b_f|b   0.872275        (655.027)
Ancestral splits for:   228
        b_f|b   0.737467        (655.195)
        b|b     0.113075        (657.07)
Ancestral splits for:   229
        f|f     0.861392        (655.04)
Ancestral splits for:   230
        f|f     0.956846        (654.935)
Ancestral splits for:   231
        f|f     0.984198        (654.906)
Ancestral splits for:   232
        f|c     0.593202        (655.413)
        f|f     0.193801        (656.531)
Ancestral splits for:   233
```

```
        f|f       0.984948        (654.906)
Ancestral splits for:     234
        f|b       0.501449        (655.581)
        f|f       0.403973        (655.797)
Ancestral splits for:     235
        f|f       0.809731        (655.102)
        f|b_f     0.179624        (656.607)
Ancestral splits for:     236
        f|f       0.994174        (654.896)
Ancestral splits for:     237
        f|f       0.956512        (654.935)
Ancestral splits for:     238
        f|f       0.899832        (654.996)
Ancestral splits for:     239
        f|f       0.991513        (654.899)
Ancestral splits for:     240
        f|f       0.392915        (655.825)
        b_f|b     0.15107         (656.781)
        b_f|f     0.15107         (656.781)
Ancestral splits for:     241
        f|f       0.812986        (655.098)
        b_f|f     0.183267        (656.587)
Ancestral splits for:     242
        f|f       0.907625        (654.987)
Ancestral splits for:     243
        f|f       0.964655        (654.927)
Ancestral splits for:     244
        f|f       0.989833        (654.901)
Ancestral splits for:     245
        f|f       0.976877        (654.914)
Ancestral splits for:     246
        f|f       0.994412        (654.896)
Ancestral splits for:     247
        f|f       0.994053        (654.897)
Ancestral splits for:     248
        a|f       0.800561        (655.113)
Ancestral splits for:     249
        f|f       0.899063        (654.997)
Ancestral splits for:     250
        f|f       0.256906        (656.25)
        b_c|f     0.167677        (656.676)
        b|f       0.166076        (656.686)
        c|f       0.165862        (656.687)
        b_f|f     0.0458394       (657.973)
        c_f|f     0.0457804       (657.974)
        b_c_f|f 0.0369511         (658.189)
Ancestral splits for:     251
        f|f       0.592476        (655.414)
        f|b_f     0.114222        (657.06)
        f|c_f     0.113819        (657.064)
        f|b_c_f 0.0805254         (657.41)
```

```
Ancestral splits for:	252
	f|f	0.986473	(654.904)
Ancestral splits for:	253
	b|b	0.981303	(654.909)
Ancestral splits for:	254
	f|f	0.999475	(654.891)
Ancestral splits for:	255
	f|f	0.991982	(654.899)
Ancestral splits for:	256
	b|f	0.52542	(655.534)
	f|f	0.131179	(656.922)
	b_f|f	0.0923926	(657.272)
	b|b_f	0.0916216	(657.281)
Ancestral splits for:	257
	f|f	0.968376	(654.923)
Ancestral splits for:	258
	b|b	0.861118	(655.04)
Ancestral splits for:	259
	b|f	0.532929	(655.52)
	b|b	0.21879	(656.41)
	b_f|f	0.126998	(656.954)
Ancestral splits for:	260
	b|b	0.751639	(655.176)
	b_f|b	0.187437	(656.565)
Ancestral splits for:	261
	b|b	0.564168	(655.463)
	b|d	0.178958	(656.611)
Ancestral splits for:	262
	b|f	0.918956	(654.975)
Ancestral splits for:	263
	b|b	0.682175	(655.273)
	b|b_f	0.104089	(657.153)
Ancestral splits for:	264
	b|b	0.685244	(655.269)
	b_f|b	0.163316	(656.703)
Ancestral splits for:	265
	b|b_f	0.925982	(654.967)
Ancestral splits for:	266
	f|f	0.681454	(655.274)
	f|b_f	0.272287	(656.191)
Ancestral splits for:	267
	f|f	0.73975	(655.192)
	b_f|f	0.103113	(657.162)
	b_f|b	0.103113	(657.162)
Ancestral splits for:	268
	f|f	0.992813	(654.898)
Ancestral splits for:	269
	f|f	0.808636	(655.103)
	b_f|f	0.143562	(656.832)
Ancestral splits for:	270
	f|f	0.650384	(655.321)
```

Ancestral splits for: 271

f|f	0.212096	(656.441)
f|a	0.152694	(656.77)
b|b	0.0735041	(657.501)
f|a_f	0.0672259	(657.59)
a|a	0.0569542	(657.756)
a_f|a	0.0466895	(657.955)
f|c	0.0442419	(658.009)
b_f|a	0.036594	(658.198)
f|a_b	0.02942	(658.417)

Ancestral splits for: 272

a_f|b	0.192751	(656.537)
b|b	0.111962	(657.08)
f|b	0.103774	(657.156)
f|f	0.0976165	(657.217)
a_b_f|b	0.0792879	(657.425)
b_f|b	0.053335	(657.822)
c_f|b	0.0409199	(658.087)
a_b|b	0.0348709	(658.247)
a|b	0.0336564	(658.282)
f|b_f	0.031682	(658.343)
a|a	0.0288326	(658.437)

Ancestral splits for: 273

a_b_f|a	0.178712	(656.613)
f|f	0.13572	(656.888)
b|b	0.121751	(656.996)
a_f|a	0.0836841	(657.371)
a_b|a	0.0732148	(657.505)
b_f|a	0.0667898	(657.597)
a|a	0.0597162	(657.709)
b_f|f	0.0445299	(658.002)
b_f|b	0.0445299	(658.002)
f|a	0.0242927	(658.608)

Ancestral splits for: 274

b|b_f	0.199382	(656.503)
f|f	0.161439	(656.714)
b|b	0.152078	(656.774)
b|a_b_f	0.142443	(656.839)
b|a_b	0.0429632	(658.038)
b|f	0.0381678	(658.156)
b|a_f	0.0363946	(658.204)
b_f|b	0.0358314	(658.219)

Ancestral splits for: 275

f|f	0.634504	(655.345)

Ancestral splits for: 276

f|f	0.977018	(654.914)

Ancestral splits for: 277

b|b	0.999215	(654.891)

Ancestral splits for: 278

b|b	0.996257	(654.894)

Ancestral splits for: 279

b|b 0.967545 (654.924)
Ancestral splits for: 280
b|b 0.999847 (654.891)
Ancestral splits for: 281
b|b 0.99916 (654.891)
Ancestral splits for: 282
b|b 0.994282 (654.896)
Ancestral splits for: 283
b|b 0.955961 (654.936)
Ancestral splits for: 284
c|c 0.98244 (654.908)
Ancestral splits for: 285
c|c 0.579155 (655.437)
a_c|c 0.202105 (656.49)
a_c|a 0.202105 (656.49)
Ancestral splits for: 286
c|c 0.999706 (654.891)
Ancestral splits for: 287
c|c 0.915885 (654.978)
Ancestral splits for: 288
c|c 0.966187 (654.925)
Ancestral splits for: 289
c|c 0.999543 (654.891)
Ancestral splits for: 290
c|c 0.872415 (655.027)
b_c|c 0.125197 (656.968)
Ancestral splits for: 291
c|c 0.932683 (654.96)
Ancestral splits for: 292
c|c 0.94231 (654.95)
Ancestral splits for: 293
c|c 0.911591 (654.983)
Ancestral splits for: 294
b|c 0.783934 (655.134)
Ancestral splits for: 295
b_c|c 0.668045 (655.294)
c|c 0.11618 (657.043)
b_c_f|c 0.100959 (657.184)
Ancestral splits for: 296
b|b 0.332001 (655.993)
b|b_c 0.293726 (656.116)
b|b_c_f 0.0941303 (657.254)
b|b_f 0.0683857 (657.573)
b_f|b 0.0522346 (657.843)
Ancestral splits for: 297
f|f 0.996707 (654.894)
Ancestral splits for: 298
f|f 0.996938 (654.894)
Ancestral splits for: 299
f|f 0.996272 (654.894)
Ancestral splits for: 300

```
        f|f     0.998589        (654.892)
Ancestral splits for:   301
        f|f     0.994199        (654.896)
Ancestral splits for:   302
        f|f     0.983241        (654.907)
Ancestral splits for:   303
        e|e     0.997694        (654.893)
Ancestral splits for:   304
        e|e     0.998972        (654.892)
Ancestral splits for:   305
        e|e     0.98317         (654.908)
Ancestral splits for:   306
        e|e     0.999166        (654.891)
Ancestral splits for:   307
        e|e     0.999627        (654.891)
Ancestral splits for:   308
        e|e     0.999414        (654.891)
Ancestral splits for:   309
        e|e     0.998402        (654.892)
Ancestral splits for:   310
        e|e     0.998973        (654.892)
Ancestral splits for:   311
        e|e     0.997526        (654.893)
Ancestral splits for:   312
        e|e     0.991717        (654.899)
Ancestral splits for:   313
        e|e     0.938172        (654.954)
Ancestral splits for:   314
        e|e     0.44318         (655.704)
        f|f     0.387435        (655.839)
Ancestral splits for:   315
        e|e     0.421337        (655.755)
        e|f     0.276679        (656.175)
        e|e_f   0.134077        (656.9)
        f|f     0.0867416       (657.335)
Ancestral splits for:   316
        f|f     0.479476        (655.626)
        f|e     0.34565         (655.953)
        f|e_f   0.100588        (657.187)
Ancestral splits for:   317
        e|f     0.412643        (655.776)
        f|f     0.366569        (655.894)
        e_f|f   0.0695685       (657.556)
Ancestral splits for:   318
        f|f     0.766247        (655.157)
Ancestral splits for:   319
        f|f     0.404135        (655.797)
        b|f     0.237542        (656.328)
        c|f     0.0758491       (657.47)
        b|e_f   0.0562427       (657.769)
Ancestral splits for:   320
```

```
        f|f     0.995946        (654.895)
Ancestral splits for:   321
        f|f     0.990899        (654.9)
Ancestral splits for:   322
        f|f     0.688708        (655.263)
        b_f|f   0.154892        (656.756)
Ancestral splits for:   323
        f|f     0.854156        (655.048)
Ancestral splits for:   324
        f|f     0.981461        (654.909)
Ancestral splits for:   325
        f|f     0.986276        (654.904)
Ancestral splits for:   326
        f|f     0.964037        (654.927)
Ancestral splits for:   327
        f|f     0.610265        (655.384)
        b|f     0.20469         (656.477)
Ancestral splits for:   328
        f|f     0.745139        (655.185)
        f|b_f   0.148279        (656.799)
Ancestral splits for:   329
        f|f     0.997485        (654.893)
Ancestral splits for:   330
        f|f     0.983888        (654.907)
Ancestral splits for:   331
        f|f     0.595234        (655.409)
        f|b     0.292508        (656.12)
Ancestral splits for:   332
        f|f     0.997893        (654.893)
Ancestral splits for:   333
        f|f     0.998736        (654.892)
Ancestral splits for:   334
        f|f     0.998471        (654.892)
Ancestral splits for:   335
        f|f     0.998032        (654.893)
Ancestral splits for:   336
        f|f     0.994916        (654.896)
Ancestral splits for:   337
        f|f     0.864635        (655.036)
        b_f|f   0.124795        (656.972)
Ancestral splits for:   338
        f|f     0.999489        (654.891)
Ancestral splits for:   339
        f|f     0.999159        (654.891)
Ancestral splits for:   340
        f|f     0.998209        (654.892)
Ancestral splits for:   341
        f|f     0.974866        (654.916)
Ancestral splits for:   342
        f|f     0.986829        (654.904)
Ancestral splits for:   343
```

```
        f|f       0.888394        (655.009)
Ancestral splits for:     344
        c|c       0.96953         (654.921)
Ancestral splits for:     345
        f|b       0.72979         (655.206)
        f|f       0.101137        (657.182)
Ancestral splits for:     346
        b_f|f     0.52096         (655.543)
        f|f       0.380674        (655.856)
Ancestral splits for:     347
        c|f       0.300037        (656.094)
        c|b_f     0.267537        (656.209)
        c|c_f     0.0591776       (657.718)
        c|b_c_f0.0566222          (657.762)
        c_f|f     0.0562938       (657.768)
        c|c       0.0504945       (657.876)
        f|f       0.0487732       (657.911)
        c|b       0.0478366       (657.931)
Ancestral splits for:     348
        c|c       0.605969        (655.391)
        c|b_c     0.387451        (655.839)
Ancestral splits for:     349
        c|c       0.70694         (655.237)
        c|b_c     0.276732        (656.175)
Ancestral splits for:     350
        c_f|c     0.379324        (655.86)
        b_c_f|c0.248169           (656.284)
        c|c       0.0586234       (657.727)
        b_c|c     0.0563102       (657.767)
Ancestral splits for:     351
        f|f       0.238509        (656.324)
        f|b_c_f 0.182988          (656.589)
        f|c_f     0.177183        (656.621)
        f|b_f     0.166096        (656.686)
        f|b_c     0.0452688       (657.986)
        f|c       0.0373256       (658.179)
        f|b       0.0330947       (658.299)
        b|b       0.0327229       (658.31)
Ancestral splits for:     352
        b|b       0.99894         (654.892)
Ancestral splits for:     353
        b|b       0.999763        (654.891)
Ancestral splits for:     354
        b|b       0.9983  (654.892)
Ancestral splits for:     355
        b|b       0.990819        (654.9)
Ancestral splits for:     356
        b|b       0.959971        (654.931)
Ancestral splits for:     357
        b_f|b     0.212758        (656.438)
        f|b       0.198355        (656.508)
```

b|b 0.155911 (656.749)
b_c_f|b 0.153422 (656.765)
c_f|b 0.152089 (656.774)
f|b_f 0.0359023 (658.218)
Ancestral splits for: 358
c|c 0.995758 (654.895)
Ancestral splits for: 359
c|c 0.99655 (654.894)
Ancestral splits for: 360
c|c 0.997965 (654.893)
Ancestral splits for: 361
c|c 0.841889 (655.063)
b_c|c 0.144918 (656.822)
Ancestral splits for: 362
c|c 0.961369 (654.93)
Ancestral splits for: 363
c|c 0.988462 (654.902)
Ancestral splits for: 364
c|c 0.966723 (654.924)
Ancestral splits for: 365
c|c 0.999299 (654.891)
Ancestral splits for: 366
c|c 0.997082 (654.893)
Ancestral splits for: 367
c|c 0.980032 (654.911)
Ancestral splits for: 368
b|c 0.60593 (655.392)
b_c|c 0.119923 (657.011)
b|b_c 0.0925462 (657.271)
c|c 0.089043 (657.309)
Ancestral splits for: 369
c|b_c 0.694439 (655.255)
c|c 0.180384 (656.603)
Ancestral splits for: 370
b|b 0.997135 (654.893)
Ancestral splits for: 371
b|b 0.975339 (654.916)
Ancestral splits for: 372
b|b 0.656085 (655.312)
b_c|b 0.124293 (656.976)
Ancestral splits for: 373
b_f|b 0.394629 (655.82)
b|b 0.275194 (656.181)
b_c_f|b 0.0648209 (657.627)
Ancestral splits for: 374
f|f 0.3666 (655.894)
f|b_f 0.172643 (656.647)
b_f|b 0.157 (656.742)
f|b 0.0926047 (657.27)
Ancestral splits for: 375
f|f 0.970626 (654.92)

```
Ancestral splits for:	376
	f|f	0.998306	(654.892)
Ancestral splits for:	377
	f|f	0.995149	(654.895)
Ancestral splits for:	378
	f|f	0.979361	(654.911)
Ancestral splits for:	379
	f|f	0.625362	(655.36)
	f|b	0.250201	(656.276)
Ancestral splits for:	380
	f|f	0.87694	(655.022)
Ancestral splits for:	381
	f|f	0.611282	(655.383)
	e|f	0.187675	(656.564)
Ancestral splits for:	382
	f|f	0.769959	(655.152)
	e_f|f	0.119393	(657.016)
Ancestral splits for:	383
	f|f	0.955871	(654.936)
Ancestral splits for:	384
	f|f	0.914006	(654.98)
Ancestral splits for:	385
	f|f	0.911017	(654.984)
Ancestral splits for:	386
	b_f|f	0.234565	(656.341)
Ancestral splits for:	387
	f|f	0.236319	(656.333)
	f|b_f	0.0991199	(657.202)
	f|b_e_f	0.0446086	(658)
	f|b_d_f	0.0446086	(658)
	f|b_c_f	0.0446086	(658)
	f|a_b_f	0.0446086	(658)
	f|b	0.0393865	(658.125)
	f|e_f	0.0349269	(658.245)
	f|a_f	0.0349269	(658.245)
	f|c_f	0.0349269	(658.245)
```